



$J = 0$

was H^0

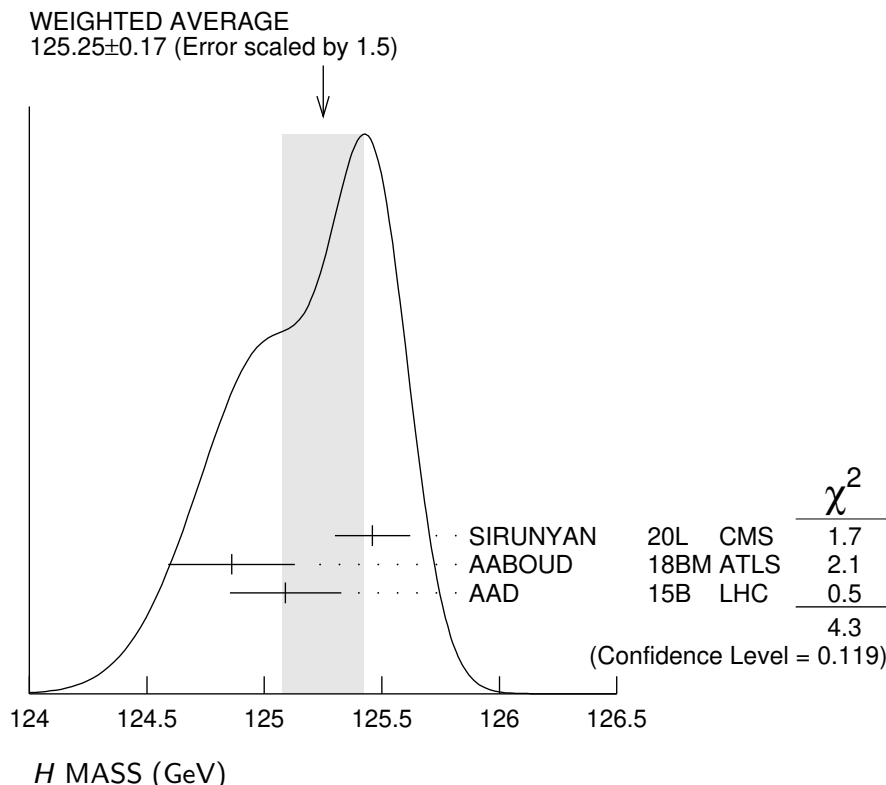
In the following H refers to the signal that has been discovered in the Higgs searches. Whereas the observed signal is labeled as a spin 0 particle and is called a Higgs Boson, the detailed properties of H and its role in the context of electroweak symmetry breaking need to be further clarified. These issues are addressed by the measurements listed below.

Concerning mass limits and cross section limits that have been obtained in the searches for neutral and charged Higgs bosons, see the sections “Searches for Neutral Higgs Bosons” and “Searches for Charged Higgs Bosons (H^\pm and $H^{\pm\pm}$)”, respectively.

H MASS

VALUE (GeV)	DOCUMENT ID	TECN	COMMENT
125.25±0.17 OUR AVERAGE			Error includes scale factor of 1.5. See the ideogram below.
125.46±0.16	¹ SIRUNYAN	20L CMS	$p p$, 13 TeV, $\gamma\gamma$, $Z Z^* \rightarrow 4\ell$
124.86±0.27	² AABOUD	18BMATLS	$p p$, 13 TeV, $\gamma\gamma$, $Z Z^* \rightarrow 4\ell$
125.09±0.21±0.11	^{2,3} AAD	15B LHC	$p p$, 7, 8 TeV
• • • We do not use the following data for averages, fits, limits, etc. • • •			
125.78±0.26	⁴ SIRUNYAN	20L CMS	$p p$, 13 TeV, $\gamma\gamma$
125.38±0.14	⁵ SIRUNYAN	20L CMS	$p p$, 7, 8, 13 TeV, $\gamma\gamma$, $Z Z^* \rightarrow 4\ell$
124.79±0.37	⁶ AABOUD	18BMATLS	$p p$, 13 TeV, $Z Z^* \rightarrow 4\ell$
124.93±0.40	⁷ AABOUD	18BMATLS	$p p$, 13 TeV, $\gamma\gamma$
124.97±0.24	^{2,8} AABOUD	18BMATLS	$p p$, 7, 8, 13 TeV, $\gamma\gamma$, $Z Z^* \rightarrow 4\ell$
125.26±0.20±0.08	⁹ SIRUNYAN	17AV CMS	$p p$, 13 TeV, $Z Z^* \rightarrow 4\ell$
125.07±0.25±0.14	³ AAD	15B LHC	$p p$, 7, 8 TeV, $\gamma\gamma$
125.15±0.37±0.15	³ AAD	15B LHC	$p p$, 7, 8 TeV, $Z Z^* \rightarrow 4\ell$
126.02±0.43±0.27	¹⁰ AAD	15B ATLS	$p p$, 7, 8 TeV, $\gamma\gamma$
124.51±0.52±0.04	¹⁰ AAD	15B ATLS	$p p$, 7, 8 TeV, $Z Z^* \rightarrow 4\ell$
125.59±0.42±0.17	¹⁰ AAD	15B CMS	$p p$, 7, 8 TeV, $Z Z^* \rightarrow 4\ell$
125.02 ^{+0.26} _{-0.27} ^{+0.14} _{-0.15}	¹⁰ KHACHATRY...	15AMCMS	$p p$, 7, 8 TeV
125.36±0.37±0.18	^{2,11} AAD	14W ATLS	$p p$, 7, 8 TeV
125.98±0.42±0.28	¹¹ AAD	14W ATLS	$p p$, 7, 8 TeV, $\gamma\gamma$
124.51±0.52±0.06	¹¹ AAD	14W ATLS	$p p$, 7, 8 TeV, $Z Z^* \rightarrow 4\ell$
125.6 ± 0.4 ± 0.2	¹² CHATRCHYAN	14AA CMS	$p p$, 7, 8 TeV, $Z Z^* \rightarrow 4\ell$
122 ± 7	¹³ CHATRCHYAN	14K CMS	$p p$, 7, 8 TeV, $\tau\tau$
124.70±0.31±0.15	¹⁴ KHACHATRY...	14P CMS	$p p$, 7, 8 TeV, $\gamma\gamma$
125.5 ± 0.2 ± 0.5	^{2,15} AAD	13AK ATLS	$p p$, 7, 8 TeV
126.8 ± 0.2 ± 0.7	¹⁵ AAD	13AK ATLS	$p p$, 7, 8 TeV, $\gamma\gamma$
124.3 ^{+0.6} _{-0.5} ^{+0.5} _{-0.3}	¹⁵ AAD	13AK ATLS	$p p$, 7, 8 TeV, $Z Z^* \rightarrow 4\ell$

$125.8 \pm 0.4 \pm 0.4$	^{2,16}	CHATRCHYAN 13J	CMS	$p\bar{p}$, 7, 8 TeV
$126.2 \pm 0.6 \pm 0.2$	¹⁶	CHATRCHYAN 13J	CMS	$p\bar{p}$, 7, 8 TeV, $ZZ^* \rightarrow 4\ell$
$126.0 \pm 0.4 \pm 0.4$	^{2,17}	AAD	12AI ATLAS	$p\bar{p}$, 7, 8 TeV
$125.3 \pm 0.4 \pm 0.5$	^{2,18}	CHATRCHYAN 12N	CMS	$p\bar{p}$, 7, 8 TeV



¹ SIRUNYAN 20L result of $H \rightarrow \gamma\gamma$ is combined with that of $H \rightarrow ZZ^* \rightarrow 4\ell$ where $\ell = e, \mu$ (SIRUNYAN 17AV).

² Combined value from $\gamma\gamma$ and $ZZ^* \rightarrow 4\ell$ final states.

³ ATLAS and CMS data are fitted simultaneously.

⁴ SIRUNYAN 20L use 35.9 fb^{-1} of $p\bar{p}$ collisions at $E_{\text{cm}} = 13 \text{ TeV}$ with $H \rightarrow \gamma\gamma$.

⁵ SIRUNYAN 20L combine 13 TeV results with 7 and 8 TeV results (KHACHATRYAN 15AM).

⁶ AABOUD 18BM use 36.1 fb^{-1} of $p\bar{p}$ collisions at $E_{\text{cm}} = 13 \text{ TeV}$ with $H \rightarrow ZZ^* \rightarrow 4\ell$ where $\ell = e, \mu$.

⁷ AABOUD 18BM use 36.1 fb^{-1} of $p\bar{p}$ collisions at $E_{\text{cm}} = 13 \text{ TeV}$ with $H \rightarrow \gamma\gamma$.

⁸ AABOUD 18BM combine 13 TeV results with 7 and 8 TeV results. Other combined results are summarized in their Fig. 4.

⁹ SIRUNYAN 17AV use 35.9 fb^{-1} of $p\bar{p}$ collisions at $E_{\text{cm}} = 13 \text{ TeV}$ with $H \rightarrow ZZ^* \rightarrow 4\ell$ where $\ell = e, \mu$.

¹⁰ KHACHATRYAN 15AM use up to 5.1 fb^{-1} of $p\bar{p}$ collisions at $E_{\text{cm}} = 7 \text{ TeV}$ and up to 19.7 fb^{-1} at $E_{\text{cm}} = 8 \text{ TeV}$.

¹¹ AAD 14W use 4.5 fb^{-1} of $p\bar{p}$ collisions at $E_{\text{cm}} = 7 \text{ TeV}$ and 20.3 fb^{-1} at 8 TeV .

¹² CHATRCHYAN 14AA use 5.1 fb^{-1} of $p\bar{p}$ collisions at $E_{\text{cm}} = 7 \text{ TeV}$ and 19.7 fb^{-1} at $E_{\text{cm}} = 8 \text{ TeV}$.

¹³ CHATRCHYAN 14K use 4.9 fb^{-1} of $p\bar{p}$ collisions at $E_{\text{cm}} = 7 \text{ TeV}$ and 19.7 fb^{-1} at $E_{\text{cm}} = 8 \text{ TeV}$.

- ¹⁴ KHACHATRYAN 14P use 5.1 fb^{-1} of pp collisions at $E_{\text{cm}} = 7 \text{ TeV}$ and 19.7 fb^{-1} at $E_{\text{cm}} = 8 \text{ TeV}$.
- ¹⁵ AAD 13AK use 4.7 fb^{-1} of pp collisions at $E_{\text{cm}} = 7 \text{ TeV}$ and 20.7 fb^{-1} at $E_{\text{cm}} = 8 \text{ TeV}$. Superseded by AAD 14W.
- ¹⁶ CHATRCHYAN 13J use 5.1 fb^{-1} of pp collisions at $E_{\text{cm}} = 7 \text{ TeV}$ and 12.2 fb^{-1} at $E_{\text{cm}} = 8 \text{ TeV}$.
- ¹⁷ AAD 12AI obtain results based on $4.6\text{--}4.8 \text{ fb}^{-1}$ of pp collisions at $E_{\text{cm}} = 7 \text{ TeV}$ and $5.8\text{--}5.9 \text{ fb}^{-1}$ at $E_{\text{cm}} = 8 \text{ TeV}$. An excess of events over background with a local significance of 5.9σ is observed at $m_H = 126 \text{ GeV}$. See also AAD 12DA.
- ¹⁸ CHATRCHYAN 12N obtain results based on $4.9\text{--}5.1 \text{ fb}^{-1}$ of pp collisions at $E_{\text{cm}} = 7 \text{ TeV}$ and $5.1\text{--}5.3 \text{ fb}^{-1}$ at $E_{\text{cm}} = 8 \text{ TeV}$. An excess of events over background with a local significance of 5.0σ is observed at about $m_H = 125 \text{ GeV}$. See also CHATRCHYAN 12BY and CHATRCHYAN 13Y.
-

H SPIN AND CP PROPERTIES

The observation of the signal in the $\gamma\gamma$ final state rules out the possibility that the discovered particle has spin 1, as a consequence of the Landau-Yang theorem. This argument relies on the assumptions that the decaying particle is an on-shell resonance and that the decay products are indeed two photons rather than two pairs of boosted photons, which each could in principle be misidentified as a single photon.

Concerning distinguishing the spin 0 hypothesis from a spin 2 hypothesis, some care has to be taken in modelling the latter in order to ensure that the discriminating power is actually based on the spin properties rather than on unphysical behavior that may affect the model of the spin 2 state.

Under the assumption that the observed signal consists of a single state rather than an overlap of more than one resonance, it is sufficient to discriminate between distinct hypotheses in the spin analyses. On the other hand, the determination of the CP properties is in general much more difficult since in principle the observed state could consist of any admixture of CP -even and CP -odd components. As a first step, the compatibility of the data with distinct hypotheses of pure CP -even and pure CP -odd states with different spin assignments has been investigated. In order to treat the case of a possible mixing of different CP states, certain cross section ratios are considered. Those cross section ratios need to be distinguished from the amount of mixing between a CP -even and a CP -odd state, as the cross section ratios depend in addition also on the coupling strengths of the CP -even and CP -odd components to the involved particles. A small relative coupling implies a small sensitivity of the corresponding cross section ratio to effects of CP mixing.

VALUE	DOCUMENT ID	TECN	COMMENT
• • • We do not use the following data for averages, fits, limits, etc. • • •			
¹ AAD	22V ATLS	WW^* ($\rightarrow e\nu\mu\nu$)+2j, 13 TeV	
² TUMASYAN	22Y CMS	$H \rightarrow \tau\tau$, 13 TeV	
³ AAD	20N ATLS	$H \rightarrow \tau\tau$, VBF, 13 TeV	
⁴ AAD	20Z ATLS	$t\bar{t}H$, $H \rightarrow \gamma\gamma$, 13 TeV	
⁵ SIRUNYAN	20AS CMS	$t\bar{t}H$, $H \rightarrow \gamma\gamma$, 13 TeV	
⁶ SIRUNYAN	19BL CMS	pp , 7, 8, 13 TeV, $ZZ^*/ZZ \rightarrow 4\ell$	
⁷ SIRUNYAN	19BZ CMS	$pp \rightarrow H+2\text{jets}$ (VBF, ggF, VH), $H \rightarrow \tau\tau$, 13 TeV	
⁸ AABOUD	18AJ ATLS	$H \rightarrow ZZ^* \rightarrow 4\ell$ ($\ell = e, \mu$), 13TeV	
⁹ SIRUNYAN	17AM CMS	$pp \rightarrow H+2j$, $H \rightarrow 4\ell$ ($\ell = e, \mu$)	

10 AAD	16 ATLS	$H \rightarrow \gamma\gamma$
11 AAD	16BL ATLS	$pp \rightarrow HjjX$ (VBF), $H \rightarrow \tau\tau$, 8 TeV
12 KHACHATRY...	16AB CMS	$pp \rightarrow WH, ZH, H \rightarrow b\bar{b}$, 8 TeV
13 AAD	15AX ATLS	$H \rightarrow WW^*$
14 AAD	15CI ATLS	$H \rightarrow ZZ^*, WW^*, \gamma\gamma$
15 AALTONEN	15 TEVA	$p\bar{p} \rightarrow WH, ZH, H \rightarrow b\bar{b}$
16 AALTONEN	15B CDF	$p\bar{p} \rightarrow WH, ZH, H \rightarrow b\bar{b}$
17 KHACHATRY...	15Y CMS	$H \rightarrow 4\ell, WW^*, \gamma\gamma$
18 ABAZOV	14F D0	$p\bar{p} \rightarrow WH, ZH, H \rightarrow b\bar{b}$
19 CHATRCHYAN 14AA	CMS	$H \rightarrow ZZ^*$
20 CHATRCHYAN 14G	CMS	$H \rightarrow WW^*$
21 KHACHATRY...	14P CMS	$H \rightarrow \gamma\gamma$
22 AAD	13AJ ATLS	$H \rightarrow \gamma\gamma, ZZ^* \rightarrow 4\ell, WW^* \rightarrow \ell\nu\ell\nu$
23 CHATRCHYAN 13J	CMS	$H \rightarrow ZZ^* \rightarrow 4\ell$

¹ AAD 22V measure the CP properties of the effective Higgs-gluon interaction using gluon fusion $H \rightarrow WW^* \rightarrow e\nu\mu\nu$ plus two jets with 36.1 fb^{-1} of data at $E_{\text{cm}} = 13 \text{ TeV}$. The measured tangent of the CP -mixing angle $\tan\alpha$ is $0.0 \pm 0.4 \pm 0.3$ assuming the standard model HVV couplings. See their Fig. 6.

² TUMASYAN 22Y measure the CP structure of the τ Yukawa coupling using 137 fb^{-1} of data at $E_{\text{cm}} = 13 \text{ TeV}$. The CP -mixing angle α for τ Yukawa coupling is measured to be $-1 \pm 19^\circ$. The data disfavour the pure CP -odd ($\alpha = 90^\circ$) at 3.0σ .

³ AAD 20N test CP invariance in H production via VBF using $H \rightarrow \tau\tau$ decay channel with 36.1 fb^{-1} at $E_{\text{cm}} = 13 \text{ TeV}$. By using the Optimal Observable method, the data constrain a parameter \tilde{d} , which is for the strength of CP violation in an effective field theory, to be $-0.090 \leq \tilde{d} \leq 0.035$ at 68% CL (see their Fig. 6).

⁴ AAD 20Z exclude a CP -mixing angle α , $|\alpha| > 43^\circ$ at 95% CL, where $\alpha = 0$ represents the Standard Model, in 139 fb^{-1} of data at $E_{\text{cm}} = 13 \text{ TeV}$. The pure CP -odd structure of the top Yukawa coupling ($\alpha = 90^\circ$) is excluded at 3.9σ .

⁵ SIRUNYAN 20AS exclude the pure CP -odd structure of the top Yukawa coupling at 3.2σ using $t\bar{t}H$, $H \rightarrow \gamma\gamma$ in 137 fb^{-1} of data at $E_{\text{cm}} = 13 \text{ TeV}$. The fractional contribution of the CP -odd component $f_{CP}^{t\bar{t}H}$ is measured to be 0.00 ± 0.33 .

⁶ SIRUNYAN 19BL measure the anomalous HVV couplings from on-shell and off-shell production in the 4ℓ final state. Data of 80.2 fb^{-1} at 13 TeV , 19.7 fb^{-1} at 8 TeV , and 5.1 fb^{-1} at 7 TeV are used. See their Tables VI and VII for anomalous HVV couplings of CP -violating and CP -conserving parameters with on- and off-shells.

⁷ SIRUNYAN 19BZ constrain anomalous HVV couplings of the Higgs boson with data of 35.9 fb^{-1} at $E_{\text{cm}} = 13 \text{ TeV}$ using Higgs boson candidates with two jets produced in VBF, ggF , and VH that decay to $\tau\tau$. See their Table 2 and Fig. 10, which show 68% CL and 95% CL intervals. Combining those with the $H \rightarrow 4\ell$ (SIRUNYAN 19BL, on-shell scenario), results shown in their Tables 3, 4, and Fig. 11 are obtained. A CP -violating parameter is set to be $f_{a3}\cos(\phi_{a3}) = (0.00 \pm 0.27) \times 10^{-3}$ and CP -conserving parameters are $f_{a2}\cos(\phi_{a2}) = (0.08 \pm 1.04) \times 10^{-3}$, $f_{\Lambda 1}\cos(\phi_{\Lambda 1}) = (0.00 \pm 0.53) \times 10^{-3}$, and $f_{\Lambda 1}^{Z\gamma}\cos(\phi_{\Lambda 1}^{Z\gamma}) = (0.0 \pm 1.1) \times 10^{-3}$.

⁸ AABOUD 18AJ study the tensor structure of the Higgs boson couplings using an effective Lagrangian using 36.1 fb^{-1} of pp collision data at $E_{\text{cm}} = 13 \text{ TeV}$. Constraints are set on the non-Standard-Model CP -even and CP -odd couplings to Z bosons and on the CP -odd coupling to gluons. See their Figs. 9 and 10, and Tables 10 and 11.

⁹ SIRUNYAN 17AM constrain anomalous couplings of the Higgs boson with 5.1 fb^{-1} of pp collisions at $E_{\text{cm}} = 7 \text{ TeV}$, 19.7 fb^{-1} at $E_{\text{cm}} = 8 \text{ TeV}$, and 38.6 fb^{-1} at $E_{\text{cm}} = 13 \text{ TeV}$. See their Table 3 and Fig. 3, which show 68% CL and 95% CL intervals. A CP

- violation parameter f_{a3} is set to be $f_{a3}\cos(\phi_{a3}) = [-0.38, 0.46]$ at 95% CL ($\phi_{a3} = 0$ or π).
- 10 AAD 16 study $H \rightarrow \gamma\gamma$ with an effective Lagrangian including CP even and odd terms in 20.3 fb^{-1} of pp collisions at $E_{\text{cm}} = 8 \text{ TeV}$. The data is consistent with the expectations for the Higgs boson of the Standard Model. Limits on anomalous couplings are also given.
 - 11 AAD 16BL study VBF $H \rightarrow \tau\tau$ with an effective Lagrangian including a CP odd term in 20.3 fb^{-1} of pp collisions at $E_{\text{cm}} = 8 \text{ TeV}$. The measurement is consistent with the expectation of the Standard Model. The CP -mixing parameter \tilde{d} (a dimensionless coupling $\tilde{d} = -(m_W^2/\Lambda^2)f_{WW}$) is constrained to the interval of $(-0.11, 0.05)$ at 68% CL under the assumption of $\tilde{d} = \tilde{d}_B$.
 - 12 KHACHATRYAN 16AB search for anomalous pseudoscalar couplings of the Higgs boson to W and Z with 18.9 fb^{-1} of pp collisions at $E_{\text{cm}} = 8 \text{ TeV}$. See their Table 5 and Figs 5 and 6 for limits on possible anomalous pseudoscalar coupling parameters.
 - 13 AAD 15AX compare the $J^{CP}=0^+$ Standard Model assignment with other J^{CP} hypotheses in 20.3 fb^{-1} of pp collisions at $E_{\text{cm}} = 8 \text{ TeV}$, using the process $H \rightarrow WW^* \rightarrow e\nu\mu\nu$. 2^+ hypotheses are excluded at 84.5–99.4%CL, 0^- at 96.5%CL, 0^+ (field strength coupling) at 70.8%CL. See their Fig. 19 for limits on possible CP mixture parameters.
 - 14 AAD 15CI compare the $J^{CP}=0^+$ Standard Model assignment with other J^{CP} hypotheses in 4.5 fb^{-1} of pp collisions at $E_{\text{cm}} = 7 \text{ TeV}$ and 20.3 fb^{-1} at $E_{\text{cm}} = 8 \text{ TeV}$, using the processes $H \rightarrow ZZ^* \rightarrow 4\ell$, $H \rightarrow \gamma\gamma$ and combine with AAD 15AX data. 0^+ (field strength coupling), 0^- and several 2^+ hypotheses are excluded at more than 99.9% CL. See their Tables 7–9 for limits on possible CP mixture parameters.
 - 15 AALTONEN 15 combine AALTONEN 15B and ABAZOV 14F data. An upper limit of 0.36 of the Standard Model production rate at 95% CL is obtained both for a 0^- and a 2^+ state. Assuming the SM event rate, the $J^{CP}=0^-$ (2^+) hypothesis is excluded at the 5.0σ (4.9σ) level.
 - 16 AALTONEN 15B compare the $J^{CP}=0^+$ Standard Model assignment with other J^{CP} hypotheses in 9.45 fb^{-1} of $p\bar{p}$ collisions at $E_{\text{cm}} = 1.96 \text{ TeV}$, using the processes $ZH \rightarrow \ell\ell b\bar{b}$, $WH \rightarrow \ell\nu b\bar{b}$, and $ZH \rightarrow \nu\nu b\bar{b}$. Bounds on the production rates of 0^- and 2^+ (graviton-like) states are set, see their tables II and III.
 - 17 KHACHATRYAN 15Y compare the $J^{CP}=0^+$ Standard Model assignment with other J^{CP} hypotheses in up to 5.1 fb^{-1} of pp collisions at $E_{\text{cm}} = 7 \text{ TeV}$ and up to 19.7 fb^{-1} at $E_{\text{cm}} = 8 \text{ TeV}$, using the processes $H \rightarrow 4\ell$, $H \rightarrow WW^*$, and $H \rightarrow \gamma\gamma$. 0^- is excluded at 99.98% CL, and several 2^+ hypotheses are excluded at more than 99% CL. Spin 1 models are excluded at more than 99.999% CL in ZZ^* and WW^* modes. Limits on anomalous couplings and several cross section fractions, treating the case of CP -mixed states, are also given.
 - 18 ABAZOV 14F compare the $J^{CP}=0^+$ Standard Model assignment with $J^{CP}=0^-$ and 2^+ (graviton-like coupling) hypotheses in up to 9.7 fb^{-1} of $p\bar{p}$ collisions at $E_{\text{cm}} = 1.96 \text{ TeV}$. They use kinematic correlations between the decay products of the vector boson and the Higgs boson in the final states $ZH \rightarrow \ell\ell b\bar{b}$, $WH \rightarrow \ell\nu b\bar{b}$, and $ZH \rightarrow \nu\nu b\bar{b}$. The 0^- (2^+) hypothesis is excluded at 97.6% CL (99.0% CL). In order to treat the case of a possible mixture of a 0^+ state with another J^{CP} state, the cross section fractions $f_X = \sigma_X / (\sigma_{0^+} + \sigma_X)$ are considered, where $X = 0^-, 2^+$. Values for f_{0^-} (f_{2^+}) above 0.80 (0.67) are excluded at 95% CL under the assumption that the total cross section is that of the SM Higgs boson.
 - 19 CHATRCHYAN 14AA compare the $J^{CP}=0^+$ Standard Model assignment with various J^{CP} hypotheses in 5.1 fb^{-1} of pp collisions at $E_{\text{cm}} = 7 \text{ TeV}$ and 19.7 fb^{-1} at $E_{\text{cm}} = 8 \text{ TeV}$. $J^{CP}=0^-$ and 1^\pm hypotheses are excluded at 99% CL, and several $J=2$

hypotheses are excluded at 95% CL. In order to treat the case of a possible mixture of a 0^+ state with another JCP state, the cross section fraction $f_{a3} = |a_3|^2 \sigma_3 / (|a_1|^2 \sigma_1 + |a_2|^2 \sigma_2 + |a_3|^2 \sigma_3)$ is considered, where the case $a_3 = 1, a_1 = a_2 = 0$ corresponds to a pure CP -odd state. Assuming $a_2 = 0$, a value for f_{a3} above 0.51 is excluded at 95% CL.

- 20 CHATRCHYAN 14G compare the $JCP = 0^+$ Standard Model assignment with $JCP = 0^-$ and 2^+ (graviton-like coupling) hypotheses in 4.9 fb^{-1} of pp collisions at $E_{\text{cm}} = 7 \text{ TeV}$ and 19.4 fb^{-1} at $E_{\text{cm}} = 8 \text{ TeV}$. Varying the fraction of the production of the 2^+ state via gg and $q\bar{q}$, 2^+ hypotheses are disfavored at CL between 83.7 and 99.8%. The 0^- hypothesis is disfavored against 0^+ at the 65.3% CL.
- 21 KHACHATRYAN 14P compare the $JCP = 0^+$ Standard Model assignment with a 2^+ (graviton-like coupling) hypothesis in 5.1 fb^{-1} of pp collisions at $E_{\text{cm}} = 7 \text{ TeV}$ and 19.7 fb^{-1} at $E_{\text{cm}} = 8 \text{ TeV}$. Varying the fraction of the production of the 2^+ state via gg and $q\bar{q}$, 2^+ hypotheses are disfavored at CL between 71 and 94%.
- 22 AAD 13AJ compare the spin 0, CP -even hypothesis with specific alternative hypotheses of spin 0, CP -odd, spin 1, CP -even and CP -odd, and spin 2, CP -even models using the Higgs boson decays $H \rightarrow \gamma\gamma$, $H \rightarrow ZZ^* \rightarrow 4\ell$ and $H \rightarrow WW^* \rightarrow \ell\nu\ell\nu$ and combinations thereof. The data are compatible with the spin 0, CP -even hypothesis, while all other tested hypotheses are excluded at confidence levels above 97.8%.
- 23 CHATRCHYAN 13J study angular distributions of the lepton pairs in the ZZ^* channel where both Z bosons decay to e or μ pairs. Under the assumption that the observed particle has spin 0, the data are found to be consistent with the pure CP -even hypothesis, while the pure CP -odd hypothesis is disfavored.

H DECAY WIDTH

The total decay width for a light Higgs boson with a mass in the observed range is not expected to be directly observable at the LHC. For the case of the Standard Model the prediction for the total width is about 4 MeV, which is three orders of magnitude smaller than the experimental mass resolution. There is no indication from the results observed so far that the natural width is broadened by new physics effects to such an extent that it could be directly observable. Furthermore, as all LHC Higgs channels rely on the identification of Higgs decay products, the total Higgs width cannot be measured indirectly without additional assumptions. The different dependence of on-peak and off-peak contributions on the total width in Higgs decays to ZZ^* and interference effects between signal and background in Higgs decays to $\gamma\gamma$ can provide additional information in this context. Constraints on the total width from the combination of on-peak and off-peak contributions in Higgs decays to ZZ^* rely on the assumption of equal on- and off-shell effective couplings. Without an experimental determination of the total width or further theoretical assumptions, only ratios of couplings can be determined at the LHC rather than absolute values of couplings.

VALUE (MeV)	CL%	DOCUMENT ID	TECN	COMMENT
3.2^{+2.4} -1.7		¹ TUMASYAN	22AMCMS	$pp, 13 \text{ TeV}, ZZ^*/ZZ \rightarrow 4\ell, ZZ \rightarrow 2\ell 2\nu$
• • • We do not use the following data for averages, fits, limits, etc. • • •				
$3.2^{+2.8}_{-2.2}$		² SIRUNYAN	19BL CMS	$pp, 7, 8, 13 \text{ TeV}, ZZ^*/ZZ \rightarrow 4\ell$
< 14.4	95	³ AABOUD	18BP ATLS	$pp, 13 \text{ TeV}, ZZ \rightarrow 4\ell, 2\ell 2\nu$
< 1100	95	⁴ SIRUNYAN	17AV CMS	$pp, 13 \text{ TeV}, ZZ^* \rightarrow 4\ell$
< 26	95	⁵ KHACHATRYAN	16BA CMS	$pp, 7, 8 \text{ TeV}, WW^{(*)}$

< 13	95	⁶ KHACHATRYAN 16BA CMS	$pp, 7, 8 \text{ TeV}, ZZ^{(*)}, WW^{(*)}$
< 22.7	95	⁷ AAD 15BE ATLAS	$pp, 8 \text{ TeV}, ZZ^{(*)}, WW^{(*)}$
< 1700	95	⁸ KHACHATRYAN 15AM CMS	$pp, 7, 8 \text{ TeV}$
$> 3.5 \times 10^{-9}$	95	⁹ KHACHATRYAN 15BA CMS	$pp, 7, 8 \text{ TeV}, \text{flight distance}$
< 46	95	¹⁰ KHACHATRYAN 15BA CMS	$pp, 7, 8 \text{ TeV}, ZZ^{(*)} \rightarrow 4\ell$
< 5000	95	¹¹ AAD 14W ATLAS	$pp, 7, 8 \text{ TeV}, \gamma\gamma$
< 2600	95	¹¹ AAD 14W ATLAS	$pp, 7, 8 \text{ TeV}, ZZ^* \rightarrow 4\ell$
< 3400	95	¹² CHATRCHYAN 14AA CMS	$pp, 7, 8 \text{ TeV}, ZZ^* \rightarrow 4\ell$
< 22	95	¹³ KHACHATRYAN 14D CMS	$pp, 7, 8 \text{ TeV}, ZZ^{(*)}$
< 2400	95	¹⁴ KHACHATRYAN 14P CMS	$pp, 7, 8 \text{ TeV}, \gamma\gamma$

¹ TUMASYAN 22AM use up to 140 fb^{-1} at $E_{\text{cm}} = 13 \text{ TeV}$. The off-shell Higgs boson production in the $ZZ \rightarrow 4\ell$ and $ZZ \rightarrow 2\ell 2\nu$ decay channels and the on-shell production in the $ZZ^* \rightarrow 4\ell$ ($\ell = e, \mu$) decay channels are used to measure the total width. The off-shell Higgs signal strength is measured to be $0.62^{+0.68}_{-0.45}$ without the constraint on the ratio of the off-shell signal strengths for gluon-fusion and gauge-boson modes. The scenario of no off-shell contribution is excluded at 3.6σ . The results are shown in their Table 1 with other constraint scenarios and the decay widths assuming the same coupling modifiers for on- and off-shell couplings (g_p and g_d in their notation). The measurement of anomalous HVV couplings is shown in their Extended Data Table 1 and Fig. 8.

² SIRUNYAN 19BL measure the width and anomalous HVV couplings from on-shell and off-shell production in the 4ℓ final state. Data of 80.2 fb^{-1} at 13 TeV , 19.7 fb^{-1} at 8 TeV , and 5.1 fb^{-1} at 7 TeV are used. The total width for the SM-like couplings is measured to be also [0.08, 9.16] MeV with 95% CL, assuming SM-like couplings for on- and off-shells (see their Table VIII). Constraints on the total width for anomalous HVV interaction cases are found in their Table IX. See their Table X for the Higgs boson signal strength in the off-shell region.

³ AABOUD 18BP use 36.1 fb^{-1} at $E_{\text{cm}} = 13 \text{ TeV}$. An observed upper limit on the off-shell Higgs signal strength of 3.8 is obtained at 95% CL using off-shell Higgs boson production in the $ZZ \rightarrow 4\ell$ and $ZZ \rightarrow 2\ell 2\nu$ decay channels ($\ell = e, \mu$). Combining with the on-shell signal strength measurements, the quoted upper limit on the Higgs boson total width is obtained, assuming the ratios of the relevant Higgs-boson couplings to the SM predictions are constant with energy from on-shell production to the high-mass range.

⁴ SIRUNYAN 17AV obtain an upper limit on the width from the $m_{4\ell}$ distribution in $ZZ^* \rightarrow 4\ell$ ($\ell = e, \mu$) decays. Data of 35.9 fb^{-1} pp collisions at $E_{\text{cm}} = 13 \text{ TeV}$ is used. The expected limit is 1.60 GeV.

⁵ KHACHATRYAN 16BA derive constraints on the total width from comparing $WW^{(*)}$ production via on-shell and off-shell H using 4.9 fb^{-1} of pp collisions at $E_{\text{cm}} = 7 \text{ TeV}$ and 19.4 fb^{-1} at 8 TeV .

⁶ KHACHATRYAN 16BA combine the $WW^{(*)}$ result with $ZZ^{(*)}$ results of KHACHATRYAN 15BA and KHACHATRYAN 14D.

⁷ AAD 15BE derive constraints on the total width from comparing $ZZ^{(*)}$ and $WW^{(*)}$ production via on-shell and off-shell H using 20.3 fb^{-1} of pp collisions at $E_{\text{cm}} = 8 \text{ TeV}$. The K factor for the background processes is assumed to be equal to that for the signal.

⁸ KHACHATRYAN 15AM combine $\gamma\gamma$ and $ZZ^* \rightarrow 4\ell$ results. The expected limit is 2.3 GeV.

⁹ KHACHATRYAN 15BA derive a lower limit on the total width from an upper limit on the decay flight distance $\tau < 1.9 \times 10^{-13} \text{ s}$. 5.1 fb^{-1} of pp collisions at $E_{\text{cm}} = 7 \text{ TeV}$ and 19.7 fb^{-1} at 8 TeV are used.

¹⁰ KHACHATRYAN 15BA derive constraints on the total width from comparing $ZZ^{(*)}$ production via on-shell and off-shell H with an unconstrained anomalous coupling. 4ℓ final states in 5.1 fb^{-1} of pp collisions at $E_{\text{cm}} = 7 \text{ TeV}$ and 19.7 fb^{-1} at $E_{\text{cm}} = 8 \text{ TeV}$ are used.

¹¹ AAD 14W use 4.5 fb^{-1} of pp collisions at $E_{\text{cm}} = 7 \text{ TeV}$ and 20.3 fb^{-1} at 8 TeV . The expected limit is 6.2 GeV .

¹² CHATRCHYAN 14AA use 5.1 fb^{-1} of pp collisions at $E_{\text{cm}} = 7 \text{ TeV}$ and 19.7 fb^{-1} at $E_{\text{cm}} = 8 \text{ TeV}$. The expected limit is 2.8 GeV .

¹³ KHACHATRYAN 14D derive constraints on the total width from comparing $ZZ^{(*)}$ production via on-shell and off-shell H . 4ℓ and $\ell\ell\nu\nu$ final states in 5.1 fb^{-1} of pp collisions at $E_{\text{cm}} = 7 \text{ TeV}$ and 19.7 fb^{-1} at $E_{\text{cm}} = 8 \text{ TeV}$ are used.

¹⁴ KHACHATRYAN 14P use 5.1 fb^{-1} of pp collisions at $E_{\text{cm}} = 7 \text{ TeV}$ and 19.7 fb^{-1} at $E_{\text{cm}} = 8 \text{ TeV}$. The expected limit is 3.1 GeV .

***H* DECAY MODES**

Mode	Fraction (Γ_i/Γ)	Confidence level
Γ_1 WW^*	$(25.7 \pm 2.5) \%$	
Γ_2 ZZ^*	$(2.80 \pm 0.30) \%$	
Γ_3 $\gamma\gamma$	$(2.50 \pm 0.20) \times 10^{-3}$	
Γ_4 $b\bar{b}$	$(53 \pm 8) \%$	
Γ_5 e^+e^-	$< 3.6 \times 10^{-4}$	95%
Γ_6 $\mu^+\mu^-$	$(2.6 \pm 1.3) \times 10^{-4}$	
Γ_7 $\tau^+\tau^-$	$(6.0 \pm 0.8) \%$	
Γ_8 $Z\gamma$	$(3.2 \pm 1.5) \times 10^{-3}$	
Γ_9 $Z\rho(770)$	$< 1.21 \%$	95%
Γ_{10} $Z\phi(1020)$	$< 3.6 \times 10^{-3}$	95%
Γ_{11} $Z\eta_c$		
Γ_{12} ZJ/ψ		
Γ_{13} $J/\psi\gamma$	$< 3.5 \times 10^{-4}$	95%
Γ_{14} $J/\psi J/\psi$	$< 1.8 \times 10^{-3}$	95%
Γ_{15} $\psi(2S)\gamma$	$< 2.0 \times 10^{-3}$	95%
Γ_{16} $\Upsilon(1S)\gamma$	$< 4.9 \times 10^{-4}$	95%
Γ_{17} $\Upsilon(2S)\gamma$	$< 5.9 \times 10^{-4}$	95%
Γ_{18} $\Upsilon(3S)\gamma$	$< 5.7 \times 10^{-4}$	95%
Γ_{19} $\Upsilon(\text{nS})\Upsilon(\text{mS})$	$< 1.4 \times 10^{-3}$	95%
Γ_{20} $\rho(770)\gamma$	$< 8.8 \times 10^{-4}$	95%
Γ_{21} $\phi(1020)\gamma$	$< 4.8 \times 10^{-4}$	95%
Γ_{22} $e\mu$	$LF < 6.1 \times 10^{-5}$	95%
Γ_{23} $e\tau$	$LF < 2.2 \times 10^{-3}$	95%
Γ_{24} $\mu\tau$	$LF < 1.5 \times 10^{-3}$	95%
Γ_{25} invisible	$< 13 \%$	95%
Γ_{26} γ invisible	$< 2.9 \%$	95%

H BRANCHING RATIOS **$\Gamma(WW^*)/\Gamma_{\text{total}}$**

VALUE	DOCUMENT ID	TECN	COMMENT	Γ_1/Γ
$0.257^{+0.026}_{-0.024}$	¹ ATLAS 22	ATLS	$pp, 13 \text{ TeV}$	

¹ ATLAS 22 report combined results (see their Extended Data Table 1) using up to 139 fb^{-1} of data at $E_{\text{cm}} = 13 \text{ TeV}$, assuming $m_H = 125.09 \text{ GeV}$. SM values for the production cross-sections are assumed. See their Fig. 2b.

 $\Gamma(ZZ^*)/\Gamma_{\text{total}}$

VALUE	DOCUMENT ID	TECN	COMMENT	Γ_2/Γ
0.028 ± 0.003	¹ ATLAS 22	ATLS	$pp, 13 \text{ TeV}$	

¹ ATLAS 22 report combined results (see their Extended Data Table 1) using up to 139 fb^{-1} of data at $E_{\text{cm}} = 13 \text{ TeV}$, assuming $m_H = 125.09 \text{ GeV}$. SM values for the production cross-sections are assumed. See their Fig. 2b.

 $\Gamma(\gamma\gamma)/\Gamma_{\text{total}}$

VALUE	DOCUMENT ID	TECN	COMMENT	Γ_3/Γ
0.0025 ± 0.0002	¹ ATLAS 22	ATLS	$pp, 13 \text{ TeV}$	

¹ ATLAS 22 report combined results (see their Extended Data Table 1) using up to 139 fb^{-1} of data at $E_{\text{cm}} = 13 \text{ TeV}$, assuming $m_H = 125.09 \text{ GeV}$. SM values for the production cross-sections are assumed. See their Fig. 2b.

 $\Gamma(b\bar{b})/\Gamma_{\text{total}}$

VALUE	DOCUMENT ID	TECN	COMMENT	Γ_4/Γ
0.53 ± 0.08	¹ ATLAS 22	ATLS	$pp, 13 \text{ TeV}$	

¹ ATLAS 22 report combined results (see their Extended Data Table 1) using up to 139 fb^{-1} of data at $E_{\text{cm}} = 13 \text{ TeV}$, assuming $m_H = 125.09 \text{ GeV}$. SM values for the production cross-sections are assumed. See their Fig. 2b.

 $\Gamma(e^+e^-)/\Gamma_{\text{total}}$

VALUE	CL%	DOCUMENT ID	TECN	COMMENT	Γ_5/Γ
$<3.6 \times 10^{-4}$	95	¹ AAD 20F	ATLS	$pp, 13 \text{ TeV}$	

• • • We do not use the following data for averages, fits, limits, etc. • • •

$<1.9 \times 10^{-3}$	95	² KHACHATRYAN 15H	CMS	$pp, 7, 8 \text{ TeV}$
-----------------------	----	------------------------------	-----	------------------------

¹ AAD 20F use 139 fb^{-1} of pp collisions at $E_{\text{cm}} = 13 \text{ TeV}$. The best-fit value of the $H \rightarrow ee$ branching fraction is $(0.0 \pm 1.7 \pm 0.6) \times 10^{-4}$ for $m_H = 125 \text{ GeV}$.

² KHACHATRYAN 15H use 5.0 fb^{-1} of pp collisions at $E_{\text{cm}} = 7 \text{ TeV}$ and 19.7 fb^{-1} at 8 TeV.

 $\Gamma(\mu^+\mu^-)/\Gamma_{\text{total}}$

VALUE (units 10^{-4})	DOCUMENT ID	TECN	COMMENT	Γ_6/Γ
2.6 ± 1.3	¹ ATLAS 22	ATLS	$pp, 13 \text{ TeV}$	

¹ ATLAS 22 report combined results (see their Extended Data Table 1) using up to 139 fb^{-1} of data at $E_{\text{cm}} = 13 \text{ TeV}$, assuming $m_H = 125.09 \text{ GeV}$. SM values for the production cross-sections are assumed. See their Fig. 2b.

$\Gamma(\tau^+\tau^-)/\Gamma_{\text{total}}$	Γ_7/Γ		
<u>VALUE</u>	<u>DOCUMENT ID</u>	<u>TECN</u>	<u>COMMENT</u>
$0.060^{+0.008}_{-0.007}$	¹ ATLAS	22	ATLS $p p$, 13 TeV

¹ ATLAS 22 report combined results (see their Extended Data Table 1) using up to 139 fb^{-1} of data at $E_{\text{cm}} = 13$ TeV, assuming $m_H = 125.09$ GeV. SM values for the production cross-sections are assumed. See their Fig. 2b.

$\Gamma(Z\gamma)/\Gamma_{\text{total}}$	Γ_8/Γ		
<u>VALUE (units 10^{-3})</u>	<u>DOCUMENT ID</u>	<u>TECN</u>	<u>COMMENT</u>
3.2 ± 1.5	¹ ATLAS	22	ATLS $p p$, 13 TeV

¹ ATLAS 22 report combined results (see their Extended Data Table 1) using up to 139 fb^{-1} of data at $E_{\text{cm}} = 13$ TeV, assuming $m_H = 125.09$ GeV. SM values for the production cross-sections are assumed. See their Fig. 2b.

$\Gamma(Z\rho(770))/\Gamma_{\text{total}}$	Γ_9/Γ			
<u>VALUE</u>	<u>CL%</u>	<u>DOCUMENT ID</u>	<u>TECN</u>	<u>COMMENT</u>
$<1.21 \times 10^{-2}$	95	¹ SIRUNYAN	20BK CMS	$p p$, 13 TeV

¹ SIRUNYAN 20BK search for $H \rightarrow Z\rho$, $Z \rightarrow e^+e^-/\mu^+\mu^-$, $\rho \rightarrow \pi^+\pi^-$ with 137 fb^{-1} of $p p$ collision data at $E_{\text{cm}} = 13$ TeV. The quoted branching fraction is for the unpolarized decay. See their Table 3 for different polarizations.

$\Gamma(Z\phi(1020))/\Gamma_{\text{total}}$	Γ_{10}/Γ			
<u>VALUE</u>	<u>CL%</u>	<u>DOCUMENT ID</u>	<u>TECN</u>	<u>COMMENT</u>
$<3.6 \times 10^{-3}$	95	¹ SIRUNYAN	20BK CMS	$p p$, 13 TeV

¹ SIRUNYAN 20BK search for $H \rightarrow Z\phi$, $Z \rightarrow e^+e^-/\mu^+\mu^-$, $\phi \rightarrow K^+K^-$ with 137 fb^{-1} of $p p$ collision data at $E_{\text{cm}} = 13$ TeV. The quoted branching fraction is for the unpolarized decay. See their Table 4 for different polarizations.

$\Gamma(Z\eta_c)/\Gamma_{\text{total}}$	Γ_{11}/Γ		
<u>VALUE</u>	<u>DOCUMENT ID</u>	<u>TECN</u>	<u>COMMENT</u>
$\bullet \bullet \bullet$ We do not use the following data for averages, fits, limits, etc. $\bullet \bullet \bullet$			

¹ AAD 20AE ATLS $p p$, 13 TeV

¹ AAD 20AE search for $H \rightarrow Z\eta_c$ with two-leptons ($e^+e^-/\mu^+\mu^-$) plus jet events using 139 fb^{-1} of $p p$ collision data at $E_{\text{cm}} = 13$ TeV. The upper limit of $\sigma(p p \rightarrow H) \cdot B(H \rightarrow Z\eta_c)$ is 110 pb at 95% CL.

$\Gamma(ZJ/\psi)/\Gamma_{\text{total}}$	Γ_{12}/Γ		
<u>VALUE</u>	<u>DOCUMENT ID</u>	<u>TECN</u>	<u>COMMENT</u>
$\bullet \bullet \bullet$ We do not use the following data for averages, fits, limits, etc. $\bullet \bullet \bullet$			

¹ AAD 20AE ATLS $p p$, 13 TeV

¹ AAD 20AE search for $H \rightarrow ZJ/\psi$ with two-leptons ($e^+e^-/\mu^+\mu^-$) plus jet events using 139 fb^{-1} of $p p$ collision data at $E_{\text{cm}} = 13$ TeV. The upper limit of $\sigma(p p \rightarrow H) \cdot B(H \rightarrow ZJ/\psi)$ is 100 pb at 95% CL.

$\Gamma(J/\psi\gamma)/\Gamma_{\text{total}}$ Γ_{13}/Γ

VALUE	CL%	DOCUMENT ID	TECN	COMMENT
$<7.6 \times 10^{-4}$	95	¹ SIRUNYAN	19AJ CMS	13 TeV, 35.9 fb^{-1}
$<3.5 \times 10^{-4}$	95	² AABOUD	18BL ATLS	13 TeV, 36.1 fb^{-1}
$\bullet \bullet \bullet$ We do not use the following data for averages, fits, limits, etc. $\bullet \bullet \bullet$				
$<1.5 \times 10^{-3}$	95	³ KHACHATRYAN...16B	CMS	8 TeV
$<1.5 \times 10^{-3}$	95	⁴ AAD	15I ATLS	8 TeV

¹SIRUNYAN 19AJ search for $H \rightarrow J/\psi\gamma$, $J/\psi \rightarrow \mu^+ \mu^-$ with 35.9 fb^{-1} of pp collision data at $E_{\text{cm}} = 13 \text{ TeV}$. The upper limit corresponds to 260 times the SM prediction and by combining the KHACHATRYAN 16B, it is 220 times the SM prediction.

²AABOUD 18BL search for $H \rightarrow J/\psi\gamma$, $J/\psi \rightarrow \mu^+ \mu^-$ with 36.1 fb^{-1} of pp collision data at $E_{\text{cm}} = 13 \text{ TeV}$.

³KHACHATRYAN 16B use 19.7 fb^{-1} of pp collision data at 8 TeV.

⁴AAD 15I use 19.7 fb^{-1} of pp collision data at 8 TeV.

 $\Gamma(J/\psi J/\psi)/\Gamma_{\text{total}}$ Γ_{14}/Γ

VALUE	CL%	DOCUMENT ID	TECN	COMMENT
$<1.8 \times 10^{-3}$	95	¹ SIRUNYAN	19BR CMS	pp at 13 TeV

¹SIRUNYAN 19BR search for $H \rightarrow J/\psi J/\psi$, $J/\psi \rightarrow \mu^+ \mu^-$ with 37.5 fb^{-1} of pp collision data at $E_{\text{cm}} = 13 \text{ TeV}$. J/ψ s from the Higgs decay are assumed to be unpolarized. For fully longitudinal (transverse) polarized J/ψ s, limits change by -22% ($+10\%$).

 $\Gamma(\psi(2S)\gamma)/\Gamma_{\text{total}}$ Γ_{15}/Γ

VALUE	CL%	DOCUMENT ID	TECN	COMMENT
$<2.0 \times 10^{-3}$	95	¹ AABOUD	18BL ATLS	13 TeV, 36.1 fb^{-1}

¹AABOUD 18BL search for $H \rightarrow \psi(2S)\gamma$, $\psi(2S) \rightarrow \mu^+ \mu^-$ with 36.1 fb^{-1} of pp collision data at $E_{\text{cm}} = 13 \text{ TeV}$.

 $\Gamma(\Upsilon(1S)\gamma)/\Gamma_{\text{total}}$ Γ_{16}/Γ

VALUE	CL%	DOCUMENT ID	TECN	COMMENT
$<4.9 \times 10^{-4}$	95	¹ AABOUD	18BL ATLS	13 TeV, 36.1 fb^{-1}

$\bullet \bullet \bullet$ We do not use the following data for averages, fits, limits, etc. $\bullet \bullet \bullet$

$<1.3 \times 10^{-3}$ 95 ²AAD 15I ATLS 8 TeV

¹AABOUD 18BL search for $H \rightarrow \Upsilon(1S)\gamma$, $\Upsilon(1S) \rightarrow \mu^+ \mu^-$ with 36.1 fb^{-1} of pp collision data at $E_{\text{cm}} = 13 \text{ TeV}$.

²AAD 15I use 19.7 fb^{-1} of pp collision data at 8 TeV.

 $\Gamma(\Upsilon(2S)\gamma)/\Gamma_{\text{total}}$ Γ_{17}/Γ

VALUE	CL%	DOCUMENT ID	TECN	COMMENT
$<5.9 \times 10^{-4}$	95	¹ AABOUD	18BL ATLS	13 TeV, 36.1 fb^{-1}

$\bullet \bullet \bullet$ We do not use the following data for averages, fits, limits, etc. $\bullet \bullet \bullet$

$<1.9 \times 10^{-3}$ 95 ²AAD 15I ATLS 8 TeV

¹AABOUD 18BL search for $H \rightarrow \Upsilon(2S)\gamma$, $\Upsilon(2S) \rightarrow \mu^+ \mu^-$ with 36.1 fb^{-1} of pp collision data at $E_{\text{cm}} = 13 \text{ TeV}$.

²AAD 15I use 19.7 fb^{-1} of pp collision data at 8 TeV.

$\Gamma(\Upsilon(3S)\gamma)/\Gamma_{\text{total}}$ Γ_{18}/Γ

VALUE	CL%	DOCUMENT ID	TECN	COMMENT
$<5.7 \times 10^{-4}$	95	1 AABOUD	18BL ATLS	13 TeV, 36.1 fb^{-1}
$\bullet \bullet \bullet$ We do not use the following data for averages, fits, limits, etc. $\bullet \bullet \bullet$				
$<1.3 \times 10^{-3}$	95	2 AAD	15I ATLS	8 TeV
¹ AABOUD 18BL search for $H \rightarrow \Upsilon(3S)\gamma$, $\Upsilon(3S) \rightarrow \mu^+ \mu^-$ with 36.1 fb^{-1} of $p p$ collision data at $E_{\text{cm}} = 13 \text{ TeV}$.				
² AAD 15I use 19.7 fb^{-1} of $p p$ collision data at 8 TeV.				

 $\Gamma(\Upsilon(nS)\Upsilon(mS))/\Gamma_{\text{total}}$ Γ_{19}/Γ

VALUE	CL%	DOCUMENT ID	TECN	COMMENT
$<1.4 \times 10^{-3}$	95	1 SIRUNYAN	19BR CMS	$p p$ at 13 TeV
¹ SIRUNYAN 19BR search for $H \rightarrow \Upsilon(nS)\Upsilon(mS)$ with $\Upsilon(nS), \Upsilon(mS) \rightarrow \mu^+ \mu^-$ ($n, m = 1, 2, 3$) for 37.5 fb^{-1} of $p p$ collision data at $E_{\text{cm}} = 13 \text{ TeV}$. Υ s from the Higgs decay are assumed to be unpolarized. For fully longitudinal (transverse) polarized Υ s, limits change by $-22\% (+10\%)$. The three Υ states selected in a mass range of 8.5–11 GeV are not distinguished.				

 $\Gamma(\rho(770)\gamma)/\Gamma_{\text{total}}$ Γ_{20}/Γ

VALUE	CL%	DOCUMENT ID	TECN	COMMENT
$<8.8 \times 10^{-4}$	95	1 AABOUD	18AU ATLS	$p p$, 13 TeV
¹ AABOUD 18AU use 35.6 fb^{-1} of $p p$ collision data at 13 TeV.				

 $\Gamma(\phi(1020)\gamma)/\Gamma_{\text{total}}$ Γ_{21}/Γ

VALUE	CL%	DOCUMENT ID	TECN	COMMENT
$<4.8 \times 10^{-4}$	95	1 AABOUD	18AU ATLS	$p p$, 13 TeV
$\bullet \bullet \bullet$ We do not use the following data for averages, fits, limits, etc. $\bullet \bullet \bullet$				
$<1.4 \times 10^{-3}$	95	2 AABOUD	16K ATLS	$p p$, 13 TeV
¹ AABOUD 18AU use 35.6 fb^{-1} of $p p$ collision data at 13 TeV.				
² AABOUD 16K use 2.7 fb^{-1} of $p p$ collision data at 13 TeV.				

 $\Gamma(e\mu)/\Gamma_{\text{total}}$ Γ_{22}/Γ

VALUE	CL%	DOCUMENT ID	TECN	COMMENT
$<6.1 \times 10^{-5}$	95	1 AAD	20F ATLS	$p p$, 13 TeV
$\bullet \bullet \bullet$ We do not use the following data for averages, fits, limits, etc. $\bullet \bullet \bullet$				
$<3.5 \times 10^{-4}$	95	2 KHACHATRYAN...16CD CMS	$p p$, 8 TeV	
¹ AAD 20F use 139 fb^{-1} of $p p$ collisions at $E_{\text{cm}} = 13 \text{ TeV}$. The best-fit value of the $H \rightarrow e\mu$ branching fraction is $(0.4 \pm 2.9 \pm 0.3) \times 10^{-5}$ for $m_H = 125 \text{ GeV}$.				
² KHACHATRYAN 16CD search for $H \rightarrow e\mu$ in 19.7 fb^{-1} of $p p$ collisions at $E_{\text{cm}} = 8 \text{ TeV}$. The limit constrains the $Y_{e\mu}$ Yukawa coupling to $\sqrt{ Y_{e\mu} ^2 + Y_{\mu e} ^2} < 5.4 \times 10^{-4}$ at 95% CL (see their Fig. 6).				

 $\Gamma(e\tau)/\Gamma_{\text{total}}$ Γ_{23}/Γ

VALUE	CL%	DOCUMENT ID	TECN	COMMENT
$< 2.2 \times 10^{-3}$	95	1 SIRUNYAN	21Z CMS	$p p$, 13 TeV
$\bullet \bullet \bullet$ We do not use the following data for averages, fits, limits, etc. $\bullet \bullet \bullet$				
$< 4.7 \times 10^{-3}$	95	2 AAD	20A ATLS	$p p$, 13 TeV

$< 6.1 \times 10^{-3}$	95	³ SIRUNYAN	18BH CMS	$p p$, 13 TeV
$< 10.4 \times 10^{-3}$	95	⁴ AAD	17 ATLAS	$p p$, 8 TeV
$< 6.9 \times 10^{-3}$	95	⁵ KHACHATRYAN	16CD CMS	$p p$, 8 TeV

¹ SIRUNYAN 21Z search for $H \rightarrow e\tau$ in 137 fb^{-1} of $p p$ collisions at $E_{\text{cm}} = 13 \text{ TeV}$.

The limit constrains the $Y_{e\tau}$ Yukawa coupling to $\sqrt{|Y_{e\tau}|^2 + |Y_{\tau e}|^2} < 1.35 \times 10^{-3}$ at 95% CL (see their Fig. 8).

² AAD 20A search for $H \rightarrow e\tau$ in 36.1 fb^{-1} of $p p$ collisions at $E_{\text{cm}} = 13 \text{ TeV}$. The limit constrains the $Y_{e\tau}$ Yukawa coupling to $\sqrt{|Y_{e\tau}|^2 + |Y_{\tau e}|^2} < 2.0 \times 10^{-3}$ at 95% CL (see their Fig. 5).

³ SIRUNYAN 18BH search for $H \rightarrow e\tau$ in 35.9 fb^{-1} of $p p$ collisions at $E_{\text{cm}} = 13 \text{ TeV}$. The limit constrains the $Y_{e\tau}$ Yukawa coupling to $\sqrt{|Y_{e\tau}|^2 + |Y_{\tau e}|^2} < 2.26 \times 10^{-3}$ at 95% CL (see their Fig. 10).

⁴ AAD 17 search for $H \rightarrow e\tau$ in 20.3 fb^{-1} of $p p$ collisions at $E_{\text{cm}} = 8 \text{ TeV}$.

⁵ KHACHATRYAN 16CD search for $H \rightarrow e\tau$ in 19.7 fb^{-1} of $p p$ collisions at $E_{\text{cm}} = 8 \text{ TeV}$. The limit constrains the $Y_{e\tau}$ Yukawa coupling to $\sqrt{|Y_{e\tau}|^2 + |Y_{\tau e}|^2} < 2.4 \times 10^{-3}$ at 95% CL (see their Fig. 6).

$\Gamma(\mu\tau)/\Gamma_{\text{total}}$

Γ_{24}/Γ

VALUE	CL%	DOCUMENT ID	TECN	COMMENT
$< 1.5 \times 10^{-3}$	95	¹ SIRUNYAN	21Z CMS	$p p$, 13 TeV
• • • We do not use the following data for averages, fits, limits, etc. • • •				
$< 2.8 \times 10^{-3}$	95	² AAD	20A ATLAS	$p p$, 13 TeV
$< 26 \times 10^{-2}$	95	³ AAIJ	18AM LHCb	$p p$, 8 TeV
$< 2.5 \times 10^{-3}$	95	⁴ SIRUNYAN	18BH CMS	$p p$, 13 TeV
$< 1.43 \times 10^{-2}$	95	⁵ AAD	17 ATLAS	$p p$, 8 TeV
$< 1.51 \times 10^{-2}$	95	⁶ KHACHATRYAN	15Q CMS	$p p$, 8 TeV

¹ SIRUNYAN 21Z search for $H \rightarrow \mu\tau$ in 137 fb^{-1} of $p p$ collisions at $E_{\text{cm}} = 13 \text{ TeV}$.

The limit constrains the $Y_{\mu\tau}$ Yukawa coupling to $\sqrt{|Y_{\mu\tau}|^2 + |Y_{\tau\mu}|^2} < 1.11 \times 10^{-3}$ at 95% CL (see their Fig. 8).

² AAD 20A search for $H \rightarrow \mu\tau$ in 36.1 fb^{-1} of $p p$ collisions at $E_{\text{cm}} = 13 \text{ TeV}$. The limit constrains the $Y_{\mu\tau}$ Yukawa coupling to $\sqrt{|Y_{\mu\tau}|^2 + |Y_{\tau\mu}|^2} < 1.5 \times 10^{-3}$ at 95% CL (see their Fig. 5).

³ AAIJ 18AM search for $H \rightarrow \mu\tau$ in 2.0 fb^{-1} of $p p$ collisions at $E_{\text{cm}} = 8 \text{ TeV}$. The limit constrains the $Y_{\mu\tau}$ Yukawa coupling to $\sqrt{|Y_{\mu\tau}|^2 + |Y_{\tau\mu}|^2} < 1.7 \times 10^{-2}$ at 95% CL assuming SM production cross sections.

⁴ SIRUNYAN 18BH search for $H \rightarrow \mu\tau$ in 35.9 fb^{-1} of $p p$ collisions at $E_{\text{cm}} = 13 \text{ TeV}$. The limit constrains the $Y_{\mu\tau}$ Yukawa coupling to $\sqrt{|Y_{\mu\tau}|^2 + |Y_{\tau\mu}|^2} < 1.43 \times 10^{-3}$ at 95% CL (see their Fig. 10).

⁵ AAD 17 search for $H \rightarrow \mu\tau$ in 20.3 fb^{-1} of $p p$ collisions at $E_{\text{cm}} = 8 \text{ TeV}$.

⁶ KHACHATRYAN 15Q search for $H \rightarrow \mu\tau$ with τ decaying electronically or hadronically in 19.7 fb^{-1} of $p p$ collisions at $E_{\text{cm}} = 8 \text{ TeV}$. The fit gives $B(H \rightarrow \mu\tau) = (0.84^{+0.39}_{-0.37})\%$ with a significance of 2.4σ .

$\Gamma(\text{invisible})/\Gamma_{\text{total}}$	Γ_{25}/Γ			
Invisible final states.				
VALUE	CL%	DOCUMENT ID	TECN	COMMENT
<0.13	95	¹ ATLAS	22	ATLS $p p, 13 \text{ TeV}$
$\bullet \bullet \bullet$ We do not use the following data for averages, fits, limits, etc. $\bullet \bullet \bullet$				
<0.19	95	² AAD	22D	ATLS $p p \rightarrow Z H, 13 \text{ TeV}$
<0.145	95	³ AAD	22P	ATLS $p p \rightarrow q q H, 13 \text{ TeV}$
<0.37	95	⁴ AAD	22S	ATLS $p p \rightarrow q q H \gamma, 13 \text{ TeV}$
<0.16	95	⁵ CMS	22	CMS $p p, 13 \text{ TeV}$
<0.18	95	⁶ TUMASYAN	22G	CMS $p p \rightarrow q q H, 8, 13 \text{ TeV}$
<0.18	95	⁷ TUMASYAN	22G	CMS $p p \rightarrow q q H, 13 \text{ TeV}$
<0.34	95	⁸ AAD	21F	ATLS $p p, 13 \text{ TeV}$
<0.29	95	⁹ SIRUNYAN	21A	CMS $p p \rightarrow Z H, 13 \text{ TeV}$
<0.278	95	¹⁰ TUMASYAN	21D	CMS $p p, 13 \text{ TeV}, \text{jet or } V(\rightarrow q \bar{q})$
<0.37	95	¹¹ AABOUD	19AI	ATLS $p p \rightarrow q q H, 13 \text{ TeV}$
<0.38	95	¹² AABOUD	19AL	ATLS $p p, 13 \text{ TeV}$
<0.26	95	¹³ AABOUD	19AL	ATLS $p p, 7, 8, 13 \text{ TeV}$
<0.22	95	¹⁴ SIRUNYAN	19AT	CMS $p p, 13 \text{ TeV}$
<0.33	95	¹⁵ SIRUNYAN	19BO	CMS $p p \rightarrow q q H, 13 \text{ TeV}$
<0.26	95	¹⁶ SIRUNYAN	19BO	CMS $p p, 13 \text{ TeV}$
<0.19	95	¹⁷ SIRUNYAN	19BO	CMS $p p, 7, 8, 13 \text{ TeV}$
<0.67	95	¹⁸ AABOUD	18	ATLS $p p \rightarrow Z H, 13 \text{ TeV}$
<0.83	95	¹⁹ AABOUD	18CA	ATLS $p p \rightarrow W H/Z H, W/Z \rightarrow jj, 13 \text{ TeV}$
<0.40	95	²⁰ SIRUNYAN	18BV	CMS $p p \rightarrow Z H, 13 \text{ TeV}$
<0.53	95	²¹ SIRUNYAN	18S	CMS $p p, 13 \text{ TeV}, \text{jet or } V(\rightarrow q \bar{q})$
<0.46	95	²² AABOUD	17BD	ATLS $p p \rightarrow H j, q q H, 13 \text{ TeV}$
<0.24	95	²³ KHACHATRY...	17F	CMS $p p, 7, 8, 13 \text{ TeV}$
<0.28	95	²⁴ AAD	16AF	ATLS $p p \rightarrow q q H, 8 \text{ TeV}$
<0.34	95	²⁵ AAD	16AN	LHC $p p, 7, 8 \text{ TeV}$
<0.78	95	²⁶ AAD	15BD	ATLS $p p \rightarrow W H/Z H, 8 \text{ TeV}$
<0.25	95	²⁷ AAD	15CX	ATLS $p p, 7, 8 \text{ TeV}$
<0.75	95	²⁸ AAD	140	ATLS $p p \rightarrow Z H, 7, 8 \text{ TeV}$
<0.58	95	²⁹ CHATRCHYAN	14B	CMS $p p \rightarrow Z H, q q H$
<0.81	95	³⁰ CHATRCHYAN	14B	CMS $p p \rightarrow Z H, 7, 8 \text{ TeV}$
<0.65	95	³¹ CHATRCHYAN	14B	CMS $p p \rightarrow q q H, 8 \text{ TeV}$

¹ ATLAS 22 report the combined results using 139 fb^{-1} of data at $E_{\text{cm}} = 13 \text{ TeV}$, where H decaying to invisible final states in VBF (AAD 22P), and $Z H, Z \rightarrow ee, \mu\mu$ (AAD 22D), assuming $\kappa_V \leq 1$ and $B_{\text{undetected}} \geq 0$.

² AAD 22D search for H decaying to invisible final states associated with a Z decaying $ee/\mu\mu$ using 139 fb^{-1} at 13 TeV . The limit is obtained for $m_H = 125 \text{ GeV}$ and assuming the SM $Z H$ production cross section. The branching ratio is obtained to be $(0.3 \pm 9.0)\%$.

³ AAD 22P search for $p p \rightarrow q q H X$ (VBF) with H decaying to invisible final states using 139 fb^{-1} of data. The quoted limit on the branching ratio is given for $m_H = 125 \text{ GeV}$ and assumes the Standard Model cross section.

⁴ AAD 22S observe electroweak $Z(\rightarrow \nu\nu)\gamma + 2\text{jets}$ production process with 139 fb^{-1} of data. This result is applicable to search for $p p \rightarrow q q H \gamma X$ (VBF+ γ) with H decaying to invisible final states. The quoted limit on the branching ratio is given for $m_H = 125 \text{ GeV}$ and assumes the Standard Model cross section.

- ⁵ CMS 22 report the combined results using (a part of) 138 fb^{-1} of data at $E_{\text{cm}} = 13 \text{ TeV}$, where H decaying to invisible final states in VBF (SIRUNYAN 19BO), associated with an energetic jet or a $V(\rightarrow q\bar{q})$ (TUMASYAN 21D), and $ZH, Z \rightarrow ee, \mu\mu$ (SIRUNYAN 21A) and assuming $\kappa_V \leq 1$ and $B_{\text{undetected}} \geq 0$.
- ⁶ TUMASYAN 22G combine $13 \text{ TeV } 101 \text{ fb}^{-1}$ results with 8 TeV (KHACHATRYAN 17F) and other 13 TeV (KHACHATRYAN 17F for 2015 and SIRUNYAN 19BO for 2016) for H decaying to invisible final states with VBF topology. The quoted limit on the branching ratio is given for $m_H = 125.38 \text{ GeV}$ and assumes the Standard Model production rates. The branching ratio is obtained to be $0.086^{+0.054}_{-0.052}$. See their Figs. 11 and 12.
- ⁷ TUMASYAN 22G search for $pp \rightarrow qqHX$ (VBF) with H decaying to invisible final states using 101 fb^{-1} of data (2017 and 2018). The quoted limit on the branching ratio is given for $m_H = 125.38 \text{ GeV}$ and assumes the Standard Model cross section. See their Figs. 11 and 12.
- ⁸ AAD 21F search for an invisibly decaying Higgs boson with an energetic jet ($p_T > 150 \text{ GeV}$) and missing transverse momentum ($> 200 \text{ GeV}$) in 139 fb^{-1} at $E_{\text{cm}} = 13 \text{ TeV}$. The quoted limit on the branching ratio is given for $m_H = 125 \text{ GeV}$.
- ⁹ SIRUNYAN 21A search for H decaying to invisible final states associated with a Z decaying $ee/\mu\mu$ using 137 fb^{-1} at 13 TeV . The limit is obtained for $m_H = 125 \text{ GeV}$ and assuming the SM ZH production cross section.
- ¹⁰ TUMASYAN 21D search for H decaying to invisible final states associated with an energetic jet or a $V, V \rightarrow q\bar{q}$ using 101 fb^{-1} at 13 TeV and the result is combined with SIRUNYAN 18S.
- ¹¹ AABOUD 19AI search for $pp \rightarrow qqHX$ (VBF) with H decaying to invisible final states using 36.1 fb^{-1} of data. The quoted limit on the branching ratio is given for $m_H = 125 \text{ GeV}$ and assumes the Standard Model rates for VBF and gluon-fusion production.
- ¹² AABOUD 19AL combine results of H decaying to invisible final states with VBF(AABOUD 19AI), ZH , and WH productions (AABOUD 18, AABOUD 18CA), which use 36.1 fb^{-1} of data at 13 TeV . The quoted limit is given for $m_H = 125 \text{ GeV}$ and assumes the Standard Model rates for gluon fusion, VBF, ZH , and WH productions.
- ¹³ AABOUD 19AL combine results of 7, 8 (AAD 15CX), and 13 TeV for H decaying to invisible final states.
- ¹⁴ SIRUNYAN 19AT perform a combined fit with visible decay using 35.9 fb^{-1} of data at 13 TeV .
- ¹⁵ SIRUNYAN 19BO search for $pp \rightarrow qqHX$ (VBF) with H decaying to invisible final states using 35.9 fb^{-1} of data. The quoted limit on the branching ratio is given for $m_H = 125.09 \text{ GeV}$ and assumes the Standard Model production rates.
- ¹⁶ SIRUNYAN 19BO combine the VBF channel with results of other 13 TeV analyses: SIRUNYAN 18BV and SIRUNYAN 18S. The quoted limit on the branching ratio is given for $m_H = 125.09 \text{ GeV}$ and assumes the Standard Model production rates.
- ¹⁷ SIRUNYAN 19BO combine $13 \text{ TeV } 35.9 \text{ fb}^{-1}$ results with 7, 8, 13 TeV (KHACHATRYAN 17F) for H decaying to invisible final states. The quoted limit on the branching ratio is given for $m_H = 125.09 \text{ GeV}$ and assumes the Standard Model production rates. The branching ratio is obtained to be $0.05 \pm 0.03 \text{ (stat)} \pm 0.07 \text{ (syst)}$.
- ¹⁸ AABOUD 18 search for $pp \rightarrow HZX, Z \rightarrow ee, \mu\mu$ with H decaying to invisible final states in 36.1 fb^{-1} at $E_{\text{cm}} = 13 \text{ TeV}$. The quoted limit on the branching ratio is given for $m_H = 125 \text{ GeV}$ and assumes the Standard Model rate for HZ production.
- ¹⁹ AABOUD 18CA search for H decaying to invisible final states using WH , and ZH productions, where W and Z hadronically decay. The data of 36.1 fb^{-1} at $E_{\text{cm}} = 13 \text{ TeV}$ is used. The quoted limit assumes SM production cross sections with combining the contributions from WH , ZH , ggF and VBF production modes.
- ²⁰ SIRUNYAN 18BV search for H decaying to invisible final states associated with a $Z, Z \rightarrow \ell\ell$ using 35.9 fb^{-1} at 13 TeV . The limit is obtained for $m_H = 125 \text{ GeV}$ and assuming the SM ZH production cross section.

- 21 SIRUNYAN 18S search for H decaying to invisible final states associated with an energetic jet or a V , $V \rightarrow q\bar{q}$ using 35.9 fb^{-1} at 13 TeV .
- 22 AABOUD 17BD search for H decaying to invisible final states with ≥ 1 jet and VBF events using 3.2 fb^{-1} of pp collisions at $E_{\text{cm}} = 13 \text{ TeV}$. A cross-section ratio R^{miss} is used in the measurement. The quoted limit is given for $m_H = 125 \text{ GeV}$.
- 23 KHACHATRYAN 17F search for H decaying to invisible final states with gluon fusion, VBF, ZH , and WH productions using 2.3 fb^{-1} of pp collisions at $E_{\text{cm}} = 13 \text{ TeV}$, 19.7 fb^{-1} at 8 TeV , and 5.1 fb^{-1} at 7 TeV . The quoted limit is given for $m_H = 125 \text{ GeV}$ and assumes the Standard Model rates for gluon fusion, VBF, ZH , and WH productions.
- 24 AAD 16AF search for $pp \rightarrow qqHX$ (VBF) with H decaying to invisible final states in 20.3 fb^{-1} at $E_{\text{cm}} = 8 \text{ TeV}$. The quoted limit on the branching ratio is given for $m_H = 125 \text{ GeV}$ and assumes the Standard Model rates for VBF and gluon-fusion production.
- 25 AAD 16AN perform fits to the ATLAS and CMS data at $E_{\text{cm}} = 7$ and 8 TeV . The branching fraction of decays into BSM particles that are invisible or into undetected decay modes is measured for $m_0 = 125.09 \text{ GeV}$.
- 26 AAD 15BD search for $pp \rightarrow HWX$ and $pp \rightarrow HZX$ with W or Z decaying hadronically and H decaying to invisible final states using data at $E_{\text{cm}} = 8 \text{ TeV}$. The quoted limit is given for $m_H = 125 \text{ GeV}$, assumes the Standard Model rates for the production processes and is based on a combination of the contributions from HW , HZ and the gluon-fusion process.
- 27 AAD 15CX search for H decaying to invisible final states with VBF, ZH , and WH productions using 20.3 fb^{-1} at 8 TeV , and 4.7 fb^{-1} at 7 TeV . The quoted limit is given for $m_H = 125.36 \text{ GeV}$ and assumes the Standard Model rates for gluon fusion, VBF, ZH , and WH productions. The upper limit is improved to 0.23 by adding the measured visible decay rates.
- 28 AAD 140 search for $pp \rightarrow HZX$, $Z \rightarrow \ell\ell$, with H decaying to invisible final states in 4.5 fb^{-1} at $E_{\text{cm}} = 7 \text{ TeV}$ and 20.3 fb^{-1} at $E_{\text{cm}} = 8 \text{ TeV}$. The quoted limit on the branching ratio is given for $m_H = 125.5 \text{ GeV}$ and assumes the Standard Model rate for HZ production.
- 29 CHATRCHYAN 14B search for $pp \rightarrow HZX$, $Z \rightarrow \ell\ell$ and $Z \rightarrow b\bar{b}$, and also $pp \rightarrow qqHX$ with H decaying to invisible final states using data at $E_{\text{cm}} = 7$ and 8 TeV . The quoted limit on the branching ratio is obtained from a combination of the limits from HZ and qqH . It is given for $m_H = 125 \text{ GeV}$ and assumes the Standard Model rates for the two production processes.
- 30 CHATRCHYAN 14B search for $pp \rightarrow HZX$ with H decaying to invisible final states and $Z \rightarrow \ell\ell$ in 4.9 fb^{-1} at $E_{\text{cm}} = 7 \text{ TeV}$ and 19.7 fb^{-1} at $E_{\text{cm}} = 8 \text{ TeV}$, and also with $Z \rightarrow b\bar{b}$ in 18.9 fb^{-1} at $E_{\text{cm}} = 8 \text{ TeV}$. The quoted limit on the branching ratio is given for $m_H = 125 \text{ GeV}$ and assumes the Standard Model rate for HZ production.
- 31 CHATRCHYAN 14B search for $pp \rightarrow qqHX$ (vector boson fusion) with H decaying to invisible final states in 19.5 fb^{-1} at $E_{\text{cm}} = 8 \text{ TeV}$. The quoted limit on the branching ratio is given for $m_H = 125 \text{ GeV}$ and assumes the Standard Model rate for qqH production.

$\Gamma(\gamma \text{ invisible})/\Gamma_{\text{total}}$	Γ_{26}/Γ			
VALUE	CL%	DOCUMENT ID	TECN	COMMENT
<0.029	95	1,2 SIRUNYAN	21L CMS	VBF, HZ , $H \rightarrow \gamma + \text{invisible}$, 13 TeV
• • • We do not use the following data for averages, fits, limits, etc. • • •				
<0.035	95	¹ SIRUNYAN	21L CMS	VBF, $H \rightarrow \gamma + \text{invisible}$, 13 TeV
<0.046	95	³ SIRUNYAN	19CG CMS	$pp \rightarrow HZ$, $H \rightarrow \gamma + \text{invisible}$, $Z \rightarrow \ell\ell$, 13 TeV

¹ SIRUNYAN 21L search for H decaying to an invisible final state plus a γ in the VBF production using 130 fb^{-1} data at $E_{\text{cm}} = 13 \text{ TeV}$. The invisible state is called a dark

photon. The quoted limit on the branching ratio is given for $m_H = 125$ GeV assuming the Standard Model rates.

²The result of the VBF production is combined with the $pp \rightarrow HZ$ result (SIRUNYAN 19CG).

³SIRUNYAN 19CG search for $pp \rightarrow HZ$, $Z \rightarrow ee$, $\mu\mu$ with H decaying to invisible final states plus a γ in 137 fb^{-1} at $E_{\text{cm}} = 13$ TeV. The quoted limit on the branching ratio is given for $m_H = 125$ GeV assuming the Standard Model rate for HZ production and is obtained in the context of a theoretical model, where the undetected (invisible) particle is massless.

H SIGNAL STRENGTHS IN DIFFERENT CHANNELS

The H signal strength in a particular final state xx is given by the cross section times branching ratio in this channel normalized to the Standard Model (SM) value, $\sigma \cdot B(H \rightarrow xx) / (\sigma \cdot B(H \rightarrow xx))_{\text{SM}}$, for the specified mass value of H . For the SM predictions, see DITTMAIER 11, DITTMAIER 12, and HEINEMEYER 13A. Results for fiducial and differential cross sections are also listed below.

Combined Final States

VALUE	DOCUMENT ID	TECN	COMMENT
1.03 ±0.04 OUR AVERAGE			
1.05 ±0.06	¹ ATLAS	22	ATLS pp , 13 TeV
1.002 ±0.057	² CMS	22	CMS pp , 13 TeV
1.09 ±0.07 ±0.04 ^{+0.08} _{-0.07}	^{3,4} AAD	16AN LHC	pp , 7, 8 TeV
1.44 ^{+0.59} _{-0.56}	⁵ AALTONEN	13M TEVA	$p\bar{p} \rightarrow HX$, 1.96 TeV
• • • We do not use the following data for averages, fits, limits, etc. • • •			
1.11 ^{+0.09} _{-0.08}	⁶ AAD	20	ATLS pp , 13 TeV
1.17 ±0.10	⁷ SIRUNYAN	19AT CMS	pp , 13 TeV
	⁸ SIRUNYAN	19BA CMS	pp , 13 TeV, differential cross sections
1.20 ±0.10 ±0.06 ^{+0.09} _{-0.08}	⁴ AAD	16AN ATLS	pp , 7, 8 TeV
0.97 ±0.09 ±0.05 ^{+0.08} _{-0.07}	⁴ AAD	16AN CMS	pp , 7, 8 TeV
1.18 ±0.10 ±0.07 ^{+0.08} _{-0.07}	⁹ AAD	16K ATLS	pp , 7, 8 TeV
0.75 ^{+0.28} _{-0.26} ^{+0.13} _{-0.11} ^{+0.08} _{-0.05}	⁹ AAD	16K ATLS	pp , 7 TeV
1.28 ±0.11 ±0.08 ±0.10	⁹ AAD	16K ATLS	pp , 8 TeV
	¹⁰ AAD	15P ATLS	pp , 8 TeV, cross section
1.00 ±0.09 ±0.07 ^{+0.08} _{-0.07}	¹¹ KHACHATRYAN...15AMCMS		pp , 7, 8 TeV
1.33 ^{+0.14} _{-0.10} ±0.15	¹² AAD	13AK ATLS	pp , 7 and 8 TeV
1.54 ^{+0.77} _{-0.73}	¹³ AALTONEN	13L CDF	$p\bar{p} \rightarrow HX$, 1.96 TeV
1.40 ^{+0.92} _{-0.88}	¹⁴ ABAZOV	13L D0	$p\bar{p} \rightarrow HX$, 1.96 TeV
1.4 ±0.3	¹⁵ AAD	12AI ATLS	$pp \rightarrow HX$, 7, 8 TeV
1.2 ±0.4	¹⁵ AAD	12AI ATLS	$pp \rightarrow HX$, 7 TeV

1.5 ± 0.4
 0.87 ± 0.23

¹⁵ AAD 12AI ATLS $p p \rightarrow H X$, 8 TeV
¹⁶ CHATRCHYAN 12N CMS $p p \rightarrow H X$, 7, 8 TeV

¹ ATLAS 22 report combined results (see their Extended Data Table 1) using up to 139 fb^{-1} of data at $E_{\text{cm}} = 13$ TeV, assuming $m_H = 125.09$ GeV. The Higgs production cross-sections, branching fractions and several ratios are found in their Figs. 2 and 3.

² CMS 22 report combined results (see their Extended Data Table 2) using 138 fb^{-1} of data at $E_{\text{cm}} = 13$ TeV, assuming $m_H = 125.38$ GeV. Signal strengths for production modes and decay channels are found in their Fig. 2.

³ AAD 16AN perform fits to the ATLAS and CMS data at $E_{\text{cm}} = 7$ and 8 TeV. The signal strengths for individual production processes are $1.03^{+0.16}_{-0.14}$ for gluon fusion, $1.18^{+0.25}_{-0.23}$ for vector boson fusion, $0.89^{+0.40}_{-0.38}$ for $W H$ production, $0.79^{+0.38}_{-0.36}$ for $Z H$ production, and $2.3^{+0.7}_{-0.6}$ for $t \bar{t} H$ production.

⁴ AAD 16AN: The uncertainties represent statistics, experimental systematics, and added in quadrature theory systematics on the background and on the signal. The quoted signal strengths are given for $m_H = 125.09$ GeV. In the fit, relative branching ratios and relative production cross sections are fixed to those in the Standard Model.

⁵ AALTONEN 13M combine all Tevatron data from the CDF and D0 Collaborations with up to 10.0 fb^{-1} and 9.7 fb^{-1} , respectively, of $p \bar{p}$ collisions at $E_{\text{cm}} = 1.96$ TeV. The quoted signal strength is given for $m_H = 125$ GeV.

⁶ AAD 20 combine results of up to 79.8 fb^{-1} of data at $E_{\text{cm}} = 13$ TeV, assuming $m_H = 125.09$ GeV: $\gamma \gamma$, ZZ^* , WW^* , $\tau \tau$, $b \bar{b}$, $\mu \mu$, invisible, and off-shell analyses (see their Table I). The signal strengths for individual production processes are 1.04 ± 0.09 for gluon fusion, $1.21^{+0.24}_{-0.22}$ for vector boson fusion, $1.30^{+0.40}_{-0.38}$ for $W H$ production, $1.05^{+0.31}_{-0.29}$ for $Z H$ production, and $1.21^{+0.26}_{-0.24}$ for $t \bar{t} H + t H$ production (see their Fig. 2 and Table IV). Several results with the simplified template cross section and κ -frameworks are presented: see their Figs. 9–11, Figs 20, 21 and Table VIII for stage-1 simplified template cross sections, their Figs. 12–17 and Tables X–XII for the κ -framework.

⁷ SIRUNYAN 19AT combine results of 35.9 fb^{-1} of data at $E_{\text{cm}} = 13$ TeV, assuming $m_H = 125.09$ GeV. The signal strengths for individual production processes are $1.22^{+0.14}_{-0.12}$ for gluon fusion, $0.73^{+0.30}_{-0.27}$ for vector boson fusion, $2.18^{+0.58}_{-0.55}$ for $W H$ production, $0.87^{+0.44}_{-0.42}$ for $Z H$ production, and $1.18^{+0.30}_{-0.27}$ for $t \bar{t} H$ production. Several results with the simplified template cross section and κ -frameworks are presented: see their Fig. 8 and Table 5 for stage-0 simplified template cross sections, their Figs. 9–18 and Tables 7–11 for the κ -framework.

⁸ SIRUNYAN 19BA measure differential cross sections for the Higgs boson transverse momentum, the number of jets, the rapidity of the Higgs boson and the transverse momentum of the leading jet using 35.9 fb^{-1} of data at $E_{\text{cm}} = 13$ TeV with $H \rightarrow \gamma \gamma$, $H \rightarrow ZZ^*$, and $H \rightarrow b \bar{b}$. The total cross section for Higgs boson production is measured to be $61.1 \pm 6.0 \pm 3.7 \text{ pb}$ using $H \rightarrow \gamma \gamma$ and $H \rightarrow ZZ^*$ channels. Several coupling measurements in the κ -framework are performed.

⁹ AAD 16K use up to 4.7 fb^{-1} of $p p$ collisions at $E_{\text{cm}} = 7$ TeV and up to 20.3 fb^{-1} at $E_{\text{cm}} = 8$ TeV. The third uncertainty in the measurement is theory systematics. The signal strengths for individual production modes are $1.23 \pm 0.14^{+0.09}_{-0.08}{}^{+0.16}_{-0.12}$ for gluon fusion, $1.23^{+0.28}_{-0.27}{}^{+0.13}_{-0.12}{}^{+0.11}_{-0.09}$ for vector boson fusion, $0.80^{+0.31}_{-0.30} \pm 0.17^{+0.10}_{-0.05}$ for $W/Z H$ production, and $1.81^{+0.52}_{-0.50}{}^{+0.58}_{-0.55}{}^{+0.31}_{-0.12}$ for $t \bar{t} H$ production. The quoted signal strengths are given for $m_H = 125.36$ GeV.

¹⁰ AAD 15P measure total and differential cross sections of the process $p p \rightarrow H X$ at $E_{\text{cm}} = 8$ TeV with 20.3 fb^{-1} . $\gamma \gamma$ and 4ℓ final states are used. $\sigma(p p \rightarrow H X) =$

- $33.0 \pm 5.3 \pm 1.6$ pb is given. See their Figs. 2 and 3 for data on differential cross sections.
- ¹¹ KHACHATRYAN 15AM use up to 5.1 fb^{-1} of $p p$ collisions at $E_{\text{cm}} = 7 \text{ TeV}$ and up to 19.7 fb^{-1} at $E_{\text{cm}} = 8 \text{ TeV}$. The third uncertainty in the measurement is theory systematics. Fits to each production mode give the value of $0.85^{+0.19}_{-0.16}$ for gluon fusion, $1.16^{+0.37}_{-0.34}$ for vector boson fusion, $0.92^{+0.38}_{-0.36}$ for $W H$, $Z H$ production, and $2.90^{+1.08}_{-0.94}$ for $t\bar{t}H$ production.
- ¹² AAD 13AK use 4.7 fb^{-1} of $p p$ collisions at $E_{\text{cm}} = 7 \text{ TeV}$ and 20.7 fb^{-1} at $E_{\text{cm}} = 8 \text{ TeV}$. The combined signal strength is based on the $\gamma\gamma$, $Z Z^* \rightarrow 4\ell$, and $W W^* \rightarrow \ell\nu\ell\nu$ channels. The quoted signal strength is given for $m_H = 125.5 \text{ GeV}$. Reported statistical error value modified following private communication with the experiment.
- ¹³ AALTONEN 13L combine all CDF results with $9.45\text{--}10.0 \text{ fb}^{-1}$ of $p\bar{p}$ collisions at $E_{\text{cm}} = 1.96 \text{ TeV}$. The quoted signal strength is given for $m_H = 125 \text{ GeV}$.
- ¹⁴ ABAZOV 13L combine all D0 results with up to 9.7 fb^{-1} of $p\bar{p}$ collisions at $E_{\text{cm}} = 1.96 \text{ TeV}$. The quoted signal strength is given for $m_H = 125 \text{ GeV}$.
- ¹⁵ AAD 12AI obtain results based on $4.6\text{--}4.8 \text{ fb}^{-1}$ of $p p$ collisions at $E_{\text{cm}} = 7 \text{ TeV}$ and $5.8\text{--}5.9 \text{ fb}^{-1}$ at $E_{\text{cm}} = 8 \text{ TeV}$. An excess of events over background with a local significance of 5.9σ is observed at $m_H = 126 \text{ GeV}$. The quoted signal strengths are given for $m_H = 126 \text{ GeV}$. See also AAD 12DA.
- ¹⁶ CHATRCHYAN 12N obtain results based on $4.9\text{--}5.1 \text{ fb}^{-1}$ of $p p$ collisions at $E_{\text{cm}} = 7 \text{ TeV}$ and $5.1\text{--}5.3 \text{ fb}^{-1}$ at $E_{\text{cm}} = 8 \text{ TeV}$. An excess of events over background with a local significance of 5.0σ is observed at about $m_H = 125 \text{ GeV}$. The combined signal strength is based on the $\gamma\gamma$, $Z Z^*$, $W W^*$, $\tau^+\tau^-$, and $b\bar{b}$ channels. The quoted signal strength is given for $m_H = 125.5 \text{ GeV}$. See also CHATRCHYAN 13Y.

WW^* Final State

VALUE	DOCUMENT ID	TECN	COMMENT
1.00±0.08 OUR AVERAGE			
0.97 ± 0.09	¹ CMS	22 CMS	$p p$, 13 TeV
$1.09^{+0.18}_{-0.16}$	^{2,3} AAD	16AN LHC	$p p$, 7, 8 TeV
$0.94^{+0.85}_{-0.83}$	⁴ AALTONEN	13M TEVA	$p\bar{p} \rightarrow H X$, 1.96 TeV
• • • We do not use the following data for averages, fits, limits, etc. • • •			
$0.5 \pm 0.4^{+0.7}_{-0.6}$	⁵ AAD	22V ATLS	$p p$, $WW^* (\rightarrow e\nu\mu\nu)$ +2j, 13 TeV
	⁶ AAD	22V ATLS	$p p$, $WW^* (\rightarrow e\nu\mu\nu)$ +2j, 13 TeV
	⁷ AABOUD	19F ATLS	$p p$, 13 TeV, cross sections
$2.5^{+0.9}_{-0.8}$	⁸ AAD	19A ATLS	$p p \rightarrow HW/HZ$, $H \rightarrow WW^*$, 13 TeV
$1.28^{+0.17}_{-0.16}$	⁹ SIRUNYAN	19AT CMS	$p p$, 13 TeV
$1.28^{+0.18}_{-0.17}$	¹⁰ SIRUNYAN	19AX CMS	$p p$, 13 TeV
$1.22^{+0.23}_{-0.21}$	³ AAD	16AN ATLS	$p p$, 7, 8 TeV
$0.90^{+0.23}_{-0.21}$	³ AAD	16AN CMS	$p p$, 7, 8 TeV
$1.18 \pm 0.16^{+0.17}_{-0.14}$	¹¹ AAD	16AO ATLS	$p p$, 8 TeV, cross sections
	¹² AAD	16K ATLS	$p p$, 7, 8 TeV

$1.09^{+0.16}_{-0.15} {}^{+0.17}_{-0.14}$	13 AAD	15AA ATLS	$p\bar{p}, 7, 8 \text{ TeV}$
$3.0 {}^{+1.3}_{-1.1} {}^{+1.0}_{-0.7}$	14 AAD	15AQ ATLS	$p\bar{p} \rightarrow H\bar{W}/Z\bar{X}, 7, 8 \text{ TeV}$
$1.16^{+0.16}_{-0.15} {}^{+0.18}_{-0.15}$	15 AAD	15AQ ATLS	$p\bar{p}, 7, 8 \text{ TeV}$
$0.72 \pm 0.12 \pm 0.10 {}^{+0.12}_{-0.10}$	16 CHATRCHYAN 14G CMS	CMS	$p\bar{p}, 7, 8 \text{ TeV}$
$0.99^{+0.31}_{-0.28}$	17 AAD	13AK ATLS	$p\bar{p}, 7 \text{ and } 8 \text{ TeV}$
$0.00^{+1.78}_{-0.00}$	18 AALTONEN	13L CDF	$p\bar{p} \rightarrow H\bar{X}, 1.96 \text{ TeV}$
$1.90^{+1.63}_{-1.52}$	19 ABAZOV	13L D0	$p\bar{p} \rightarrow H\bar{X}, 1.96 \text{ TeV}$
1.3 ± 0.5	20 AAD	12AI ATLS	$p\bar{p} \rightarrow H\bar{X}, 7, 8 \text{ TeV}$
0.5 ± 0.6	20 AAD	12AI ATLS	$p\bar{p} \rightarrow H\bar{X}, 7 \text{ TeV}$
1.9 ± 0.7	20 AAD	12AI ATLS	$p\bar{p} \rightarrow H\bar{X}, 8 \text{ TeV}$
$0.60^{+0.42}_{-0.37}$	21 CHATRCHYAN 12N CMS	CMS	$p\bar{p} \rightarrow H\bar{X}, 7, 8 \text{ TeV}$

¹ CMS 22 report combined results (see their Extended Data Table 2) using up to 138 fb^{-1} of data at $E_{\text{cm}} = 13 \text{ TeV}$, assuming $m_H = 125.38 \text{ GeV}$. See their Fig. 2 right.

² AAD 16AN perform fits to the ATLAS and CMS data at $E_{\text{cm}} = 7$ and 8 TeV . The signal strengths for individual production processes are 0.84 ± 0.17 for gluon fusion, 1.2 ± 0.4 for vector boson fusion, $1.6 {}^{+1.2}_{-1.0}$ for WH production, $5.9 {}^{+2.6}_{-2.2}$ for ZH production, and $5.0 {}^{+1.8}_{-1.7}$ for $t\bar{t}H$ production.

³ AAD 16AN: In the fit, relative production cross sections are fixed to those in the Standard Model. The quoted signal strength is given for $m_H = 125.09 \text{ GeV}$.

⁴ AALTONEN 13M combine all Tevatron data from the CDF and D0 Collaborations with up to 10.0 fb^{-1} and 9.7 fb^{-1} , respectively, of $p\bar{p}$ collisions at $E_{\text{cm}} = 1.96 \text{ TeV}$. The quoted signal strength is given for $m_H = 125 \text{ GeV}$.

⁵ AAD 22V measure the signal strength for ggF+2jets with 36.1 fb^{-1} data at 13 TeV .

⁶ AAD 22V probe the Higgs couplings to longitudinally and transversely polarized W and Z using VBF ($H \rightarrow WW^* \rightarrow e\nu\mu\nu$ plus two jets) with 36.1 fb^{-1} of data at $E_{\text{cm}} = 13 \text{ TeV}$. The ratios of the polarization-dependent couplings $g_{HV_LV_L}$ and $g_{HV_TV_T}$ to the Higgs- V coupling predicted by the SM, $a_L = g_{HV_LV_L}/g_{HVV}^{\text{SM}}$ and $a_T = g_{HV_TV_T}/g_{HVV}^{\text{SM}}$ are measured to be $0.91 {}^{+0.10}_{-0.18} {}^{+0.09}_{-0.17}$ and $1.2 \pm 0.4 {}^{+0.2}_{-0.3}$, respectively, assuming the standard Hgg coupling. These measurements are translated into pseudo-observables of κ_{VV} and ϵ_{VV} : $\kappa_{VV} = 0.91 {}^{+0.10}_{-0.18} {}^{+0.09}_{-0.17}$ and $\epsilon_{VV} = 0.13 {}^{+0.28}_{-0.20} {}^{+0.08}_{-0.10}$, where $\kappa_{VV} = 1$ and $\epsilon_{VV} = 0$ for the SM. See their Tables 9 and 10.

⁷ AABOUD 19F measure cross-sections times the $H \rightarrow WW^*$ branching fraction in the $H \rightarrow WW^* \rightarrow e\nu\mu\nu$ channel using 36.1 fb^{-1} of $p\bar{p}$ collisions at $E_{\text{cm}} = 13 \text{ TeV}$: $\sigma_{ggF} \times B(H \rightarrow WW^*) = 11.4 {}^{+1.2}_{-1.1} {}^{+1.8}_{-1.7} \text{ pb}$ and $\sigma_{VBF} \times B(H \rightarrow WW^*) = 0.50 {}^{+0.24}_{-0.22} \pm 0.17 \text{ pb}$.

⁸ AAD 19A use 36.1 fb^{-1} data at 13 TeV . The cross section times branching fraction values are measured to be $0.67 {}^{+0.31}_{-0.27} {}^{+0.18}_{-0.14} \text{ pb}$ for WH , $H \rightarrow WW^*$ and $0.54 {}^{+0.31}_{-0.24} {}^{+0.15}_{-0.07} \text{ pb}$ for ZH , $H \rightarrow WW^*$.

⁹ SIRUNYAN 19AT perform a combine fit to 35.9 fb^{-1} of data at $E_{\text{cm}} = 13 \text{ TeV}$.

¹⁰ SIRUNYAN 19AX measure the signal strengths, cross sections and so on using gluon fusion, VBF and VH production processes with 35.9 fb^{-1} of data. The quoted signal

strength is given for $m_H = 125.09$ GeV. Signal strengths for each production process is found in their Fig. 9. Measured cross sections and ratios to the SM predictions in the stage-0 simplified template cross section framework are shown in their Fig. 10. $\kappa_F = 1.52^{+0.48}_{-0.41}$ and $\kappa_V = 1.10 \pm 0.08$ are obtained (see their Fig. 11 (right)).

- 11 AAD 16AO measure fiducial total and differential cross sections of gluon fusion process at $E_{cm} = 8$ TeV with 20.3 fb^{-1} using $H \rightarrow WW^* \rightarrow e\nu\mu\nu$. The measured fiducial total cross section is 36.0 ± 9.7 fb in their fiducial region (Table 7). See their Fig. 6 for fiducial differential cross sections. The results are given for $m_H = 125$ GeV.
- 12 AAD 16K use up to 4.7 fb^{-1} of $p\bar{p}$ collisions at $E_{cm} = 7$ TeV and up to 20.3 fb^{-1} at $E_{cm} = 8$ TeV. The quoted signal strength is given for $m_H = 125.36$ GeV.
- 13 AAD 15AA use 4.5 fb^{-1} of $p\bar{p}$ collisions at $E_{cm} = 7$ TeV and 20.3 fb^{-1} at $E_{cm} = 8$ TeV. The signal strength for the gluon fusion and vector boson fusion mode is $1.02 \pm 0.19^{+0.22}_{-0.18}$ and $1.27^{+0.44}_{-0.40} + 0.30$, respectively. The quoted signal strengths are given for $m_H = 125.36$ GeV.
- 14 AAD 15AQ use 4.5 fb^{-1} of $p\bar{p}$ collisions at $E_{cm} = 7$ TeV and 20.3 fb^{-1} at $E_{cm} = 8$ TeV. The quoted signal strength is given for $m_H = 125.36$ GeV.
- 15 AAD 15AQ combine their result on W/ZH production with the results of AAD 15AA (gluon fusion and vector boson fusion, slightly updated). The quoted signal strength is given for $m_H = 125.36$ GeV.
- 16 CHATRCHYAN 14G use 4.9 fb^{-1} of $p\bar{p}$ collisions at $E_{cm} = 7$ TeV and 19.4 fb^{-1} at $E_{cm} = 8$ TeV. The last uncertainty in the measurement is theory systematics. The quoted signal strength is given for $m_H = 125.6$ GeV.
- 17 AAD 13AK use 4.7 fb^{-1} of $p\bar{p}$ collisions at $E_{cm} = 7$ TeV and 20.7 fb^{-1} at $E_{cm} = 8$ TeV. The quoted signal strength is given for $m_H = 125.5$ GeV. Superseded by AAD 15AA.
- 18 AALTONEN 13L combine all CDF results with $9.45\text{--}10.0 \text{ fb}^{-1}$ of $p\bar{p}$ collisions at $E_{cm} = 1.96$ TeV. The quoted signal strength is given for $m_H = 125$ GeV.
- 19 ABAZOV 13L combine all D0 results with up to 9.7 fb^{-1} of $p\bar{p}$ collisions at $E_{cm} = 1.96$ TeV. The quoted signal strength is given for $m_H = 125$ GeV.
- 20 AAD 12AI obtain results based on 4.7 fb^{-1} of $p\bar{p}$ collisions at $E_{cm} = 7$ TeV and 5.8 fb^{-1} at $E_{cm} = 8$ TeV. The quoted signal strengths are given for $m_H = 126$ GeV. See also AAD 12DA.
- 21 CHATRCHYAN 12N obtain results based on 4.9 fb^{-1} of $p\bar{p}$ collisions at $E_{cm} = 7$ TeV and 5.1 fb^{-1} at $E_{cm} = 8$ TeV. The quoted signal strength is given for $m_H = 125.5$ GeV. See also CHATRCHYAN 13Y.

ZZ^* Final State

VALUE	CL%	DOCUMENT ID	TECN	COMMENT
1.02 ± 0.08 OUR AVERAGE				
$0.97^{+0.12}_{-0.11}$		¹ CMS	22 CMS	$p\bar{p}$, 13 TeV
1.01 ± 0.11		^{2,3} AAD	20AQ ATLS	$p\bar{p}$, 13 TeV
$1.29^{+0.26}_{-0.23}$		^{4,5} AAD	16AN LHC	$p\bar{p}$, 7, 8 TeV
• • • We do not use the following data for averages, fits, limits, etc. • • •				
		⁶ SIRUNYAN	21AE CMS	$p\bar{p}$, 13 TeV, couplings
$0.94 \pm 0.07^{+0.09}_{-0.08}$		⁷ SIRUNYAN	21S CMS	$p\bar{p}$, 13 TeV
		^{2,8} AAD	20AQ ATLS	$p\bar{p}$, 13 TeV
		⁹ AAD	20BA ATLS	$p\bar{p}$, 13 TeV cross sections
<6.5	95	¹⁰ AABOUD	19N ATLS	$p\bar{p}$, 13 TeV, off-shell
$1.06^{+0.19}_{-0.17}$		¹¹ SIRUNYAN	19AT CMS	$p\bar{p}$, 13 TeV

$1.28^{+0.21}_{-0.19}$		¹² AABOUD	18AJ ATLS	pp , 13 TeV
<3.8	95	¹³ AABOUD	18BP ATLS	pp , 13 TeV, off-shell
$1.05^{+0.15+0.11}_{-0.14-0.09}$		¹⁴ SIRUNYAN	17AV CMS	pp , 13 TeV
$1.52^{+0.40}_{-0.34}$		⁵ AAD	16AN ATLS	pp , 7, 8 TeV
$1.04^{+0.32}_{-0.26}$		⁵ AAD	16AN CMS	pp , 7, 8 TeV
$1.46^{+0.35+0.19}_{-0.31-0.13}$		¹⁵ AAD	16K ATLS	pp , 7, 8 TeV
		¹⁶ KHACHATRY...	16AR CMS	pp , 7, 8 TeV cross sections
$1.44^{+0.34+0.21}_{-0.31-0.11}$		¹⁷ AAD	15F ATLS	$pp \rightarrow HX$, 7, 8 TeV
		¹⁸ AAD	14AR ATLS	pp , 8 TeV, cross sections
$0.93^{+0.26+0.13}_{-0.23-0.09}$		¹⁹ CHATRCHYAN	14AA CMS	pp , 7, 8 TeV
$1.43^{+0.40}_{-0.35}$		²⁰ AAD	13AK ATLS	pp , 7 and 8 TeV
$0.80^{+0.35}_{-0.28}$		²¹ CHATRCHYAN	13J CMS	$pp \rightarrow HX$, 7, 8 TeV
1.2 ± 0.6		²² AAD	12AI ATLS	$pp \rightarrow HX$, 7, 8 TeV
1.4 ± 1.1		²² AAD	12AI ATLS	$pp \rightarrow HX$, 7 TeV
1.1 ± 0.8		²² AAD	12AI ATLS	$pp \rightarrow HX$, 8 TeV
$0.73^{+0.45}_{-0.33}$		²³ CHATRCHYAN	12N CMS	$pp \rightarrow HX$, 7, 8 TeV

¹ CMS 22 report combined results (see their Extended Data Table 2) using up to 138 fb^{-1} of data at $E_{\text{cm}} = 13 \text{ TeV}$, assuming $m_H = 125.38 \text{ GeV}$. See their Fig. 2 right.

² AAD 20AQ perform analyses using $H \rightarrow ZZ^* \rightarrow 4\ell$ ($\ell = e, \mu$) with data of 139 fb^{-1} at $E_{\text{cm}} = 13 \text{ TeV}$. Results are given for $m_H = 125 \text{ GeV}$.

³ AAD 20AQ measured the inclusive cross section times branching ratio for $H \rightarrow ZZ^*$ decay ($|y(H)| < 2.5$) to be $1.34 \pm 0.12 \text{ pb}$ (with $1.33 \pm 0.08 \text{ pb}$ expected in the SM).

⁴ AAD 16AN perform fits to the ATLAS and CMS data at $E_{\text{cm}} = 7$ and 8 TeV . The signal strengths for individual production processes are $1.13^{+0.34}_{-0.31}$ for gluon fusion and $0.1^{+1.1}_{-0.6}$ for vector boson fusion.

⁵ AAD 16AN: In the fit, relative production cross sections are fixed to those in the Standard Model. The quoted signal strength is given for $m_H = 125.09 \text{ GeV}$.

⁶ SIRUNYAN 21AE obtains constraints on anomalous couplings to vector bosons (W, Z , and gluon) and top quark using $H \rightarrow ZZ^* \rightarrow 4\ell$ ($\ell = e, \mu$) with data of 137 fb^{-1} at $E_{\text{cm}} = 13 \text{ TeV}$. Their Table 5 and Figs 14–17 show (effective) couplings to gluon and top with combining gluon fusion, $t\bar{t}H$ and tH production channels and the result of $t\bar{t}H$, $H \rightarrow \gamma\gamma$ (SIRUNYAN 20AS). Their Tables 6–9 and Figs 18–22 show couplings to W and Z for different assumptions and bases (Higgs and Warsaw).

⁷ SIRUNYAN 21S measure cross sections with the $H \rightarrow ZZ^* \rightarrow 4\ell$ ($\ell = e, \mu$) channel using 137 fb^{-1} data at $E_{\text{cm}} = 13 \text{ TeV}$. Results are given for $m_H = 125.38 \text{ GeV}$. The signal strengths for individual production processes in their Table 4. Cross sections are given in their Table 6 and Fig. 14, which are based on the simplified template cross section framework (reduced stage-1.2).

⁸ AAD 20AQ present several results for the channel $H \rightarrow ZZ^* \rightarrow 4\ell$ ($\ell = e, \mu$) with the simplified template cross section with κ -frameworks and the effective field theory (EFT) approach; see their Table 8 and Fig. 10 for simplified template cross sections. $\kappa_V = 1.02 \pm 0.06$ and $\kappa_F = 0.88 \pm 0.16$ are obtained, see their Fig. 12 for the κ -framework. See their Tables 9 and 10 and Figs. 16–18 for the EFT-framework.

- ⁹ AAD 20BA measure the cross section for $pp \rightarrow H \rightarrow ZZ^* \rightarrow 4\ell$ ($\ell = e, \mu$) using 139 fb^{-1} at $E_{\text{cm}} = 13 \text{ TeV}$. They give $\sigma \cdot B = 3.28 \pm 0.30 \pm 0.11 \text{ fb}$ in their fiducial region, where $3.41 \pm 0.18 \text{ fb}$ is expected in the Standard Model for $m_H = 125 \text{ GeV}$. Various differential cross sections are also given; see their Figs. 19-39. Constraints on Yukawa couplings for bottom and charm quarks are given in their Table 9 and Fig. 41.
- ¹⁰ AABOUD 19N measure the spectrum of the four-lepton invariant mass $m_{4\ell}$ ($\ell = e$ or μ) using 36.1 fb^{-1} of data at $E_{\text{cm}} = 13 \text{ TeV}$. The quoted signal strength upper limit is obtained from $180 \text{ GeV} < m_{4\ell} < 1200 \text{ GeV}$.
- ¹¹ SIRUNYAN 19AT perform a combine fit to 35.9 fb^{-1} of data at $E_{\text{cm}} = 13 \text{ TeV}$.
- ¹² AABOUD 18AJ perform analyses using $H \rightarrow ZZ^* \rightarrow 4\ell$ ($\ell = e, \mu$) with data of 36.1 fb^{-1} at $E_{\text{cm}} = 13 \text{ TeV}$. Results are given for $m_H = 125.09 \text{ GeV}$. The inclusive cross section times branching ratio for $H \rightarrow ZZ^*$ decay ($|\eta(H)| < 2.5$) is measured to be $1.73^{+0.26}_{-0.24} \text{ pb}$ (with $1.34^{+0.09}_{-0.09} \text{ pb}$ expected in the SM).
- ¹³ AABOUD 18BP measure an off-shell Higgs boson production using $ZZ \rightarrow 4\ell$ and $ZZ \rightarrow 2\ell 2\nu$ ($\ell = e, \mu$) decay channels with 36.1 fb^{-1} of data at $E_{\text{cm}} = 13 \text{ TeV}$. The quoted signal strength upper limit is obtained from a combination of these two channels, where $220 \text{ GeV} < m_{4\ell} < 2000 \text{ GeV}$ for $ZZ \rightarrow 4\ell$ and $250 \text{ GeV} < m_T^{ZZ} < 2000 \text{ GeV}$ for $ZZ \rightarrow 2\ell 2\nu$ (m_T^{ZZ} is defined in their Section 5). See their Table 2 for each measurement.
- ¹⁴ SIRUNYAN 17AV use 35.9 fb^{-1} of pp collisions at $E_{\text{cm}} = 13 \text{ TeV}$. The quoted signal strength, obtained from the analysis of $H \rightarrow ZZ^* \rightarrow 4\ell$ ($\ell = e, \mu$) decays, is given for $m_H = 125.09 \text{ GeV}$. The signal strengths for different production modes are given in their Table 3. The fiducial and differential cross sections are shown in their Fig. 10.
- ¹⁵ AAD 16K use up to 4.7 fb^{-1} of pp collisions at $E_{\text{cm}} = 7 \text{ TeV}$ and up to 20.3 fb^{-1} at $E_{\text{cm}} = 8 \text{ TeV}$. The quoted signal strength is given for $m_H = 125.36 \text{ GeV}$.
- ¹⁶ KHACHATRYAN 16AR use data of 5.1 fb^{-1} at $E_{\text{cm}} = 7 \text{ TeV}$ and 19.7 fb^{-1} at 8 TeV . The fiducial cross sections for the production of 4 leptons via $H \rightarrow 4\ell$ decays are measured to be $0.56^{+0.67+0.21}_{-0.44-0.06} \text{ fb}$ at 7 TeV and $1.11^{+0.41+0.14}_{-0.35-0.10} \text{ fb}$ at 8 TeV in their fiducial region (Table 2). The differential cross sections at $E_{\text{cm}} = 8 \text{ TeV}$ are also shown in Figs. 4 and 5. The results are given for $m_H = 125 \text{ GeV}$.
- ¹⁷ AAD 15F use 4.5 fb^{-1} of pp collisions at $E_{\text{cm}} = 7 \text{ TeV}$ and 20.3 fb^{-1} at $E_{\text{cm}} = 8 \text{ TeV}$. The quoted signal strength is given for $m_H = 125.36 \text{ GeV}$. The signal strength for the gluon fusion production mode is $1.66^{+0.45+0.25}_{-0.41-0.15}$, while the signal strength for the vector boson fusion production mode is $0.26^{+1.60+0.36}_{-0.91-0.23}$.
- ¹⁸ AAD 14AR measure the cross section for $pp \rightarrow H \rightarrow ZZ^* \rightarrow 4\ell$ ($\ell = e, \mu$) using 20.3 fb^{-1} at $E_{\text{cm}} = 8 \text{ TeV}$. They give $\sigma \cdot B = 2.11^{+0.53}_{-0.47} \pm 0.08 \text{ fb}$ in their fiducial region, where $1.30 \pm 0.13 \text{ fb}$ is expected in the Standard Model for $m_H = 125.4 \text{ GeV}$. Various differential cross sections are also given; see their Fig. 2.
- ¹⁹ CHATRCHYAN 14AA use 5.1 fb^{-1} of pp collisions at $E_{\text{cm}} = 7 \text{ TeV}$ and 19.7 fb^{-1} at $E_{\text{cm}} = 8 \text{ TeV}$. The quoted signal strength is given for $m_H = 125.6 \text{ GeV}$. The signal strength for the gluon fusion and $t\bar{t}H$ production mode is $0.80^{+0.46}_{-0.36}$, while the signal strength for the vector boson fusion and WH, ZH production mode is $1.7^{+2.2}_{-2.1}$.
- ²⁰ AAD 13AK use 4.7 fb^{-1} of pp collisions at $E_{\text{cm}} = 7 \text{ TeV}$ and 20.7 fb^{-1} at $E_{\text{cm}} = 8 \text{ TeV}$. The quoted signal strength is given for $m_H = 125.5 \text{ GeV}$.
- ²¹ CHATRCHYAN 13J obtain results based on $ZZ \rightarrow 4\ell$ final states in 5.1 fb^{-1} of pp collisions at $E_{\text{cm}} = 7 \text{ TeV}$ and 12.2 fb^{-1} at $E_{\text{cm}} = 8 \text{ TeV}$. The quoted signal strength is given for $m_H = 125.8 \text{ GeV}$. Superseded by CHATRCHYAN 14AA.

²² AAD 12AI obtain results based on 4.7–4.8 fb⁻¹ of $p p$ collisions at $E_{\text{cm}} = 7$ TeV and 5.8 fb⁻¹ at $E_{\text{cm}} = 8$ TeV. The quoted signal strengths are given for $m_H = 126$ GeV. See also AAD 12DA.

²³ CHATRCHYAN 12N obtain results based on 4.9–5.1 fb⁻¹ of $p p$ collisions at $E_{\text{cm}} = 7$ TeV and 5.1–5.3 fb⁻¹ at $E_{\text{cm}} = 8$ TeV. An excess of events over background with a local significance of 5.0 σ is observed at about $m_H = 125$ GeV. The quoted signal strengths are given for $m_H = 125.5$ GeV. See also CHATRCHYAN 12BY and CHATRCHYAN 13Y.

$\gamma\gamma$ Final State

VALUE	DOCUMENT ID	TECN	COMMENT
1.10±0.07 OUR AVERAGE			
1.13±0.09	1 CMS	22 CMS	$p p$, 13 TeV
0.99 ^{+0.15} _{-0.14}	2 AABOUD	18BO ATLS	$p p$, 13 TeV, 36.1 fb ⁻¹
1.14 ^{+0.19} _{-0.18}	3,4 AAD	16AN LHC	$p p$, 7, 8 TeV
5.97 ^{+3.39} _{-3.12}	5 AALTONEN	13M TEVA	$p\bar{p} \rightarrow HX$, 1.96 TeV
• • • We do not use the following data for averages, fits, limits, etc. • • •			
1.12±0.09	6 AAD	22N ATLS	$p p$, 13 TeV, diff. x-sections
1.20 ^{+0.18} _{-0.14}	7 SIRUNYAN	21O CMS	$p p$, 13 TeV
1.18 ^{+0.17} _{-0.14}	8 SIRUNYAN	19AT CMS	$p p$, 13 TeV
1.14 ^{+0.27} _{-0.25}	9 SIRUNYAN	19L CMS	$p p$, 13 TeV, diff. x-section
1.11 ^{+0.25} _{-0.23}	10 SIRUNYAN	18DS CMS	$p p$, $H \rightarrow \gamma\gamma$, 13 TeV, floated m_H
1.17±0.23 ^{+0.10+0.12} _{-0.08-0.08}	4 AAD	16AN ATLS	$p p$, 7, 8 TeV
1.14±0.21 ^{+0.09+0.13} _{-0.05-0.09}	11 KHACHATRY...16G CMS		$p p$, 8 TeV, diff. x-section
1.55 ^{+0.33} _{-0.28}	12 AAD	14BC ATLS	$p p \rightarrow HX$, 7, 8 TeV
7.81 ^{+4.61} _{-4.42}	13 AAD	14BJ ATLS	$p p$, 8 TeV, diff. x-section
4.20 ^{+4.60} _{-4.20}	14 KHACHATRY...14P CMS		$p p$, 7, 8 TeV
1.8 ± 0.5	15 AAD	13AK ATLS	$p p$, 7 and 8 TeV
2.2 ± 0.7	16 AALTONEN	13L CDF	$p\bar{p} \rightarrow HX$, 1.96 TeV
1.5 ± 0.6	17 ABAZOV	13L D0	$p\bar{p} \rightarrow HX$, 1.96 TeV
1.54 ^{+0.46} _{-0.42}	18 AAD	12AI ATLS	$p p \rightarrow HX$, 7, 8 TeV
1.54 ^{+0.46} _{-0.42}	18 AAD	12AI ATLS	$p p \rightarrow HX$, 7 TeV
1.54 ^{+0.46} _{-0.42}	18 AAD	12AI ATLS	$p p \rightarrow HX$, 8 TeV
1.54 ^{+0.46} _{-0.42}	19 CHATRCHYAN 12N CMS		$p p \rightarrow HX$, 7, 8 TeV

¹ CMS 22 report combined results (see their Extended Data Table 2) using up to 138 fb⁻¹ of data at $E_{\text{cm}} = 13$ TeV, assuming $m_H = 125.38$ GeV. See their Fig. 2 right.

² AABOUD 18BO use 36.1 fb⁻¹ of $p p$ collisions at $E_{\text{cm}} = 13$ TeV. The signal strengths for the individual production modes are: $0.81^{+0.19}_{-0.18}$ for gluon fusion, $2.0^{+0.6}_{-0.5}$ for vector boson fusion, $0.7^{+0.9}_{-0.8}$ for VH production ($V = W, Z$), and 0.5 ± 0.6 for $t\bar{t}H$ and tH production. Other measurements of cross sections and couplings are summarized in their Section 10. The quoted values are given for $m_H = 125.09$ GeV.

- ³ AAD 16AN perform fits to the ATLAS and CMS data at $E_{\text{cm}} = 7$ and 8 TeV. The signal strengths for individual production processes are $1.10^{+0.23}_{-0.22}$ for gluon fusion, 1.3 ± 0.5 for vector boson fusion, $0.5^{+1.3}_{-1.2}$ for WH production, $0.5^{+3.0}_{-2.5}$ for ZH production, and $2.2^{+1.6}_{-1.3}$ for $t\bar{t}H$ production.
- ⁴ AAD 16AN: In the fit, relative production cross sections are fixed to those in the Standard Model. The quoted signal strength is given for $m_H = 125.09$ GeV.
- ⁵ AALTONEN 13M combine all Tevatron data from the CDF and D0 Collaborations with up to 10.0 fb^{-1} and 9.7 fb^{-1} , respectively, of $p\bar{p}$ collisions at $E_{\text{cm}} = 1.96$ TeV. The quoted signal strength is given for $m_H = 125$ GeV.
- ⁶ AAD 22N measure fiducial and differential cross sections of $pp \rightarrow H \rightarrow \gamma\gamma$ at $E_{\text{cm}} = 13$ TeV with 139 fb^{-1} data. The quoted results are given for $m_H = 125.09$ GeV. The inclusive fiducial $\sigma \cdot B$ is $67 \pm 5 \pm 4$ fb with their defined fiducial region. Other fiducial $\sigma \cdot B$ are in their Table 3. Differential $\sigma \cdot B$ are shown in their Figs. 8–13, 15, 25–32, 35, 36. Double-differential $\sigma \cdot B$ are in their Figs. 14, 33, 34. Modifications of the b - and c -quark Yukawa couplings to H , κ_b and κ_c at 95% CL are in their Table 6 and Fig. 18. Wilson coefficients at 95% CL are in their Table 7 and Fig. 21.
- ⁷ SIRUNYAN 21O measures cross sections and couplings with the $H \rightarrow \gamma\gamma$ channel using 137 fb^{-1} data at $E_{\text{cm}} = 13$ TeV. Results are given for $m_H = 125.38$ GeV. The signal strengths for individual production processes are given in their Fig. 16. Cross sections are given in their Tables 12 and 13 and Figs. 18 and 20, which are based on the simplified template cross section framework (reduced stage-1.2). Results in the κ -framework are given in their Fig. 22.
- ⁸ SIRUNYAN 19AT perform a combine fit to 35.9 fb^{-1} of data at $E_{\text{cm}} = 13$ TeV.
- ⁹ SIRUNYAN 19L measure fiducial and differential cross sections of the process $pp \rightarrow H \rightarrow \gamma\gamma$ at $E_{\text{cm}} = 13$ TeV with 35.9 fb^{-1} . See their Figs. 4–11.
- ¹⁰ SIRUNYAN 18DS use 35.9 fb^{-1} of $pp \rightarrow H$ collisions with $H \rightarrow \gamma\gamma$ at $E_{\text{cm}} = 13$ TeV. The Higgs mass is floated in the measurement of a signal strength. The result is $1.18^{+0.12}_{-0.11}(\text{stat.})^{+0.09}_{-0.07}(\text{syst.})^{+0.07}_{-0.06}(\text{theory})$, which is largely insensitive to the Higgs mass around 125 GeV.
- ¹¹ KHACHATRYAN 16G measure fiducial and differential cross sections of the process $pp \rightarrow HX$, $H \rightarrow \gamma\gamma$ at $E_{\text{cm}} = 8$ TeV with 19.7 fb^{-1} . See their Figs. 4–6 and Table 1 for data.
- ¹² AAD 14BC use 4.5 fb^{-1} of pp collisions at $E_{\text{cm}} = 7$ TeV and 20.3 fb^{-1} at $E_{\text{cm}} = 8$ TeV. The last uncertainty in the measurement is theory systematics. The quoted signal strength is given for $m_H = 125.4$ GeV. The signal strengths for the individual production modes are: 1.32 ± 0.38 for gluon fusion, 0.8 ± 0.7 for vector boson fusion, 1.0 ± 1.6 for WH production, $0.1^{+3.7}_{-0.1}$ for ZH production, and $1.6^{+2.7}_{-1.8}$ for $t\bar{t}H$ production.
- ¹³ AAD 14BJ measure fiducial and differential cross sections of the process $pp \rightarrow HX$, $H \rightarrow \gamma\gamma$ at $E_{\text{cm}} = 8$ TeV with 20.3 fb^{-1} . See their Table 3 and Figs. 3–12 for data.
- ¹⁴ KHACHATRYAN 14P use 5.1 fb^{-1} of pp collisions at $E_{\text{cm}} = 7$ TeV and 19.7 fb^{-1} at $E_{\text{cm}} = 8$ TeV. The last uncertainty in the measurement is theory systematics. The quoted signal strength is given for $m_H = 124.7$ GeV. The signal strength for the gluon fusion and $t\bar{t}H$ production mode is $1.13^{+0.37}_{-0.31}$, while the signal strength for the vector boson fusion and WH , ZH production mode is $1.16^{+0.63}_{-0.58}$.
- ¹⁵ AAD 13AK use 4.7 fb^{-1} of pp collisions at $E_{\text{cm}} = 7$ TeV and 20.7 fb^{-1} at $E_{\text{cm}} = 8$ TeV. The quoted signal strength is given for $m_H = 125.5$ GeV.
- ¹⁶ AALTONEN 13L combine all CDF results with $9.45\text{--}10.0 \text{ fb}^{-1}$ of $p\bar{p}$ collisions at $E_{\text{cm}} = 1.96$ TeV. The quoted signal strength is given for $m_H = 125$ GeV.
- ¹⁷ ABAZOV 13L combine all D0 results with up to 9.7 fb^{-1} of $p\bar{p}$ collisions at $E_{\text{cm}} = 1.96$ TeV. The quoted signal strength is given for $m_H = 125$ GeV.

¹⁸ AAD 12AI obtain results based on 4.8 fb^{-1} of pp collisions at $E_{\text{cm}} = 7 \text{ TeV}$ and 5.9 fb^{-1} at $E_{\text{cm}} = 8 \text{ TeV}$. The quoted signal strengths are given for $m_H = 126 \text{ GeV}$. See also AAD 12DA.

¹⁹ CHATRCHYAN 12N obtain results based on 5.1 fb^{-1} of pp collisions at $E_{\text{cm}} = 7 \text{ TeV}$ and 5.3 fb^{-1} at $E_{\text{cm}} = 8 \text{ TeV}$. The quoted signal strength is given for $m_H = 125.5 \text{ GeV}$. See also CHATRCHYAN 13Y.

$c\bar{c}$ Final State

VALUE	CL%	DOCUMENT ID	TECN	COMMENT
$8 \pm 22 \text{ OUR AVERAGE}$		Error includes scale factor of 1.9.		
– $9 \pm 10 \pm 11$	1,2 AAD	22W ATLS	$pp \rightarrow WH/ZH$, 13 TeV	
$37 \pm 17^{+11}_{-9}$	3 SIRUNYAN	20AE CMS	pp , 13 TeV	

• • • We do not use the following data for averages, fits, limits, etc. • • •

– $9 \pm 10 \pm 12$	1,4 AAD	22W ATLS	$pp \rightarrow WH/ZH$, 13 TeV
< 110	95	5 AABOUD	18M ATLS pp , 13 TeV

¹ AAD 22W search for VH , $H \rightarrow c\bar{c}$ ($V = W, Z$) using 139 fb^{-1} of pp collision data at $E_{\text{cm}} = 13 \text{ TeV}$. The results are given for $m_H = 125 \text{ GeV}$.

² The analysis of VH , $H \rightarrow c\bar{c}$ is combined with VH , $H \rightarrow b\bar{b}$ (AAD 21AB). The ratio $-\kappa_c/\kappa_b-$ is constrained to be less than 4.5 at 95% CL. See their Fig. 7.

³ SIRUNYAN 20AE use 35.9 fb^{-1} of pp collisions at $E_{\text{cm}} = 13 \text{ TeV}$. The measured best fit value of $\sigma(pp \rightarrow VH) \cdot B(H \rightarrow c\bar{c})$ is $2.40^{+1.12+0.65}_{-1.11-0.61} \text{ pb}$ (equivalent to < 4.5 pb at 95% CL upper limit, i.e. 70 times the standard model), where V is $W \rightarrow \ell\nu$, $Z \rightarrow \ell\ell$, or $Z \rightarrow \nu\nu$ ($\ell = e, \mu$). The quoted values are given for $m_H = 125 \text{ GeV}$.

⁴ The upper limit at 95% CL is 26 times the SM prediction. See their Fig. 2. The constraint on the charm Yukawa coupling modifier κ_c is measured to be $|\kappa_c| < 8.5$ at 95% CL. See their Fig. 4.

⁵ AABOUD 18M use 36.1 fb^{-1} of pp collisions at $E_{\text{cm}} = 13 \text{ TeV}$. The upper limit on $\sigma(pp \rightarrow ZH) \cdot B(H \rightarrow c\bar{c})$ is 2.7 pb at 95% CL. This corresponds to 110 times the standard model. The quoted values are given for $m_H = 125 \text{ GeV}$.

$b\bar{b}$ Final State

VALUE	DOCUMENT ID	TECN	COMMENT
$0.99 \pm 0.12 \text{ OUR AVERAGE}$			
$1.05^{+0.22}_{-0.21}$	1 CMS	22 CMS	pp , 13 TeV
$1.02^{+0.12+0.14}_{-0.11-0.13}$	2 AAD	21AB ATLS	$pp \rightarrow HW/HZ$, $H \rightarrow b\bar{b}$, 13 TeV, 139 fb^{-1}
$0.95 \pm 0.32^{+0.20}_{-0.17}$	3 AAD	21AJ ATLS	VBF, $H \rightarrow b\bar{b}$, pp , 13 TeV, 126 fb^{-1}
$0.70^{+0.29}_{-0.27}$	4,5 AAD	16AN LHC	pp , 7, 8 TeV
$1.59^{+0.69}_{-0.72}$	6 AALTONEN	13M TEVA	$p\bar{p} \rightarrow HX$, 1.96 TeV

• • • We do not use the following data for averages, fits, limits, etc. • • •

0.8 ± 3.2	7 AAD	22X ATLS	boosted $H \rightarrow b\bar{b}$, pp , 13 TeV
$0.95 \pm 0.18^{+0.19}_{-0.18}$	2 AAD	21AB ATLS	$pp \rightarrow HW$, $H \rightarrow b\bar{b}$, 13 TeV, 139 fb^{-1}
$1.08 \pm 0.17^{+0.18}_{-0.15}$	2 AAD	21AB ATLS	$pp \rightarrow HZ$, $H \rightarrow b\bar{b}$, 13 TeV, 139 fb^{-1}

$0.72^{+0.29}_{-0.28}{}^{+0.26}_{-0.22}$	⁸ AAD	21H ATLS	$p\bar{p} \rightarrow HW/HZ, H \rightarrow b\bar{b}$, boosted W/Z , 13 TeV, 139 fb^{-1}
1.3 ± 1.0	⁹ AAD	21M ATLS	$VBF+\gamma, H \rightarrow b\bar{b}, p\bar{p}$, 13 TeV, 132 fb^{-1}
$3.7 \pm 1.2 {}^{+0.11}_{-0.9}$	¹⁰ SIRUNYAN	20BL CMS	boosted $H \rightarrow b\bar{b}$, $p\bar{p}$, 13 TeV
	¹¹ AABOUD	19U ATLS	$p\bar{p} \rightarrow VH, H \rightarrow b\bar{b}$, 13 TeV, cross sections
1.12 ± 0.29	¹² SIRUNYAN	19AT CMS	$p\bar{p}$, 13 TeV
$1.16^{+0.27}_{-0.25}$	¹³ AABOUD	18BN ATLS	$p\bar{p} \rightarrow HW/HZ, H \rightarrow b\bar{b}$, 13 TeV, 79.8 fb^{-1}
$0.98^{+0.22}_{-0.21}$	¹⁴ AABOUD	18BN ATLS	$p\bar{p} \rightarrow HW/HZ, H \rightarrow b\bar{b}$, 7, 8, 13 TeV
1.01 ± 0.20	¹⁵ AABOUD	18BN ATLS	$p\bar{p} \rightarrow HX, ggF, VBF, VH, t\bar{t}H$ 7, 8, 13 TeV
$2.5 {}^{+1.4}_{-1.3}$	^{16,17} AABOUD	18BQ ATLS	$p\bar{p} \rightarrow HX, VBF, ggF, VH, t\bar{t}H$, 13 TeV
$3.0 {}^{+1.7}_{-1.6}$	^{16,18} AABOUD	18BQ ATLS	$p\bar{p} \rightarrow HX, VBF$, 13 TeV
	¹⁹ AALTONEN	18C CDF	$p\bar{p} \rightarrow HX$, 1.96 TeV
$1.19^{+0.40}_{-0.38}$	²⁰ SIRUNYAN	18AE CMS	$p\bar{p} \rightarrow HW/HZ, H \rightarrow b\bar{b}$, 13 TeV
$1.06^{+0.31}_{-0.29}$	²¹ SIRUNYAN	18AE CMS	$p\bar{p} \rightarrow HW/HZ, H \rightarrow b\bar{b}$, 7, 8, 13 TeV
1.06 ± 0.26	²² SIRUNYAN	18DB CMS	$p\bar{p} \rightarrow HW/HZ, H \rightarrow b\bar{b}$, 13 TeV, 77.2 fb^{-1}
1.01 ± 0.22	²³ SIRUNYAN	18DB CMS	$p\bar{p} \rightarrow HW/HZ, H \rightarrow b\bar{b}$, 7, 8, 13 TeV
1.04 ± 0.20	²⁴ SIRUNYAN	18DB CMS	$p\bar{p} \rightarrow HX, ggF, VBF, VH, t\bar{t}H$ 7, 8, 13 TeV
$2.3 {}^{+1.8}_{-1.6}$	²⁵ SIRUNYAN	18E CMS	$p\bar{p} \rightarrow HX$, boosted, 13 TeV
$1.20^{+0.24}_{-0.23}{}^{+0.34}_{-0.28}$	²⁶ AABOUD	17BA ATLS	$p\bar{p} \rightarrow HW/ZX, H \rightarrow b\bar{b}$, 13 TeV, 36.1 fb^{-1}
$0.90 \pm 0.18 {}^{+0.21}_{-0.19}$	²⁷ AABOUD	17BA ATLS	$p\bar{p} \rightarrow HW/ZX, H \rightarrow b\bar{b}$, 7, 8, 13 TeV
$-0.8 \pm 1.3 {}^{+1.8}_{-1.9}$	²⁸ AABOUD	16X ATLS	$p\bar{p} \rightarrow HX, VBF$, 8 TeV
0.62 ± 0.37	⁵ AAD	16AN ATLS	$p\bar{p}$, 7, 8 TeV
$0.81 {}^{+0.45}_{-0.43}$	⁵ AAD	16AN CMS	$p\bar{p}$, 7, 8 TeV
$0.63 {}^{+0.31}_{-0.30}{}^{+0.24}_{-0.23}$	²⁹ AAD	16K ATLS	$p\bar{p}$, 7, 8 TeV
$0.52 \pm 0.32 \pm 0.24$	³⁰ AAD	15G ATLS	$p\bar{p} \rightarrow HW/ZX$, 7, 8 TeV
$2.8 {}^{+1.6}_{-1.4}$	³¹ KHACHATRY...15Z	CMS	$p\bar{p} \rightarrow HX, VBF$, 8 TeV
$1.03 {}^{+0.44}_{-0.42}$	³² KHACHATRY...15Z	CMS	$p\bar{p}$, 8 TeV, combined
1.0 ± 0.5	³³ CHATRCHYAN14AI	CMS	$p\bar{p} \rightarrow HW/ZX$, 7, 8 TeV
$1.72 {}^{+0.92}_{-0.87}$	³⁴ AALTONEN	13L CDF	$p\bar{p} \rightarrow HX$, 1.96 TeV
$1.23 {}^{+1.24}_{-1.17}$	³⁵ ABAZOV	13L D0	$p\bar{p} \rightarrow HX$, 1.96 TeV
0.5 ± 2.2	³⁶ AAD	12AI ATLS	$p\bar{p} \rightarrow HW/ZX$, 7 TeV

³⁷ AALTONEN 12T TEVA $p\bar{p} \rightarrow HW/ZX$, 1.96 TeV
 $0.48^{+0.81}_{-0.70}$

³⁸ CHATRCHYAN 12N CMS $pp \rightarrow HW/ZX$, 7, 8 TeV

¹ CMS 22 report combined results (see their Extended Data Table 2) using up to 138 fb^{-1} of data at $E_{\text{cm}} = 13$ TeV, assuming $m_H = 125.38$ GeV. See their Fig. 2 right.

² AAD 21AB search for VH , $H \rightarrow b\bar{b}$ ($V = W, Z$) using 139 fb^{-1} of pp collision data at $E_{\text{cm}} = 13$ TeV. The results are given for $m_H = 125$ GeV. Cross sections are given in their Table 13 and Fig. 7, which are based on the simplified template cross section framework (reduced stage-1.2). Wilson coefficients of the Warsaw-basis operators are given in their Fig. 9.

³ AAD 21AJ present measurements of $H \rightarrow b\bar{b}$ in the VBF production mode. The inclusive VBF cross sections with and without the branching ratio of $H \rightarrow b\bar{b}$ are $2.07 \pm 0.70^{+0.46}_{-0.37}$ fb and $3.56 \pm 1.21^{+0.80}_{-0.64}$ fb, respectively. The latter is obtained assuming the SM value of $B(H \rightarrow b\bar{b}) = 0.5809$ and $m_H = 125$ GeV.

⁴ AAD 16AN perform fits to the ATLAS and CMS data at $E_{\text{cm}} = 7$ and 8 TeV. The signal strengths for individual production processes are 1.0 ± 0.5 for WH production, 0.4 ± 0.4 for ZH production, and 1.1 ± 1.0 for $t\bar{t}H$ production.

⁵ AAD 16AN: In the fit, relative production cross sections are fixed to those in the Standard Model. The quoted signal strength is given for $m_H = 125.09$ GeV.

⁶ AALTONEN 13M combine all Tevatron data from the CDF and D0 Collaborations with up to 10.0 fb^{-1} and 9.7 fb^{-1} , respectively, of $p\bar{p}$ collisions at $E_{\text{cm}} = 1.96$ TeV. The quoted signal strength is given for $m_H = 125$ GeV.

⁷ AAD 22X measure cross sections using a boosted $H \rightarrow b\bar{b}$ with large-radius jets. The data is 136 fb^{-1} of pp collisions at $E_{\text{cm}} = 13$ TeV. All the results are given for $m_H = 125$ GeV. The inclusive signal strength is given using data with a H candidate jet $p_T > 250$ GeV. The fiducial H production cross section ($p_T(H) > 450$ GeV and $|y(H)| < 2$) is < 115 fb (95% CL) and the upper limits for other four different p_T regions are shown in their Fig 12. The measured fiducial H production cross section ($p_T(H) > 1$ TeV) is $2.3 \pm 3.9(\text{stat}) \pm 1.3(\text{syst}) \pm 0.5(\text{theory})$ fb.

⁸ AAD 21H present measurements of $H \rightarrow b\bar{b}$ with a boosted vector boson ($p_T > 250$ GeV) using 139 fb^{-1} of pp collision data at $E_{\text{cm}} = 13$ TeV. Cross sections are given in their Table 6 and Fig. 4, which are based on the simplified template cross section framework (reduced stage-1.2). Wilson coefficients of the Warsaw-basis operators are given in their Fig. 5.

⁹ AAD 21M search for VBF+ γ , $H \rightarrow b\bar{b}$ using 132 fb^{-1} of pp collision data at $E_{\text{cm}} = 13$ TeV.

¹⁰ SIRUNYAN 20BL search for boosted $H \rightarrow b\bar{b}$ (a H candidate jet $p_T > 450$ GeV) using 137 fb^{-1} of pp collision data at $E_{\text{cm}} = 13$ TeV. The quoted signal strength corresponds to a significance of 2.5 standard deviations and is given for $m_H = 125$ GeV. A differential fiducial cross section as a function of Higgs boson p_T for ggF is shown in their Fig. 7, assuming the other production modes occur at the expected SM rates. The reported value is $3.7 \pm 1.2^{+0.8+0.8}_{-0.7-0.5}$ where the last uncertainty comes from theoretical modeling. We have combined the systematic uncertainties in quadrature.

¹¹ AABOUD 19U measure cross sections of $pp \rightarrow VH$, $H \rightarrow b\bar{b}$ production as a function of the gauge boson transverse momentum using data of 79.8 fb^{-1} . The kinematic fiducial volumes used is based on the simplified template cross section framework (reduced stage-1). See their Table 3 and Fig. 3.

¹² SIRUNYAN 19AT perform a combine fit to 35.9 fb^{-1} of data at $E_{\text{cm}} = 13$ TeV.

¹³ AABOUD 18BN search for VH , $H \rightarrow b\bar{b}$ ($V = W, Z$) using 79.8 fb^{-1} of pp collision data at $E_{\text{cm}} = 13$ TeV. The quoted signal strength corresponds to a significance of 4.9 standard deviations and is given for $m_H = 125$ GeV.

¹⁴ AABOUD 18BN combine results of 79.8 fb^{-1} at $E_{\text{cm}} = 13$ TeV with results of VH at $E_{\text{cm}} = 7$ and 8 TeV.

- 15 AABOUD 18BN combine results of VH at $E_{cm} = 7, 8$ and 13 TeV with results of VBF (+gluon fusion) and $t\bar{t}H$ at $E_{cm} = 7, 8$, and 13 TeV to perform a search for the $H \rightarrow b\bar{b}$ decay. The quoted signal strength assumes a SM production strength and corresponds to a significance of 5.4 standard deviations.
- 16 AABOUD 18BQ search for $H \rightarrow b\bar{b}$ produced through vector-boson fusion (VBF) and VBF+ γ with 30.6 fb^{-1} pp collision data at $E_{cm} = 13$ TeV. The quoted signal strength is given for $m_H = 125$ GeV.
- 17 The signal strength is measured including all production modes (VBF, ggF, VH , $t\bar{t}H$).
- 18 The signal strength is measured for VBF-only and others (ggF, VH , $t\bar{t}H$) are constrained to Standard Model expectations with uncertainties described in their Section VIII B.
- 19 AALTONEN 18C use 5.4 fb^{-1} of $p\bar{p}$ collisions at $E_{cm} = 1.96$ TeV. The upper limit at 95% CL on $p\bar{p} \rightarrow H \rightarrow b\bar{b}$ is 33 times the SM prediction, which corresponds to a cross section of 40.6 pb .
- 20 SIRUNYAN 18AE use 35.9 fb^{-1} of pp collision data at $E_{cm} = 13$ TeV. The quoted signal strength corresponds to 3.3 standard deviations and is given for $m_H = 125.09$ GeV.
- 21 SIRUNYAN 18AE combine the result of 35.9 fb^{-1} at $E_{cm} = 13$ TeV with the results obtained from data of up to 5.1 fb^{-1} at $E_{cm} = 7$ TeV and up to 18.9 fb^{-1} at $E_{cm} = 8$ TeV (CHATRCHYAN 14AI and KHACHATRYAN 15Z). The quoted signal strength corresponds to 3.8 standard deviations and is given for $m_H = 125.09$ GeV.
- 22 SIRUNYAN 18DB search for VH , $H \rightarrow b\bar{b}$ ($V = W, Z$) using 77.2 fb^{-1} of pp collision data at $E_{cm} = 13$ TeV. The quoted signal strength corresponds to a significance of 4.4 standard deviations and is given for $m_H = 125.09$ GeV.
- 23 SIRUNYAN 18DB combine the result of 77.2 fb^{-1} at $E_{cm} = 13$ TeV with the results obtained from data of up to 5.1 fb^{-1} at $E_{cm} = 7$ TeV and up to 18.9 fb^{-1} at $E_{cm} = 8$ TeV. The quoted signal strength corresponds to a significance of 4.8 standard deviations and is given for $m_H = 125.09$ GeV.
- 24 SIRUNYAN 18DB combine results of 77.2 fb^{-1} at $E_{cm} = 13$ TeV with results of gluon fusion (ggF), VBF and $t\bar{t}H$ at $E_{cm} = 7$ TeV, 8 TeV and 13 TeV to perform a search for the $H \rightarrow b\bar{b}$ decay. The quoted signal strength assumes a SM production strength and corresponds to a significance of 5.6 standard deviations and is given for $m_H = 125.09$ GeV.
- 25 SIRUNYAN 18E use 35.9 fb^{-1} at $E_{cm} = 13$ TeV. The quoted signal strength is given for $m_H = 125$ GeV. They measure $\sigma \cdot B$ for gluon fusion production of $H \rightarrow b\bar{b}$ with $p_T > 450$ GeV, $|\eta| < 2.5$ to be $74 \pm 48^{+17}_{-10}$ fb.
- 26 AABOUD 17BA use 36.1 fb^{-1} at $E_{cm} = 13$ TeV. The quoted signal strength is given for $m_H = 125$ GeV. They give $\sigma(WH) \cdot B(H \rightarrow b\bar{b}) = 1.08^{+0.54}_{-0.47}$ pb and $\sigma(ZH) \cdot B(H \rightarrow b\bar{b}) = 0.57^{+0.26}_{-0.23}$ pb.
- 27 AABOUD 17BA combine 7, 8 and 13 TeV analyses. The quoted signal strength is given for $m_H = 125$ GeV.
- 28 AABOUD 16X search for vector-boson fusion production of H decaying to $b\bar{b}$ in 20.2 fb^{-1} of pp collisions at $E_{cm} = 8$ TeV. The quoted signal strength is given for $m_H = 125$ GeV.
- 29 AAD 16K use up to 4.7 fb^{-1} of pp collisions at $E_{cm} = 7$ TeV and up to 20.3 fb^{-1} at $E_{cm} = 8$ TeV. The quoted signal strength is given for $m_H = 125.36$ GeV.
- 30 AAD 15G use 4.7 fb^{-1} of pp collisions at $E_{cm} = 7$ TeV and 20.3 fb^{-1} at $E_{cm} = 8$ TeV. The quoted signal strength is given for $m_H = 125.36$ GeV.
- 31 KHACHATRYAN 15Z search for vector-boson fusion production of H decaying to $b\bar{b}$ in up to 19.8 fb^{-1} of pp collisions at $E_{cm} = 8$ TeV. The quoted signal strength is given for $m_H = 125$ GeV.
- 32 KHACHATRYAN 15Z combined vector boson fusion, WH , ZH production, and $t\bar{t}H$ production results. The quoted signal strength is given for $m_H = 125$ GeV.

- ³³ CHATRCHYAN 14AI use up to 5.1 fb^{-1} of $p\bar{p}$ collisions at $E_{\text{cm}} = 7 \text{ TeV}$ and up to 18.9 fb^{-1} at $E_{\text{cm}} = 8 \text{ TeV}$. The quoted signal strength is given for $m_H = 125 \text{ GeV}$. See also CHATRCHYAN 14AJ.
- ³⁴ AALTONEN 13L combine all CDF results with $9.45\text{--}10.0 \text{ fb}^{-1}$ of $p\bar{p}$ collisions at $E_{\text{cm}} = 1.96 \text{ TeV}$. The quoted signal strength is given for $m_H = 125 \text{ GeV}$.
- ³⁵ ABAZOV 13L combine all D0 results with up to 9.7 fb^{-1} of $p\bar{p}$ collisions at $E_{\text{cm}} = 1.96 \text{ TeV}$. The quoted signal strength is given for $m_H = 125 \text{ GeV}$.
- ³⁶ AAD 12AI obtain results based on $4.6\text{--}4.8 \text{ fb}^{-1}$ of $p\bar{p}$ collisions at $E_{\text{cm}} = 7 \text{ TeV}$. The quoted signal strengths are given in their Fig. 10 for $m_H = 126 \text{ GeV}$. See also Fig. 13 of AAD 12DA.
- ³⁷ AALTONEN 12T combine AALTONEN 12Q, AALTONEN 12R, AALTONEN 12S, ABAZOV 12O, ABAZOV 12P, and ABAZOV 12K. An excess of events over background is observed which is most significant in the region $m_H = 120\text{--}135 \text{ GeV}$, with a local significance of up to 3.3σ . The local significance at $m_H = 125 \text{ GeV}$ is 2.8σ , which corresponds to $(\sigma(HW) + \sigma(HZ)) \cdot B(H \rightarrow b\bar{b}) = (0.23^{+0.09}_{-0.08}) \text{ pb}$, compared to the Standard Model expectation at $m_H = 125 \text{ GeV}$ of $0.12 \pm 0.01 \text{ pb}$. Superseded by AALTONEN 13M.
- ³⁸ CHATRCHYAN 12N obtain results based on 5.0 fb^{-1} of $p\bar{p}$ collisions at $E_{\text{cm}}=7 \text{ TeV}$ and 5.1 fb^{-1} at $E_{\text{cm}}=8 \text{ TeV}$. The quoted signal strength is given for $m_H=125.5 \text{ GeV}$. See also CHATRCHYAN 13Y.

$\mu^+ \mu^-$ Final State

VALUE	CL %	DOCUMENT ID	TECN	COMMENT
1.21±0.35 OUR AVERAGE				
$1.21^{+0.45}_{-0.42}$		¹ CMS	22	CMS $p\bar{p}$, 13 TeV
1.2 ± 0.6		² AAD	21	ATLS $p\bar{p}$, 13 TeV
• • • We do not use the following data for averages, fits, limits, etc. • • •				
$1.19^{+0.40+0.15}_{-0.39-0.14}$		³ SIRUNYAN	21C	CMS $p\bar{p}$, 13 TeV
$0.68^{+1.25}_{-1.24}$		⁴ SIRUNYAN	19AT	CMS $p\bar{p}$, 13 TeV
0.7 ± 1.0	$+0.2$ -0.1	⁵ SIRUNYAN	19E	CMS $p\bar{p}$, 13 TeV, 35.9 fb^{-1}
1.0 ± 1.0	± 0.1	⁵ SIRUNYAN	19E	CMS $p\bar{p}$, 7, 8, 13 TeV
-0.1 ± 1.4		⁶ AABOUD	17Y	ATLS $p\bar{p}$, 7, 8, 13 TeV
-0.1 ± 1.5		⁶ AABOUD	17Y	ATLS $p\bar{p}$, 13 TeV
0.1 ± 2.5		⁷ AAD	16AN LHC	$p\bar{p}$, 7, 8 TeV
-0.6 ± 3.6		⁷ AAD	16AN ATLS	$p\bar{p}$, 7, 8 TeV
$0.9^{+3.6}_{-3.5}$		⁷ AAD	16AN CMS	$p\bar{p}$, 7, 8 TeV
< 7.4	95	⁸ KHACHATRY...15H	CMS	$p\bar{p} \rightarrow HX$, 7, 8 TeV
< 7.0	95	⁹ AAD	14AS	ATLS $p\bar{p} \rightarrow HX$, 7, 8 TeV

¹ CMS 22 report combined results (see their Extended Data Table 2) using up to 138 fb^{-1} of data at $E_{\text{cm}} = 13 \text{ TeV}$, assuming $m_H = 125.38 \text{ GeV}$. See their Fig. 2 right.

² AAD 21 search for $H \rightarrow \mu^+ \mu^-$ using 139 fb^{-1} of $p\bar{p}$ collision data at $E_{\text{cm}} = 13 \text{ TeV}$. The quoted signal strength corresponds to a significance of 2.0 standard deviations and is given for $m_H = 125.09 \text{ GeV}$. The upper limit on the cross section times branching fraction is 2.2 times the SM prediction at 95% CL, which corresponds to the branching fraction upper limit of 4.7×10^{-4} (assuming SM production cross sections).

³ SIRUNYAN 21 search for $H \rightarrow \mu^+ \mu^-$ using 137 fb^{-1} of $p\bar{p}$ collision data at $E_{\text{cm}} = 13 \text{ TeV}$. The quoted signal strength corresponds to a significance of 3.0 standard deviations and is given for $m_H = 125.38 \text{ GeV}$.

⁴ SIRUNYAN 19AT perform a combine fit to 35.9 fb^{-1} of data at $E_{\text{cm}} = 13 \text{ TeV}$.

⁵ SIRUNYAN 19E search for $H \rightarrow \mu^+ \mu^-$ using 35.9 fb^{-1} of $p p$ collisions at $E_{\text{cm}} = 13 \text{ TeV}$ and combine with results of 7 TeV (5.0 fb^{-1}) and 8 TeV (19.7 fb^{-1}). The upper limit at 95% CL on the signal strength is 2.9, which corresponds to the SM Higgs boson branching fraction to a muon pair of 6.4×10^{-4} .

⁶ AABOUD 17Y use 36.1 fb^{-1} of $p p$ collisions at $E_{\text{cm}} = 13 \text{ TeV}$, 20.3 fb^{-1} at 8 TeV and 4.5 fb^{-1} at 7 TeV. The quoted signal strength is given for $m_H = 125 \text{ GeV}$.

⁷ AAD 16AN: In the fit, relative production cross sections are fixed to those in the Standard Model. The quoted signal strength is given for $m_H = 125.09 \text{ GeV}$.

⁸ KHACHATRYAN 15H use 5.0 fb^{-1} of $p p$ collisions at $E_{\text{cm}} = 7 \text{ TeV}$ and 19.7 fb^{-1} at 8 TeV. The quoted signal strength is given for $m_H = 125 \text{ GeV}$.

⁹ AAD 14AS search for $H \rightarrow \mu^+ \mu^-$ in 4.5 fb^{-1} of $p p$ collisions at $E_{\text{cm}} = 7 \text{ TeV}$ and 20.3 fb^{-1} at $E_{\text{cm}} = 8 \text{ TeV}$. The quoted signal strength is given for $m_H = 125.5 \text{ GeV}$.

$\tau^+ \tau^-$ Final State

VALUE	DOCUMENT ID	TECN	COMMENT
0.91 ± 0.09 OUR AVERAGE			
0.85 ± 0.10	¹ CMS	22 CMS	$p p$, 13 TeV
$1.09^{+0.18}_{-0.17} {}^{+0.26}_{-0.22} {}^{+0.16}_{-0.11}$	² AABOUD	19AQ ATLS	$p p$, 13 TeV
$1.11^{+0.24}_{-0.22}$	^{3,4} AAD	16AN LHC	$p p$, 7, 8 TeV
$1.68^{+2.28}_{-1.68}$	⁵ AALTONEN	13M TEVA	$p \bar{p} \rightarrow H X$, 1.96 TeV
• • • We do not use the following data for averages, fits, limits, etc. • • •			
$2.5^{+1.4}_{-1.3}$	⁶ AAD	22Q ATLS	$p p$, 13 TeV
$1.24^{+0.29}_{-0.27}$	⁷ SIRUNYAN	19AF CMS	$p p \rightarrow H W/H Z$, $H \rightarrow \tau \tau$, 13 TeV
$1.02^{+0.26}_{-0.24}$	⁸ SIRUNYAN	19AF CMS	$p p$, 13 TeV
$1.09^{+0.27}_{-0.26}$	⁹ SIRUNYAN	19AT CMS	$p p$, 13 TeV
0.98 ± 0.18	¹⁰ SIRUNYAN	18Y CMS	$p p$, 13 TeV
2.3 ± 1.6	¹¹ SIRUNYAN	18Y CMS	$p p$, 7, 8, 13 TeV
$1.41^{+0.40}_{-0.36}$	¹² AAD	16AC ATLS	$p p \rightarrow H W/Z X$, 8 TeV
$0.88^{+0.30}_{-0.28}$	⁴ AAD	16AN ATLS	$p p$, 7, 8 TeV
$1.44^{+0.30}_{-0.29} {}^{+0.29}_{-0.23}$	¹³ AAD	16K ATLS	$p p$, 7, 8 TeV
$1.43^{+0.27}_{-0.26} {}^{+0.32}_{-0.25} \pm 0.09$	¹⁴ AAD	15AH ATLS	$p p \rightarrow H X$, 7, 8 TeV
0.78 ± 0.27	¹⁵ CHATRCHYAN	14K CMS	$p p \rightarrow H X$, 7, 8 TeV
$0.00^{+8.44}_{-0.00}$	¹⁶ AALTONEN	13L CDF	$p \bar{p} \rightarrow H X$, 1.96 TeV
$3.96^{+4.11}_{-3.38}$	¹⁷ ABAZOV	13L D0	$p \bar{p} \rightarrow H X$, 1.96 TeV
$0.4^{+1.6}_{-2.0}$	¹⁸ AAD	12AI ATLS	$p p \rightarrow H X$, 7 TeV
$0.09^{+0.76}_{-0.74}$	¹⁹ CHATRCHYAN	12N CMS	$p p \rightarrow H X$, 7, 8 TeV

¹ CMS 22 report combined results (see their Extended Data Table 2) using up to 138 fb^{-1} of data at $E_{\text{cm}} = 13 \text{ TeV}$, assuming $m_H = 125.38 \text{ GeV}$. See their Fig. 2 right.

² AABOUD 19AQ use 36.1 fb^{-1} of data. The first, second and third quoted errors are statistical, experimental systematic and theory systematic uncertainties, respectively. The quoted signal strength is given for $m_H = 125 \text{ GeV}$ and corresponds to 4.4 standard deviations. Combining with 7 TeV and 8 TeV results (AAD 15AH), the observed significance is 6.4 standard deviations. The cross sections in the $H \rightarrow \tau\tau$ decay channel ($m_H = 125 \text{ GeV}$) are measured to $3.77^{+0.60}_{-0.59} \text{ (stat)}^{+0.87}_{-0.74} \text{ (syst)}$ pb for the inclusive, $0.28 \pm 0.09^{+0.11}_{-0.09}$ pb for VBF, and $3.1 \pm 1.0^{+1.6}_{-1.3}$ pb for gluon-fusion production. See their Table XI for the cross sections in the framework of simplified template cross sections.

³ AAD 16AN perform fits to the ATLAS and CMS data at $E_{\text{cm}} = 7$ and 8 TeV. The signal strengths for individual production processes are 1.0 ± 0.6 for gluon fusion, 1.3 ± 0.4 for vector boson fusion, -1.4 ± 1.4 for WH production, $2.2^{+2.2}_{-1.8}$ for ZH production, and $-1.9^{+3.7}_{-3.3}$ for $t\bar{t}H$ production.

⁴ AAD 16AN: In the fit, relative production cross sections are fixed to those in the Standard Model. The quoted signal strength is given for $m_H = 125.09 \text{ GeV}$.

⁵ AALTONEN 13M combine all Tevatron data from the CDF and D0 Collaborations with up to 10.0 fb^{-1} and 9.7 fb^{-1} , respectively, of $p\bar{p}$ collisions at $E_{\text{cm}} = 1.96 \text{ TeV}$. The quoted signal strength is given for $m_H = 125 \text{ GeV}$.

⁶ AAD 22Q measure cross sections of $pp \rightarrow H \rightarrow \tau\tau$ at $E_{\text{cm}} = 13 \text{ TeV}$ with 139 fb^{-1} data. The quoted results are given for $m_H = 125.09 \text{ GeV}$ and $|y(H)| < 2.5$ is required. The inclusive fiducial $\sigma \cdot B$ is $2.94 \pm 0.21^{+0.37}_{-0.32}$ pb. The fiducial $\sigma \cdot B$ for the four dominant production modes are $2.65 \pm 0.41^{+0.91}_{-0.67}$ pb for ggF, $0.197 \pm 0.028^{+0.032}_{-0.026}$ pb for VBF, $0.115 \pm 0.058^{+0.042}_{-0.040}$ pb for VH , $0.033 \pm 0.031^{+0.022}_{-0.017}$ pb for $t\bar{t}H$. The cross sections using simplified template cross section framework (STXS) are given in their Fig. 14(a) and Table 15. The STXS bins (a reduced stage 1.2) are defined in their Fig. 1.

⁷ SIRUNYAN 19AF use 35.9 fb^{-1} of data. The quoted signal strength is given for $m_H = 125 \text{ GeV}$ and corresponds to 2.3 standard deviations.

⁸ SIRUNYAN 19AF use 35.9 fb^{-1} of data. HW/Z channels are added with a few updates on gluon fusion and vector boson fusion with respect to SIRUNYAN 18Y. The quoted signal strength is given for $m_H = 125 \text{ GeV}$ and corresponds to 5.5 standard deviations. The signal strengths for the individual production modes are: $1.12^{+0.53}_{-0.50}$ for gluon fusion, $1.13^{+0.45}_{-0.42}$ for vector boson fusion, $3.39^{+1.68}_{-1.54}$ for WH and $1.23^{+1.62}_{-1.35}$ for ZH . See their Fig. 7 for other couplings (κ_V, κ_f).

⁹ SIRUNYAN 19AT perform a combine fit to 35.9 fb^{-1} of data at $E_{\text{cm}} = 13 \text{ TeV}$. This combination is based on SIRUNYAN 18Y.

¹⁰ SIRUNYAN 18Y use 35.9 fb^{-1} of pp collisions at $E_{\text{cm}} = 13 \text{ TeV}$. The quoted signal strength is given for $m_H = 125.09 \text{ GeV}$ and corresponds to 4.9 standard deviations.

¹¹ SIRUNYAN 18Y combine the result of 35.9 fb^{-1} at $E_{\text{cm}} = 13 \text{ TeV}$ with the results obtained from data of 4.9 fb^{-1} at $E_{\text{cm}} = 7 \text{ TeV}$ and 19.7 fb^{-1} at $E_{\text{cm}} = 8 \text{ TeV}$ (KHACHATRYAN 15AM). The quoted signal strength is given for $m_H = 125.09 \text{ GeV}$ and corresponds to 5.9 standard deviations.

¹² AAD 16AC measure the signal strength with $pp \rightarrow HW/ZX$ processes using 20.3 fb^{-1} of $E_{\text{cm}} = 8 \text{ TeV}$. The quoted signal strength is given for $m_H = 125 \text{ GeV}$.

¹³ AAD 16K use up to 4.7 fb^{-1} of pp collisions at $E_{\text{cm}} = 7 \text{ TeV}$ and up to 20.3 fb^{-1} at $E_{\text{cm}} = 8 \text{ TeV}$. The quoted signal strength is given for $m_H = 125.36 \text{ GeV}$.

¹⁴ AAD 15AH use 4.5 fb^{-1} of pp collisions at $E_{\text{cm}} = 7 \text{ TeV}$ and 20.3 fb^{-1} at $E_{\text{cm}} = 8 \text{ TeV}$. The third uncertainty in the measurement is theory systematics. The signal strength for the gluon fusion mode is $2.0 \pm 0.8^{+1.2}_{-0.8} \pm 0.3$ and that for vector boson fusion and W/ZH production modes is $1.24^{+0.49}_{-0.45}^{+0.31}_{-0.29} \pm 0.08$. The quoted signal strength is given for $m_H = 125.36 \text{ GeV}$.

- ¹⁵ CHATRCHYAN 14K use 4.9 fb^{-1} of $p\bar{p}$ collisions at $E_{\text{cm}} = 7 \text{ TeV}$ and 19.7 fb^{-1} at $E_{\text{cm}} = 8 \text{ TeV}$. The quoted signal strength is given for $m_H = 125 \text{ GeV}$. See also CHATRCHYAN 14AJ.
- ¹⁶ AALTONEN 13L combine all CDF results with $9.45\text{--}10.0 \text{ fb}^{-1}$ of $p\bar{p}$ collisions at $E_{\text{cm}} = 1.96 \text{ TeV}$. The quoted signal strength is given for $m_H = 125 \text{ GeV}$.
- ¹⁷ ABAZOV 13L combine all D0 results with up to 9.7 fb^{-1} of $p\bar{p}$ collisions at $E_{\text{cm}} = 1.96 \text{ TeV}$. The quoted signal strength is given for $m_H = 125 \text{ GeV}$.
- ¹⁸ AAD 12AI obtain results based on 4.7 fb^{-1} of $p\bar{p}$ collisions at $E_{\text{cm}} = 7 \text{ TeV}$. The quoted signal strengths are given in their Fig. 10 for $m_H = 126 \text{ GeV}$. See also Fig. 13 of AAD 12DA.
- ¹⁹ CHATRCHYAN 12N obtain results based on 4.9 fb^{-1} of $p\bar{p}$ collisions at $E_{\text{cm}} = 7 \text{ TeV}$ and 5.1 fb^{-1} at $E_{\text{cm}} = 8 \text{ TeV}$. The quoted signal strength is given for $m_H = 125.5 \text{ GeV}$. See also CHATRCHYAN 13Y .

Z γ Final State

VALUE	CL%	DOCUMENT ID	TECN	COMMENT
• • • We do not use the following data for averages, fits, limits, etc. • • •				
$2.59^{+1.07}_{-0.96}$		¹ CMS	22 CMS	$p\bar{p}$, 13 TeV
< 3.6	95	² AAD	20AG ATLS	$p\bar{p}$, 13 TeV
< 7.4	95	³ SIRUNYAN	18DQ CMS	$p\bar{p}$, 13 TeV
< 6.6	95	⁴ AABOUD	17AW ATLS	$p\bar{p}$, 13 TeV
< 11	95	⁵ AAD	14J ATLS	$p\bar{p}$, 7, 8 TeV
< 9.5	95	⁶ CHATRCHYAN 13BK	CMS	$p\bar{p}$, 7, 8 TeV

¹ CMS 22 report combined results (see their Extended Data Table 2) using up to 138 fb^{-1} of data at $E_{\text{cm}} = 13 \text{ TeV}$, assuming $m_H = 125.38 \text{ GeV}$. See their Fig. 2 right.

² AAD 20AG search for $H \rightarrow Z\gamma$, $Z \rightarrow ee$, $\mu\mu$ in 139 fb^{-1} of $p\bar{p}$ collisions at $E_{\text{cm}} = 13 \text{ TeV}$. The signal strength is $2.0 \pm 0.9^{+0.4}_{-0.3}$ at $m_H = 125.09 \text{ GeV}$, which corresponds to a significance of 2.2σ . The upper limit of $\sigma(p\bar{p} \rightarrow H) \cdot B(H \rightarrow Z\gamma)$ is 305 fb at 95% CL.

³ SIRUNYAN 18DQ search for $H \rightarrow Z\gamma$, $Z \rightarrow ee$, $\mu\mu$ in 35.9 fb^{-1} of $p\bar{p}$ collisions at $E_{\text{cm}} = 13 \text{ TeV}$. The quoted signal strength (see their Figs. 6 and 7) is given for $m_H = 125 \text{ GeV}$.

⁴ AABOUD 17AW search for $H \rightarrow Z\gamma$, $Z \rightarrow ee$, $\mu\mu$ in 36.1 fb^{-1} of $p\bar{p}$ collisions at $E_{\text{cm}} = 13 \text{ TeV}$. The quoted signal strength is given for $m_H = 125.09 \text{ GeV}$. The upper limit on the branching ratio of $H \rightarrow Z\gamma$ is 1.0% at 95% CL assuming the SM Higgs boson production.

⁵ AAD 14J search for $H \rightarrow Z\gamma \rightarrow \ell\ell\gamma$ in 4.5 fb^{-1} of $p\bar{p}$ collisions at $E_{\text{cm}} = 7 \text{ TeV}$ and 20.3 fb^{-1} at $E_{\text{cm}} = 8 \text{ TeV}$. The quoted signal strength is given for $m_H = 125.5 \text{ GeV}$.

⁶ CHATRCHYAN 13BK search for $H \rightarrow Z\gamma \rightarrow \ell\ell\gamma$ in 5.0 fb^{-1} of $p\bar{p}$ collisions at $E_{\text{cm}} = 7 \text{ TeV}$ and 19.6 fb^{-1} at $E_{\text{cm}} = 8 \text{ TeV}$. A limit on cross section times branching ratio which corresponds to (4–25) times the expected Standard Model cross section is given in the range $m_H = 120\text{--}160 \text{ GeV}$ at 95% CL. The quoted limit is given for $m_H = 125 \text{ GeV}$, where 10 is expected for no signal.

$\gamma^*\gamma$ Final State

VALUE	CL%	DOCUMENT ID	TECN	COMMENT
$1.5^{+0.2}_{-0.1}$		¹ AAD	21I ATLS	$p\bar{p}$, 13 TeV, $H \rightarrow \ell\ell\gamma$, 139 fb^{-1}

• • • We do not use the following data for averages, fits, limits, etc. • • •

<4.0	95	² SIRUNYAN	18DQ CMS	$p p \rightarrow H X, 13 \text{ TeV},$ $H \rightarrow \gamma^* \gamma$
<6.7	95	³ KHACHATRYAN	16B CMS	$p p, 8 \text{ TeV}, e e \gamma, \mu \mu \gamma$

¹ AAD 21I search for $H \rightarrow \ell \ell \gamma$ ($\ell = e, \mu$) in 139 fb^{-1} of $p p$ collisions at $E_{\text{cm}} = 13 \text{ TeV}$. The mass of dilepton $m_{\ell \ell}$ is smaller than 30 GeV. This region is dominated by the decay through γ^* . The quoted signal strength corresponds to a significance of 3.2 standard deviations and is given for $m_H = 125.09 \text{ GeV}$. The cross section times the branching ratio of $H \rightarrow \ell \ell \gamma$ for $m_{\ell \ell} < 30 \text{ GeV}$ is measured to be $8.7 \pm 2.7^{+0.7}_{-0.6} \text{ fb}$.

² SIRUNYAN 18DQ search for $H \rightarrow \gamma^* \gamma, \gamma^* \rightarrow \mu \mu$ in 35.9 fb^{-1} of $p p$ collisions at $E_{\text{cm}} = 13 \text{ TeV}$. The mass of γ^* is smaller than 50 GeV except in J/ψ and Υ mass regions. The quoted signal strength (see their Figs. 6 and 7) is given for $m_H = 125 \text{ GeV}$.

³ KHACHATRYAN 16B search for $H \rightarrow \gamma^* \gamma \rightarrow e^+ e^- \gamma$ and $\mu^+ \mu^- \gamma$ (with $m(e^+ e^-) < 3.5 \text{ GeV}$ and $m(\mu^+ \mu^-) < 20 \text{ GeV}$) in 19.7 fb^{-1} of $p p$ collisions at $E_{\text{cm}} = 8 \text{ TeV}$. See their Fig. 6 for limits on individual channels.

Higgs couplings

Fermion coupling (κ_F)

VALUE	DOCUMENT ID	TECN	COMMENT
-------	-------------	------	---------

0.95 ± 0.05	¹ ATLAS	22 ATLS	$p p, 13 \text{ TeV}$
--------------------	--------------------	---------	-----------------------

• • • We do not use the following data for averages, fits, limits, etc. • • •

0.906	² CMS	22 CMS	$p p, 13 \text{ TeV}$
-------	------------------	--------	-----------------------

¹ ATLAS 22 report combined results (see their Extended Data Table 1) using up to 139 fb^{-1} of data at $E_{\text{cm}} = 13 \text{ TeV}$, assuming $m_H = 125.09 \text{ GeV}$, $\kappa_V \geq 0$, and $\kappa_F \geq 0$ ($B_{\text{inv}} = B_{\text{undetected}} = 0$). See their Fig. 4.

² CMS 22 report combined results (see their Extended Data Table 2) using up to 138 fb^{-1} of data at $E_{\text{cm}} = 13 \text{ TeV}$, assuming $m_H = 125.38 \text{ GeV}$. No uncertainty is given while their Fig. 3 left shows 68% and 95% CL contours.

Gauge boson coupling (κ_V)

VALUE	DOCUMENT ID	TECN	COMMENT
-------	-------------	------	---------

1.035 ± 0.031	¹ ATLAS	22 ATLS	$p p, 13 \text{ TeV}$
----------------------	--------------------	---------	-----------------------

• • • We do not use the following data for averages, fits, limits, etc. • • •

1.014	² CMS	22 CMS	$p p, 13 \text{ TeV}$
-------	------------------	--------	-----------------------

¹ ATLAS 22 report combined results (see their Extended Data Table 1) using up to 139 fb^{-1} of data at $E_{\text{cm}} = 13 \text{ TeV}$, assuming $m_H = 125.09 \text{ GeV}$, $\kappa_V \geq 0$, and $\kappa_F \geq 0$ ($B_{\text{inv}} = B_{\text{undetected}} = 0$). See their Fig. 4.

² CMS 22 report combined results (see their Extended Data Table 2) using up to 138 fb^{-1} of data at $E_{\text{cm}} = 13 \text{ TeV}$, assuming $m_H = 125.38 \text{ GeV}$. See their Fig. 3 left.

W boson coupling (κ_W)

VALUE	DOCUMENT ID	TECN	COMMENT
-------	-------------	------	---------

• • • We do not use the following data for averages, fits, limits, etc. • • •

1.02 ± 0.05	^{1,2} ATLAS	22 ATLS	$p p, 13 \text{ TeV}$
-------------	----------------------	---------	-----------------------

1.05 ± 0.06	^{1,3} ATLAS	22 ATLS	$p p, 13 \text{ TeV}$
-------------	----------------------	---------	-----------------------

1.00 ^{+0.00} _{-0.02}	^{1,4} ATLAS	22 ATLS	$p p, 13 \text{ TeV}$
--	----------------------	---------	-----------------------

1.06 ± 0.07	^{5,6} CMS	22 CMS	$p p, 13 \text{ TeV}$
-------------	--------------------	--------	-----------------------

1.02 ± 0.08	5,7 CMS	22 CMS	$p p, 13 \text{ TeV}$	
¹ ATLAS 22 report combined results (see their Extended Data Table 1) using up to 139 fb^{-1} of data at $E_{\text{cm}} = 13 \text{ TeV}$, assuming $m_H = 125.09 \text{ GeV}$.				
² All modifiers(κ) > 0 , and $\kappa_c = \kappa_t$ ($B_{\text{inv}} = B_{\text{undetected}} = 0$) are assumed. Only SM particles assume to contribute to the loop-induced processes. See their Fig. 5, which shows both $\kappa_c = \kappa_t$ and κ_c floating.				
³ $B_{\text{inv}} = B_{\text{undetected}} = 0$ is assumed. Coupling strength modifiers including effective photon, $Z\gamma$ and gluon are measured. See their Fig. 6.				
⁴ B_{inv} floating, $B_{\text{undetected}} \geq 0$, and $\kappa_V \leq 1$ are assumed. Coupling strength modifiers including effective photon, $Z\gamma$ and gluon are measured. See their Fig. 6.				
⁵ CMS 22 report combined results (see their Extended Data Table 2) using up to 138 fb^{-1} of data at $E_{\text{cm}} = 13 \text{ TeV}$, assuming $m_H = 125.38 \text{ GeV}$.				
⁶ Only SM particles assume to contribute to the loop-induced processes. See their Fig. 3 right.				
⁷ Coupling strength modifiers including effective photon, $Z\gamma$ and gluon are measured. See their Fig. 4 left.				

Z boson coupling (κ_Z)

VALUE	DOCUMENT ID	TECN	COMMENT
$\bullet \bullet \bullet$ We do not use the following data for averages, fits, limits, etc. $\bullet \bullet \bullet$			
$0.99^{+0.06}_{-0.05}$	1,2 ATLAS	22 ATLS	$p p, 13 \text{ TeV}$
0.99 ± 0.06	1,3 ATLAS	22 ATLS	$p p, 13 \text{ TeV}$
$0.98^{+0.02}_{-0.05}$	1,4 ATLAS	22 ATLS	$p p, 13 \text{ TeV}$
1.04 ± 0.07	5,6 CMS	22 CMS	$p p, 13 \text{ TeV}$
1.04 ± 0.07	5,7 CMS	22 CMS	$p p, 13 \text{ TeV}$

- ¹ ATLAS 22 report combined results (see their Extended Data Table 1) using up to 139 fb^{-1} of data at $E_{\text{cm}} = 13 \text{ TeV}$, assuming $m_H = 125.09 \text{ GeV}$.
- ² All modifiers(κ) > 0 , and $\kappa_c = \kappa_t$ ($B_{\text{inv}} = B_{\text{undetected}} = 0$) are assumed. Only SM particles assume to contribute to the loop-induced processes. See their Fig. 5, which shows both $\kappa_c = \kappa_t$ and κ_c floating.
- ³ $B_{\text{inv}} = B_{\text{undetected}} = 0$ is assumed. Coupling strength modifiers including effective photon, $Z\gamma$ and gluon are measured. See their Fig. 6.
- ⁴ B_{inv} floating, $B_{\text{undetected}} \geq 0$, and $\kappa_V \leq 1$ are assumed. Coupling strength modifiers including effective photon, $Z\gamma$ and gluon are measured. See their Fig. 6.
- ⁵ CMS 22 report combined results (see their Extended Data Table 2) using up to 138 fb^{-1} of data at $E_{\text{cm}} = 13 \text{ TeV}$, assuming $m_H = 125.38 \text{ GeV}$.
- ⁶ Only SM particles assume to contribute to the loop-induced processes. See their Fig. 3 right.
- ⁷ Coupling strength modifiers including effective photon, $Z\gamma$ and gluon are measured. See their Fig. 4 left.

top Yukawa coupling (κ_t)

VALUE	CL%	DOCUMENT ID	TECN	COMMENT
$\bullet \bullet \bullet$ We do not use the following data for averages, fits, limits, etc. $\bullet \bullet \bullet$				
0.95 ± 0.07		1,2 ATLAS	22 ATLS	$p p, 13 \text{ TeV}$
0.94 ± 0.11		1,3 ATLAS	22 ATLS	$p p, 13 \text{ TeV}$
0.94 ± 0.11		1,4 ATLAS	22 ATLS	$p p, 13 \text{ TeV}$
$0.95^{+0.07}_{-0.08}$		5,6 CMS	22 CMS	$p p, 13 \text{ TeV}$

$1.01^{+0.11}_{-0.10}$	5,7 CMS	22 CMS	$p p, 13 \text{ TeV}$
$[-0.9, -0.7] \text{ or } [0.7, 1.1]$	95	8 SIRUNYAN	21R CMS $p p, 13 \text{ TeV}$
<1.7	95	9 SIRUNYAN	20C CMS $p p, 13 \text{ TeV}$
<1.67	95	10 SIRUNYAN	19BY CMS $p p, 13 \text{ TeV}$
<2.1	95	11 SIRUNYAN	18BU CMS $p p, 13 \text{ TeV}$

¹ ATLAS 22 report combined results (see their Extended Data Table 1) using up to 139 fb^{-1} of data at $E_{\text{cm}} = 13 \text{ TeV}$, assuming $m_H = 125.09 \text{ GeV}$.

² All modifiers(κ) > 0 , and $\kappa_c = \kappa_t$ ($B_{\text{inv}} = B_{\text{undetected}} = 0$) are assumed. Only SM particles assume to contribute to the loop-induced processes. See their Fig. 5, which shows both $\kappa_c = \kappa_t$ and κ_c floating.

³ $B_{\text{inv}} = B_{\text{undetected}} = 0$ is assumed. Coupling strength modifiers including effective photon, $Z\gamma$ and gluon are measured. See their Fig. 6.

⁴ B_{inv} floating, $B_{\text{undetected}} \geq 0$, and $\kappa_V \leq 1$ are assumed. Coupling strength modifiers including effective photon, $Z\gamma$ and gluon are measured. See their Fig. 6.

⁵ CMS 22 report combined results (see their Extended Data Table 2) using up to 138 fb^{-1} of data at $E_{\text{cm}} = 13 \text{ TeV}$, assuming $m_H = 125.38 \text{ GeV}$.

⁶ Only SM particles assume to contribute to the loop-induced processes. See their Fig. 3 right.

⁷ Coupling strength modifiers including effective photon, $Z\gamma$ and gluon are measured. See their Fig. 4 left.

⁸ SIRUNYAN 21R constrain the ratio of the top quark Yukawa coupling y_t to its Standard Model value from $t\bar{t}H$ and tH production rates using 137 fb^{-1} $p p$ collision data at $E_{\text{cm}} = 13 \text{ TeV}$. Assuming a SM Higgs couplings to τ 's, the joint interval $-0.9 < \kappa_t (=y_t/y_t^{SM}) < -0.7$ and $0.7 < \kappa_t < 1.1$ is obtained at 95% CL (see their Fig. 17).

⁹ SIRUNYAN 20C search for the production of four top quarks with same-sign and multilepton final states with 137 fb^{-1} $p p$ collision data at $E_{\text{cm}} = 13 \text{ TeV}$. The results constraint the ratio of the top quark Yukawa coupling y_t to its Standard Model value by comparing to the central value of a theoretical prediction (see their Refs. [1-2]), yielding $|y_t/y_t^{SM}| < 1.7$ at 95% CL. See their Fig. 5.

¹⁰ SIRUNYAN 19BY measure the top quark Yukawa coupling from $t\bar{t}$ kinematic distributions, the invariant mass of the top quark pair and the rapidity difference between t and \bar{t} , in the $\ell + \text{jets}$ final state with 35.8 fb^{-1} $p p$ collision data at $E_{\text{cm}} = 13 \text{ TeV}$. The results constraint the ratio of the top quark Yukawa coupling to its the Standard Model to be $1.07^{+0.34}_{-0.43}$ with an upper limit of 1.67 at 95% CL (see their Table III).

¹¹ SIRUNYAN 18BU search for the production of four top quarks with same-sign and multilepton final states with 35.9 fb^{-1} $p p$ collision data at $E_{\text{cm}} = 13 \text{ TeV}$. The results constraint the ratio of the top quark Yukawa coupling y_t to its the Standard Model by comparing to the central value of a theoretical prediction (see their Ref. [16]), yielding $|y_t/y_t^{SM}| < 2.1$ at 95% CL.

bottom Yukawa coupling (κ_b)

VALUE	DOCUMENT ID	TECN	COMMENT
$\bullet \bullet \bullet$ We do not use the following data for averages, fits, limits, etc. $\bullet \bullet \bullet$			
0.90 ± 0.11	1,2 ATLAS	22 ATLS	$p p, 13 \text{ TeV}$
0.89 ± 0.11	1,3 ATLAS	22 ATLS	$p p, 13 \text{ TeV}$
$0.82^{+0.09}_{-0.08}$	1,4 ATLAS	22 ATLS	$p p, 13 \text{ TeV}$
$1.02^{+0.15}_{-0.17}$	5,6 CMS	22 CMS	$p p, 13 \text{ TeV}$

$0.99^{+0.17}_{-0.16}$ 5,7 CMS 22 CMS $p p$, 13 TeV

¹ ATLAS 22 report combined results (see their Extended Data Table 1) using up to 139fb^{-1} of data at $E_{\text{cm}} = 13 \text{ TeV}$, assuming $m_H = 125.09 \text{ GeV}$.

² All modifiers (κ) > 0 , and $\kappa_c = \kappa_t$ ($B_{\text{inv}} = B_{\text{undetected}} = 0$) are assumed. Only SM particles assume to contribute to the loop-induced processes. See their Fig. 5, which shows both $\kappa_c = \kappa_t$ and κ_c floating.

³ $B_{\text{inv}} = B_{\text{undetected}} = 0$ is assumed. Coupling strength modifiers including effective photon, $Z\gamma$ and gluon are measured. See their Fig. 6.

⁴ B_{inv} floating, $B_{\text{undetected}} \geq 0$, and $\kappa_V \leq 1$ are assumed. Coupling strength modifiers including effective photon, $Z\gamma$ and gluon are measured. See their Fig. 6.

⁵ CMS 22 report combined results (see their Extended Data Table 2) using up to 138 fb^{-1} of data at $E_{\text{cm}} = 13 \text{ TeV}$, assuming $m_H = 125.38 \text{ GeV}$.

⁶ Only SM particles assume to contribute to the loop-induced processes. See their Fig. 3 right.

⁷ Coupling strength modifiers including effective photon, $Z\gamma$ and gluon are measured. See their Fig. 4 left.

charm Yukawa coupling (κ_c)

VALUE	DOCUMENT ID	TECN	COMMENT
-------	-------------	------	---------

• • • We do not use the following data for averages, fits, limits, etc. • • •

$0.03^{+3.02}_{-0.03}$ 1 ATLAS 22 ATLS $p p$, 13 TeV

¹ ATLAS 22 report combined results (see their Extended Data Table 1) using up to 139 fb^{-1} of data at $E_{\text{cm}} = 13 \text{ TeV}$, assuming $m_H = 125.09 \text{ GeV}$, and all modifiers (κ) > 0 ($B_{\text{inv}} = B_{\text{undetected}} = 0$). Only SM particles assume to contribute to the loop-induced processes. See their Fig. 5, which shows both $\kappa_c = \kappa_t$ and κ_c floating.

tau Yukawa coupling (κ_τ)

VALUE	DOCUMENT ID	TECN	COMMENT
-------	-------------	------	---------

• • • We do not use the following data for averages, fits, limits, etc. • • •

0.94 ± 0.07 1,2 ATLAS 22 ATLS $p p$, 13 TeV

0.93 ± 0.07 1,3 ATLAS 22 ATLS $p p$, 13 TeV

$0.91^{+0.07}_{-0.06}$ 1,4 ATLAS 22 ATLS $p p$, 13 TeV

0.93 ± 0.08 5,6 CMS 22 CMS $p p$, 13 TeV

0.92 ± 0.08 5,7 CMS 22 CMS $p p$, 13 TeV

¹ ATLAS 22 report combined results (see their Extended Data Table 1) using up to 139 fb^{-1} of data at $E_{\text{cm}} = 13 \text{ TeV}$, assuming $m_H = 125.09 \text{ GeV}$.

² All modifiers(κ) > 0 , and $\kappa_c = \kappa_t$ ($B_{\text{inv}} = B_{\text{undetected}} = 0$) are assumed. Only SM particles assume to contribute to the loop-induced processes. See their Fig. 5, which shows both $\kappa_c = \kappa_t$ and κ_c floating.

³ $B_{\text{inv}} = B_{\text{undetected}} = 0$ is assumed. Coupling strength modifiers including effective photon, $Z\gamma$ and gluon are measured. See their Fig. 6.

⁴ B_{inv} floating, $B_{\text{undetected}} \geq 0$, and $\kappa_V \leq 1$ are assumed. Coupling strength modifiers including effective photon, $Z\gamma$ and gluon are measured. See their Fig. 6.

⁵ CMS 22 report combined results (see their Extended Data Table 2) using up to 138 fb^{-1} of data at $E_{\text{cm}} = 13 \text{ TeV}$, assuming $m_H = 125.38 \text{ GeV}$.

⁶ Only SM particles assume to contribute to the loop-induced processes. See their Fig. 3 right.

⁷ Coupling strength modifiers including effective photon, $Z\gamma$ and gluon are measured. See their Fig. 4 left.

muon Yukawa coupling (κ_μ)

VALUE	DOCUMENT ID	TECN	COMMENT
• • • We do not use the following data for averages, fits, limits, etc. • • •			
1.07 ^{+0.25} _{-0.31}	1,2 ATLAS	22	ATLS $p p$, 13 TeV
1.06 ^{+0.25} _{-0.30}	1,3 ATLAS	22	ATLS $p p$, 13 TeV
1.04 ^{+0.23} _{-0.30}	1,4 ATLAS	22	ATLS $p p$, 13 TeV
1.12 ± 0.20	5,6 CMS	22	CMS $p p$, 13 TeV
1.12 ^{+0.21} _{-0.22}	5,7 CMS	22	CMS $p p$, 13 TeV
¹ ATLAS 22 report combined results (see their Extended Data Table 1) using up to 139 fb^{-1} of data at $E_{\text{cm}} = 13 \text{ TeV}$, assuming $m_H = 125.09 \text{ GeV}$. ² All modifiers(κ) > 0 , and $\kappa_c = \kappa_t$ ($B_{\text{inv}} = B_{\text{undetected}} = 0$) are assumed. Only SM particles assume to contribute to the loop-induced processes. See their Fig. 5, which shows both $\kappa_c = \kappa_t$ and κ_c floating. ³ $B_{\text{inv}} = B_{\text{undetected}} = 0$ is assumed. Coupling strength modifiers including effective photon, $Z\gamma$ and gluon are measured. See their Fig. 6. ⁴ B_{inv} floating, $B_{\text{undetected}} \geq 0$, and $\kappa_V \leq 1$ are assumed. Coupling strength modifiers including effective photon, $Z\gamma$ and gluon are measured. See their Fig. 6. ⁵ CMS 22 report combined results (see their Extended Data Table 2) using up to 138 fb^{-1} of data at $E_{\text{cm}} = 13 \text{ TeV}$, assuming $m_H = 125.38 \text{ GeV}$. ⁶ Only SM particles assume to contribute to the loop-induced processes. See their Fig. 3 right. ⁷ Coupling strength modifiers including effective photon, $Z\gamma$ and gluon are measured. See their Fig. 4 left.			

photon effective coupling (κ_γ)

VALUE	DOCUMENT ID	TECN	COMMENT
• • • We do not use the following data for averages, fits, limits, etc. • • •			
1.01 ± 0.06	1,2 ATLAS	22	ATLS $p p$, 13 TeV
0.98 ± 0.05	1,3 ATLAS	22	ATLS $p p$, 13 TeV
1.10 ± 0.08	4 CMS	22	CMS $p p$, 13 TeV
¹ ATLAS 22 report combined results (see their Extended Data Table 1) using up to 139 fb^{-1} of data at $E_{\text{cm}} = 13 \text{ TeV}$, assuming $m_H = 125.09 \text{ GeV}$. Coupling strength modifiers including effective photon, $Z\gamma$ and gluon are measured. See their Fig. 6. ² $B_{\text{inv}} = B_{\text{undetected}} = 0$ is assumed. ³ B_{inv} floating, $B_{\text{undetected}} \geq 0$, and $\kappa_V \leq 1$ are assumed. ⁴ CMS 22 report combined results (see their Extended Data Table 2) using up to 138 fb^{-1} of data at $E_{\text{cm}} = 13 \text{ TeV}$, assuming $m_H = 125.38 \text{ GeV}$. Coupling strength modifiers including effective photon, $Z\gamma$ and gluon are measured. See their Fig. 4 left.			

gluon effective coupling (κ_{gluon})

VALUE	DOCUMENT ID	TECN	COMMENT
• • • We do not use the following data for averages, fits, limits, etc. • • •			
0.95 ± 0.07	1,2 ATLAS	22	ATLS $p p$, 13 TeV
0.94 ^{+0.07} _{-0.06}	1,3 ATLAS	22	ATLS $p p$, 13 TeV

0.92 ± 0.08

⁴ CMS

22 CMS pp , 13 TeV

¹ ATLAS 22 report combined results (see their Extended Data Table 1) using up to 139fb^{-1} of data at $E_{\text{cm}} = 13$ TeV, assuming $m_H = 125.09$ GeV. Coupling strength modifiers including effective photon, $Z\gamma$ and gluon are measured. See their Fig. 6.

² $B_{\text{inv}} = B_{\text{undetected}} = 0$ is assumed.

³ B_{inv} floating, $B_{\text{undetected}} \geq 0$, and $\kappa_V \leq 1$ are assumed.

⁴ CMS 22 report combined results (see their Extended Data Table 2) using up to 138 fb^{-1} of data at $E_{\text{cm}} = 13$ TeV, assuming $m_H = 125.38$ GeV. Coupling strength modifiers including effective photon, $Z\gamma$ and gluon are measured. See their Fig. 4 left.

$Z\gamma$ effective coupling ($\kappa_{Z\gamma}$)

VALUE	DOCUMENT ID	TECN	COMMENT
$\bullet \bullet \bullet$ We do not use the following data for averages, fits, limits, etc. $\bullet \bullet \bullet$			
$1.38^{+0.31}_{-0.37}$	1,2 ATLAS	22 ATLS	pp , 13 TeV
$1.35^{+0.29}_{-0.36}$	1,3 ATLAS	22 ATLS	pp , 13 TeV
$1.65^{+0.34}_{-0.37}$	⁴ CMS	22 CMS	pp , 13 TeV
¹ ATLAS 22 report combined results (see their Extended Data Table 1) using up to 139fb^{-1} of data at $E_{\text{cm}} = 13$ TeV, assuming $m_H = 125.09$ GeV. Coupling strength modifiers including effective photon, $Z\gamma$ and gluon are measured. See their Fig. 6.			
² $B_{\text{inv}} = B_{\text{undetected}} = 0$ is assumed.			
³ B_{inv} floating, $B_{\text{undetected}} \geq 0$, and $\kappa_V \leq 1$ are assumed.			
⁴ CMS 22 report combined results (see their Extended Data Table 2) using up to 138 fb^{-1} of data at $E_{\text{cm}} = 13$ TeV, assuming $m_H = 125.38$ GeV. Coupling strength modifiers including effective photon, $Z\gamma$ and gluon are measured. See their Fig. 4 left.			

OTHER H PRODUCTION PROPERTIES

$t\bar{t}H$ Production

Signal strength relative to the Standard Model cross section.

VALUE	DOCUMENT ID	TECN	COMMENT
1.10 ± 0.18 OUR AVERAGE			
$0.92 \pm 0.19^{+0.17}_{-0.13}$	1 SIRUNYAN	21R CMS	pp , 13 TeV, $H \rightarrow \tau\tau$, WW^* , ZZ^*
1.2 ± 0.3	2 AABOUD	18AC ATLS	pp , 13 TeV, $H \rightarrow b\bar{b}\tau\tau$, $\gamma\gamma$, WW^* , ZZ^*
$1.9^{+0.8}_{-0.7}$	3 AAD	16AN ATLS	pp , 7, 8 TeV
$\bullet \bullet \bullet$ We do not use the following data for averages, fits, limits, etc. $\bullet \bullet \bullet$			
$0.35^{+0.36}_{-0.34}$	⁴ AAD	22M ATLS	pp , 13 TeV, $H \rightarrow b\bar{b}$
$1.43^{+0.33+0.21}_{-0.31-0.15}$	5 AAD	20Z ATLS	pp , 13 TeV, $H \rightarrow \gamma\gamma$
$1.38^{+0.36}_{-0.29}$	6 SIRUNYAN	20AS CMS	pp , 13 TeV, $H \rightarrow \gamma\gamma$
$0.72 \pm 0.24 \pm 0.38$	7 SIRUNYAN	19R CMS	pp , 13 TeV, $H \rightarrow b\bar{b}$
$1.6^{+0.5}_{-0.4}$	8 AABOUD	18AC ATLS	pp , 13 TeV, $H \rightarrow \tau\tau$, WW^* , ZZ^*
	⁹ AABOUD	18BK ATLS	pp , 13 TeV, $H \rightarrow b\bar{b}\tau\tau$, $\gamma\gamma$, WW^* , ZZ^*

$0.84^{+0.64}_{-0.61}$	10 AABOUD	18T ATLS	$p p, 13 \text{ TeV}, H \rightarrow b\bar{b}$
0.9 ± 1.5	11 SIRUNYAN	18BD CMS	$p p, 13 \text{ TeV}, H \rightarrow b\bar{b}$
$1.23^{+0.45}_{-0.43}$	12 SIRUNYAN	18BQ CMS	$p p, 13 \text{ TeV}, H \rightarrow \tau\tau, WW^*, ZZ^*$
$1.26^{+0.31}_{-0.26}$	13 SIRUNYAN	18L CMS	$p p, 7, 8, 13 \text{ TeV}, H \rightarrow b\bar{b}, \tau\tau, \gamma\gamma, WW^*, ZZ^*$
1.7 ± 0.8	14 AAD	16AL ATLS	$p p, 7, 8 \text{ TeV}, H \rightarrow b\bar{b}, \tau\tau, \gamma\gamma, WW^*, \text{and } ZZ^*$
$2.3^{+0.7}_{-0.6}$	3,15 AAD	16AN LHC	$p p, 7, 8 \text{ TeV}$
$2.9^{+1.0}_{-0.9}$	3 AAD	16AN CMS	$p p, 7, 8 \text{ TeV}$
$1.81^{+0.52+0.58+0.31}_{-0.50-0.55-0.12}$	16 AAD	16K ATLS	$p p, 7, 8 \text{ TeV}$
$1.4^{+2.1}_{-1.4}{}^{+0.6}_{-0.3}$	17 AAD	15 ATLS	$p p, 7, 8 \text{ TeV}$
1.5 ± 1.1	18 AAD	15BC ATLS	$p p, 8 \text{ TeV}$
$2.1^{+1.4}_{-1.2}$	19 AAD	15T ATLS	$p p, 8 \text{ TeV}$
$1.2^{+1.6}_{-1.5}$	20 KHACHATRY...15AN CMS		$p p, 8 \text{ TeV}$
$2.8^{+1.0}_{-0.9}$	21 KHACHATRY...14H CMS		$p p, 7, 8 \text{ TeV}$
$9.49^{+6.60}_{-6.28}$	22 AALTONEN	13L CDF	$p\bar{p}, 1.96 \text{ TeV}$
$< 5.8 \text{ at 95\% CL}$	23 CHATRCHYAN	13X CMS	$p p, 7, 8 \text{ TeV}, H \rightarrow b\bar{b}$

¹ SIRUNYAN 21R search for $t\bar{t}H$ in final states with electrons, muons and hadronically decaying τ leptons ($H \rightarrow WW^*, ZZ^*, \tau\tau$) with 137 fb^{-1} of $p p$ collision data at $E_{\text{cm}} = 13 \text{ TeV}$. The quoted signal strength corresponds to a significance of 4.7 standard deviations and is given for $m_H = 125 \text{ GeV}$.

² AABOUD 18AC combine results of $t\bar{t}H, H \rightarrow \tau\tau, WW^* (\rightarrow \ell\nu\ell\nu, \ell\nu q\bar{q}), ZZ^* (\rightarrow \ell\ell\nu\nu, \ell\ell q\bar{q})$ with results of $t\bar{t}H, H \rightarrow b\bar{b}$ (AABOUD 18T), $\gamma\gamma$ (AABOUD 18BO), $ZZ^* (\rightarrow 4\ell)$ (AABOUD 18AJ) in 36.1 fb^{-1} of $p p$ collisions at $E_{\text{cm}} = 13 \text{ TeV}$. The quoted signal strength is given for $m_H = 125 \text{ GeV}$. See their Table 14.

³ AAD 16AN: In the fit, relative branching ratios are fixed to those in the Standard Model. The quoted signal strength is given for $m_H = 125.09 \text{ GeV}$.

⁴ AAD 22M measure $H \rightarrow b\bar{b}$ in $t\bar{t}H$ production using 139 fb^{-1} of data at $E_{\text{cm}} = 13 \text{ TeV}$. See their Fig. 14. The signal strengths and 95% CL cross section upper limits with simplified template cross section bins are given in their Figs. 18 and 19, respectively.

⁵ AAD 20Z measure $\sigma_{t\bar{t}H} \cdot B(H \rightarrow \gamma\gamma)$ to be $1.64^{+0.38+0.17}_{-0.36-0.14} \text{ fb}$ in 139 fb^{-1} of data at $E_{\text{cm}} = 13 \text{ TeV}$.

⁶ SIRUNYAN 20AS measure $\sigma_{t\bar{t}H} \cdot B(H \rightarrow \gamma\gamma)$ to be $1.56^{+0.34}_{-0.32} \text{ fb}$ in 137 fb^{-1} of data at $E_{\text{cm}} = 13 \text{ TeV}$.

⁷ SIRUNYAN 19R search for $t\bar{t}H$ production with H decaying to $b\bar{b}$ in 35.9 fb^{-1} of data at $E_{\text{cm}} = 13 \text{ TeV}$. The quoted signal strength is given for $m_H = 125 \text{ GeV}$.

⁸ AABOUD 18AC search for $t\bar{t}H$ production with H decaying to $\tau\tau, WW^* (\rightarrow \ell\nu\ell\nu, \ell\nu q\bar{q}), ZZ^* (\rightarrow \ell\ell\nu\nu, \ell\ell q\bar{q})$ in 36.1 fb^{-1} of $p p$ collisions at $E_{\text{cm}} = 13 \text{ TeV}$. The quoted signal strength is given for $m_H = 125 \text{ GeV}$. See their Table 13 and Fig. 13.

⁹ AABOUD 18BK use 79.8 fb^{-1} data for $t\bar{t}H$ production with $H \rightarrow \gamma\gamma$ and $ZZ^* \rightarrow 4\ell$ ($\ell = e, \mu$) and 36.1 fb^{-1} for other decay channels at $E_{\text{cm}} = 13 \text{ TeV}$. A significance of 5.8 standard deviations is observed for $m_H = 125.09 \text{ GeV}$ and its signal strength without

- the uncertainty of the $t\bar{t}H$ cross section is $1.32^{+0.28}_{-0.26}$. Combining with results of 7 and 8 TeV (AAD 16K), the significance is 6.3 standard deviations. Assuming Standard Model branching fractions, the total $t\bar{t}H$ production cross section at 13 TeV is measured to be $670 \pm 90^{+110}_{-100}$ fb.
- 10 AABOUD 18T search for $t\bar{t}H$ production with H decaying to $b\bar{b}$ in 36.1 fb^{-1} of pp collisions at $E_{\text{cm}} = 13$ TeV. The quoted signal strength is given for $m_H = 125$ GeV.
 - 11 SIRUNYAN 18BD search for $t\bar{t}H$, $H \rightarrow b\bar{b}$ in the all-jet final state with 35.9 fb^{-1} pp collision data at $E_{\text{cm}} = 13$ TeV. The quoted signal strength is given for $m_H = 125$ GeV.
 - 12 SIRUNYAN 18BQ search for $t\bar{t}H$ in final states with electrons, muons and hadronically decaying τ leptons ($H \rightarrow WW^*$, ZZ^* , $\tau\tau$) with 35.9 fb^{-1} of pp collision data at $E_{\text{cm}} = 13$ TeV. The quoted signal strength corresponds to a significance of 3.2 standard deviations and is given for $m_H = 125$ GeV.
 - 13 SIRUNYAN 18L use up to 5.1, 19.7 and 35.9 fb^{-1} of pp collisions at $E_{\text{cm}} = 7$, 8, and 13 TeV, respectively. The quoted signal strength corresponds to a significance of 5.2 standard deviations and is given for $m_H = 125.09$ GeV. H decay channels of WW^* , ZZ^* , $\gamma\gamma$, $\tau\tau$, and $b\bar{b}$ are used. See their Table 1 and Fig. 2 for results on individual channels.
 - 14 AAD 16AL search for $t\bar{t}H$ production with H decaying to $\gamma\gamma$ in 4.5 fb^{-1} of pp collisions at $E_{\text{cm}} = 7$ TeV and $b\bar{b}$, $\tau\tau$, $\gamma\gamma$, WW^* , and ZZ^* in 20.3 fb^{-1} at $E_{\text{cm}} = 8$ TeV. The quoted signal strength is given for $m_H = 125$ GeV. This paper combines the results of previous papers, and the new result of this paper only is: $\mu = 1.6 \pm 2.6$.
 - 15 AAD 16AN perform fits to the ATLAS and CMS data at $E_{\text{cm}} = 7$ and 8 TeV.
 - 16 AAD 16K use up to 4.7 fb^{-1} of pp collisions at $E_{\text{cm}} = 7$ TeV and up to 20.3 fb^{-1} at $E_{\text{cm}} = 8$ TeV. The third uncertainty in the measurement is theory systematics. The quoted signal strength is given for $m_H = 125.36$ GeV.
 - 17 AAD 15 search for $t\bar{t}H$ production with H decaying to $\gamma\gamma$ in 4.5 fb^{-1} of pp collisions at $E_{\text{cm}} = 7$ TeV and 20.3 fb^{-1} at $E_{\text{cm}} = 8$ TeV. The quoted result on the signal strength is equivalent to an upper limit of 6.7 at 95% CL and is given for $m_H = 125.4$ GeV.
 - 18 AAD 15BC search for $t\bar{t}H$ production with H decaying to $b\bar{b}$ in 20.3 fb^{-1} of pp collisions at $E_{\text{cm}} = 8$ TeV. The corresponding upper limit is 3.4 at 95% CL. The quoted signal strength is given for $m_H = 125$ GeV.
 - 19 AAD 15T search for $t\bar{t}H$ production with H resulting in multilepton final states (mainly from WW^* , $\tau\tau$, ZZ^*) in 20.3 fb^{-1} of pp collisions at $E_{\text{cm}} = 8$ TeV. The quoted result on the signal strength is given for $m_H = 125$ GeV and corresponds to an upper limit of 4.7 at 95% CL. The data sample is independent from AAD 15 and AAD 15BC.
 - 20 KHACHATRYAN 15AN search for $t\bar{t}H$ production with H decaying to $b\bar{b}$ in 19.5 fb^{-1} of pp collisions at $E_{\text{cm}} = 8$ TeV. The quoted result on the signal strength is equivalent to an upper limit of 4.2 at 95% CL and is given for $m_H = 125$ GeV.
 - 21 KHACHATRYAN 14H search for $t\bar{t}H$ production with H decaying to $b\bar{b}$, $\tau\tau$, $\gamma\gamma$, WW^* , and ZZ^* , in 5.1 fb^{-1} of pp collisions at $E_{\text{cm}} = 7$ TeV and 19.7 fb^{-1} at $E_{\text{cm}} = 8$ TeV. The quoted signal strength is given for $m_H = 125.6$ GeV.
 - 22 AALTONEN 13L combine all CDF results with $9.45\text{--}10.0 \text{ fb}^{-1}$ of $p\bar{p}$ collisions at $E_{\text{cm}} = 1.96$ TeV. The quoted signal strength is given for $m_H = 125$ GeV.
 - 23 CHATRCHYAN 13X search for $t\bar{t}H$ production followed by $H \rightarrow b\bar{b}$, one top decaying to $\ell\nu$ and the other to either $\ell\nu$ or $q\bar{q}$ in 5.0 fb^{-1} and 5.1 fb^{-1} of pp collisions at $E_{\text{cm}} = 7$ and 8 TeV. A limit on cross section times branching ratio which corresponds to (4.0–8.6) times the expected Standard Model cross section is given for $m_H = 110\text{--}140$ GeV at 95% CL. The quoted limit is given for $m_H = 125$ GeV, where 5.2 is expected for no signal.

***HH* Production Cross Section in *pp* Collisions**

The *HH* production cross section relative to the SM prediction.

<u>VALUE</u>	<u>CL%</u>	<u>DOCUMENT ID</u>	<u>TECN</u>	<u>COMMENT</u>
• • • We do not use the following data for averages, fits, limits, etc. • • •				
< 4.2	95	¹ AAD	22Y ATLS	13 TeV, $\gamma\gamma b\bar{b}$
< 3.4	95	² CMS	22 CMS	13 TeV, $b\bar{b}Z Z^*$, $b\bar{b}\gamma\gamma$, $b\bar{b}\tau\tau$, $b\bar{b}b\bar{b}$, multilepton
< 3.9	95	³ TUMASYAN	22AN CMS	13 TeV, $b\bar{b}b\bar{b}$
< 7.7	95	⁴ SIRUNYAN	21K CMS	13 TeV, $\gamma\gamma b\bar{b}$
< 6.9	95	⁵ AAD	20C ATLS	13 TeV, $b\bar{b}\gamma\gamma$, $b\bar{b}\tau\tau$, $b\bar{b}b\bar{b}$, $b\bar{b}WW^*$, $WW^*\gamma\gamma$, WW^*WW^*
< 40	95	⁶ AAD	20E ATLS	13 TeV, $HH \rightarrow b\bar{b}\ell\nu\ell\nu$
< 840	95	⁷ AAD	20X ATLS	13 TeV, VBF, $b\bar{b}b\bar{b}$
< 12.9	95	⁸ AABOUD	19A ATLS	13 TeV, $b\bar{b}b\bar{b}$
< 300	95	⁹ AABOUD	19O ATLS	13 TeV, $b\bar{b}WW^*$
< 160	95	¹⁰ AABOUD	19T ATLS	13 TeV, WW^*WW^*
< 24	95	¹¹ SIRUNYAN	19 CMS	13 TeV, $\gamma\gamma b\bar{b}$
< 75	95	¹² SIRUNYAN	19AB CMS	13 TeV, $b\bar{b}b\bar{b}$
< 22.2	95	¹³ SIRUNYAN	19BE CMS	13 TeV, $b\bar{b}\gamma\gamma b\bar{b}\tau\tau$, $b\bar{b}b\bar{b}$, $b\bar{b}WW^*$, $b\bar{b}ZZ^*$
< 179	95	¹⁴ SIRUNYAN	19H CMS	13 TeV, $b\bar{b}b\bar{b}$
< 230	95	¹⁵ AABOUD	18BU ATLS	13 TeV, $\gamma\gamma WW^*$
< 12.7	95	¹⁶ AABOUD	18CQ ATLS	13 TeV, $b\bar{b}\tau\tau$
< 22	95	¹⁷ AABOUD	18CW ATLS	13 TeV, $\gamma\gamma b\bar{b}$
< 30	95	¹⁸ SIRUNYAN	18A CMS	13 TeV, $b\bar{b}\tau\tau$
< 79	95	¹⁹ SIRUNYAN	18F CMS	13 TeV, $b\bar{b}\ell\nu\ell\nu$
< 43	95	²⁰ SIRUNYAN	17CN CMS	8 TeV, $b\bar{b}\tau\tau$, $\gamma\gamma b\bar{b}$, $b\bar{b}b\bar{b}$
< 108	95	²¹ AABOUD	16I ATLS	13 TeV, $b\bar{b}b\bar{b}$
< 74	95	²² KHACHATRYAN...16BQ CMS	16BQ CMS	8 TeV, $\gamma\gamma b\bar{b}$
< 70	95	²³ AAD	15CE ATLS	8 TeV, $b\bar{b}b\bar{b}$, $b\bar{b}\tau\tau$, $\gamma\gamma b\bar{b}$, $\gamma\gamma WW$

¹ AAD 22Y search for non-resonant *HH* production using $HH \rightarrow \gamma\gamma b\bar{b}$ with data of 139 fb^{-1} at $E_{\text{cm}} = 13$ TeV. The upper limit on the $pp \rightarrow HH$ production cross section at 95% CL is measured to be 130 fb, which corresponds to 4.2 times the SM prediction.

² CMS 22 report combined results (see their Extended Data Table 2) using 138 fb^{-1} of data at $E_{\text{cm}} = 13$ TeV. See their Fig. 5 (left) for different final states and these combination.

³ TUMASYAN 22AN search for non-resonant *HH* production using $HH \rightarrow b\bar{b}b\bar{b}$ with data of 138 fb^{-1} at $E_{\text{cm}} = 13$ TeV. The upper limit on the $pp \rightarrow HH$ production cross section at 95% CL is measured to be 120 fb, which corresponds to 3.9 times the SM prediction.

⁴ SIRUNYAN 21K search for non-resonant *HH* production using $HH \rightarrow \gamma\gamma b\bar{b}$ with data of 137 fb^{-1} at $E_{\text{cm}} = 13$ TeV. The upper limit on the $pp \rightarrow HH \rightarrow \gamma\gamma b\bar{b}$ production cross section at 95% CL is measured to be 0.67 fb, which corresponds to about 7.7 times the SM prediction.

⁵ AAD 20C combine results of up to 36.1 fb^{-1} data at $E_{\text{cm}} = 13$ TeV for $pp \rightarrow HH \rightarrow b\bar{b}\gamma\gamma$, $b\bar{b}\tau\tau$, $b\bar{b}b\bar{b}$, $b\bar{b}WW^*$, $WW^*\gamma\gamma$, WW^*WW^* (AABOUD 18CW, AABOUD 18CQ, AABOUD 19A, AABOUD 19O, AABOUD 18BU, and AABOUD 19T).

⁶ AAD 20E search non-resonant for *HH* production using $HH \rightarrow b\bar{b}\ell\nu\ell\nu$, where one of the Higgs bosons decays to $b\bar{b}$ and the other decays to either WW^* , ZZ^* , or $\tau\tau$, with data of 139 fb^{-1} at $E_{\text{cm}} = 13$ TeV. The upper limit on the $pp \rightarrow HH$ production

cross section at 95% CL is measured to be 1.2 pb, which corresponds to about 40 times the SM prediction.

- ⁷AAD 20X search for $HH \rightarrow b\bar{b}b\bar{b}$ process via VBF with data of 126 fb^{-1} at $E_{\text{cm}} = 13 \text{ TeV}$. The upper limit on the SM non-resonant HH production cross section is 1460 fb at 95% CL, which corresponds to 840 times the SM prediction.
- ⁸AABOUD 19A search for HH production using $HH \rightarrow b\bar{b}b\bar{b}$ with data of 36.1 fb^{-1} at $E_{\text{cm}} = 13 \text{ TeV}$. The upper limit on the $pp \rightarrow HH \rightarrow b\bar{b}b\bar{b}$ production cross section at 95% is measured to be 147 fb , which corresponds to about 12.9 times the SM prediction.
- ⁹AABOUD 19O search for HH production using $HH \rightarrow b\bar{b}WW^*$ with data of 36.1 fb^{-1} at $E_{\text{cm}} = 13 \text{ TeV}$. The upper limit on the $pp \rightarrow HH$ production cross section at 95% CL is calculated to be 10 pb from the observed upper limit on the $pp \rightarrow HH \rightarrow b\bar{b}WW^*$ production cross section of 2.5 pb assuming the SM branching fractions. The former corresponds to about 300 times the SM prediction.
- ¹⁰AABOUD 19T search for HH production using $HH \rightarrow WW^*WW^*$ with data of 36.1 fb^{-1} at $E_{\text{cm}} = 13 \text{ TeV}$. The upper limit on the $pp \rightarrow HH$ production cross section at 95% is measured to be 5.3 pb , which corresponds to about 160 times the SM prediction.
- ¹¹SIRUNYAN 19 search for HH production using $HH \rightarrow \gamma\gamma b\bar{b}$ with data of 35.9 fb^{-1} at $E_{\text{cm}} = 13 \text{ TeV}$. The upper limit on the $pp \rightarrow HH \rightarrow \gamma\gamma b\bar{b}$ production cross section at 95% CL is measured to be 2.0 fb , which corresponds to about 24 times the SM prediction.
- ¹²SIRUNYAN 19AB search for HH production using $HH \rightarrow b\bar{b}b\bar{b}$, where 4 heavy flavor jets from two Higgs bosons are resolved, with data of 35.9 fb^{-1} at $E_{\text{cm}} = 13 \text{ TeV}$. The upper limit on the $pp \rightarrow HH \rightarrow b\bar{b}b\bar{b}$ production cross section at 95% is measured to be 847 fb , which corresponds to about 75 times the SM prediction.
- ¹³SIRUNYAN 19BE combine results of $13 \text{ TeV } 35.9 \text{ fb}^{-1}$ data: SIRUNYAN 19, SIRUNYAN 18A, SIRUNYAN 19AB, SIRUNYAN 19H, and SIRUNYAN 18F.
- ¹⁴SIRUNYAN 19H search for HH production using $HH \rightarrow b\bar{b}b\bar{b}$, where one of $b\bar{b}$ pairs is highly boosted and the other one is resolved, with data of 35.9 fb^{-1} at $E_{\text{cm}} = 13 \text{ TeV}$. The upper limit on the $pp \rightarrow HH \rightarrow b\bar{b}b\bar{b}$ production cross section at 95% is measured to be 1980 fb , which corresponds to about 179 times the SM prediction.
- ¹⁵AABOUD 18BU search for HH production using $\gamma\gamma WW^*$ with the final state of $\gamma\gamma\ell\nu jj$ using data of 36.1 fb^{-1} at $E_{\text{cm}} = 13 \text{ TeV}$. The upper limit on the $pp \rightarrow HH$ production cross section at 95% CL is measured to be 7.7 pb , which corresponds to about 230 times the SM prediction. The upper limit on the $pp \rightarrow HH \rightarrow \gamma\gamma WW^*$ at 95% CL is measured to be 7.5 fb (see thier Table 6).
- ¹⁶AABOUD 18CQ search for HH production using $HH \rightarrow b\bar{b}\tau\tau$ with data of 36.1 fb^{-1} at $E_{\text{cm}} = 13 \text{ TeV}$. The upper limit on the $pp \rightarrow HH \rightarrow b\bar{b}\tau\tau$ production cross section at 95% is measured to be 30.9 fb , which corresponds to about 12.7 times the SM prediction.
- ¹⁷AABOUD 18CW search for HH production using $HH \rightarrow \gamma\gamma b\bar{b}$ with data of 36.1 fb^{-1} at $E_{\text{cm}} = 13 \text{ TeV}$. The upper limit on the $pp \rightarrow HH$ production cross section at 95% is measured to be 0.73 pb , which corresponds to about 22 times the SM prediction.
- ¹⁸SIRUNYAN 18A search for HH production using $HH \rightarrow b\bar{b}\tau\tau$ with data of 35.9 fb^{-1} at $E_{\text{cm}} = 13 \text{ TeV}$. The upper limit on the $gg \rightarrow HH \rightarrow b\bar{b}\tau\tau$ production cross section is measured to be 75.4 fb , which corresponds to about 30 times the SM prediction.
- ¹⁹SIRUNYAN 18F search non-resonant for HH production using $HH \rightarrow b\bar{b}\ell\nu\ell\nu$, where $\ell\nu\ell\nu$ is either $WW \rightarrow \ell\nu\ell\nu$ or $ZZ \rightarrow \ell\ell\nu\nu$ (ℓ is e , μ or a leptonically decaying τ), with data of 35.9 fb^{-1} at $E_{\text{cm}} = 13 \text{ TeV}$. The upper limit on the $HH \rightarrow b\bar{b}\ell\nu\ell\nu$ production cross section at 95% CL is measured to be 72 fb , which corresponds to about 79 times the SM prediction.
- ²⁰SIRUNYAN 17CN search for HH production using $HH \rightarrow b\bar{b}\tau\tau$ with data of 18.3 fb^{-1} at $E_{\text{cm}} = 8 \text{ TeV}$. Results are then combined with the published results of the $HH \rightarrow \gamma\gamma b\bar{b}$ and $HH \rightarrow b\bar{b}b\bar{b}$, which use data of up to 19.7 fb^{-1} at $E_{\text{cm}} = 8 \text{ TeV}$. The

upper limit on the $gg \rightarrow HH$ production cross section is measured to be 0.59 pb from $b\bar{b}\tau\tau$, which corresponds to about 59 times the SM prediction (gluon fusion). The combined upper limit is 0.43 pb, which is about 43 times the SM prediction. The quoted values are given for $m_H = 125$ GeV.

- 21 AABOUD 16I search for HH production using $HH \rightarrow b\bar{b}b\bar{b}$ with data of 3.2 fb^{-1} at $E_{\text{cm}} = 13 \text{ TeV}$. The upper limit on the $pp \rightarrow HH \rightarrow b\bar{b}b\bar{b}$ production cross section is measured to be 1.22 pb. This result corresponds to about 108 times the SM prediction (gluon fusion), which is $11.3^{+0.9}_{-1.0} \text{ fb}$ (NNLO+NNLL) including top quark mass effects. The quoted values are given for $m_H = 125$ GeV.
- 22 KHACHATRYAN 16BQ search for HH production using $HH \rightarrow \gamma\gamma b\bar{b}$ with data of 19.7 fb^{-1} at $E_{\text{cm}} = 8 \text{ TeV}$. The upper limit on the $gg \rightarrow HH \rightarrow \gamma\gamma b\bar{b}$ production is measured to be 1.85 fb, which corresponds to about 74 times the SM prediction and is translated into 0.71 pb for $gg \rightarrow HH$ production cross section.
- 23 AAD 15CE search for HH production using $HH \rightarrow b\bar{b}\tau\tau$ and $HH \rightarrow \gamma\gamma WW$ with data of 20.3 fb^{-1} at $E_{\text{cm}} = 8 \text{ TeV}$. These results are then combined with the published results of the $HH \rightarrow \gamma\gamma b\bar{b}$ and $HH \rightarrow b\bar{b}b\bar{b}$, which use data of up to 20.3 fb^{-1} at $E_{\text{cm}} = 8 \text{ TeV}$. The upper limits on the $gg \rightarrow HH$ production cross section are measured to be 1.6 pb, 11.4 pb, 2.2 pb and 0.62 pb from $b\bar{b}\tau\tau$, $\gamma\gamma WW$, $\gamma\gamma b\bar{b}$ and $b\bar{b}b\bar{b}$, respectively. The combined upper limit is 0.69 pb, which corresponds to about 70 times the SM prediction. The quoted results are given for $m_H = 125.4$ GeV. See their Table 4.

Higgs trilinear self coupling modifier κ_λ

Signal strength relative to the SM prediction, $\kappa_\lambda = \lambda_{H\bar{H}H} / \lambda_{H\bar{H}H}^{\text{SM}}$.

VALUE	CL%	DOCUMENT ID	TECN	COMMENT
• • • We do not use the following data for averages, fits, limits, etc. • • •				
– 1.5 to 6.7	95	¹ AAD	22Y ATLAS	$13 \text{ TeV}, \gamma\gamma b\bar{b}$
– 1.24 to 6.49	95	² CMS	22 CMS	$13 \text{ TeV}, b\bar{b}Z Z^*, b\bar{b}\gamma\gamma, b\bar{b}\tau\tau, b\bar{b}b\bar{b}$, multilepton
– 2.3 to 9.4	95	³ TUMASYAN	22AN CMS	$13 \text{ TeV}, b\bar{b}b\bar{b}$
– 3.3 to 8.5	95	⁴ SIRUNYAN	21K CMS	$13 \text{ TeV}, \gamma\gamma b\bar{b}$
– 5.0 to 12.0	95	⁵ AAD	20C ATLAS	$13 \text{ TeV}, b\bar{b}\gamma\gamma, b\bar{b}\tau\tau, b\bar{b}b\bar{b}, b\bar{b}WW^*, WW^*\gamma\gamma, WW^*WW^*$
– 11 to 17	95	⁶ SIRUNYAN	19 CMS	$13 \text{ TeV}, \gamma\gamma b\bar{b}$
– 11.8 to 18.8	95	⁷ SIRUNYAN	19BE CMS	$13 \text{ TeV}, b\bar{b}\gamma\gamma b\bar{b}\tau\tau, b\bar{b}b\bar{b}, b\bar{b}WW^*, b\bar{b}Z Z^*$
– 8.2 to 13.2	95	⁸ AABOUD	18CW ATLAS	$13 \text{ TeV}, \gamma\gamma b\bar{b}$
		⁹ SIRUNYAN	18A CMS	$13 \text{ TeV}, b\bar{b}\tau\tau$
– 17 to 22.5	95	¹⁰ KHACHATRYAN 16BQ	CMS	$8 \text{ TeV}, \gamma\gamma b\bar{b}$

¹ AAD 22Y search for non-resonant HH production using $HH \rightarrow \gamma\gamma b\bar{b}$ with data of 139 fb^{-1} at $E_{\text{cm}} = 13 \text{ TeV}$. The quoted κ_λ is obtained from their Fig. 12 where the theory uncertainties are not included while a negative log-likelihood scan vs. κ_λ is shown in their Fig. 13 with the theory uncertainties, which provides $\kappa_\lambda = 2.8^{+2.0}_{-2.2}$ for the 1σ confidence interval.

² CMS 22 report combined results (see their Extended Data Table 2) using 138 fb^{-1} of data at $E_{\text{cm}} = 13 \text{ TeV}$. See their Fig. 6 (left).

³ TUMASYAN 22AN search for non-resonant HH production using $HH \rightarrow b\bar{b}b\bar{b}$ with data of 138 fb^{-1} at $E_{\text{cm}} = 13 \text{ TeV}$. The upper limit on the $pp \rightarrow HH$ production cross section at 95% CL is shown as a function of κ_λ in their Fig. 2 (top).

⁴ SIRUNYAN 21K search for non-resonant HH production using $HH \rightarrow \gamma\gamma b\bar{b}$ with data of 137 fb^{-1} at $E_{\text{cm}} = 13 \text{ TeV}$.

- ⁵ AAD 20C combine results of up to 36.1 fb^{-1} data at $E_{\text{cm}} = 13 \text{ TeV}$ for $pp \rightarrow HH \rightarrow b\bar{b}\gamma\gamma, b\bar{b}\tau\tau, b\bar{b}b\bar{b}, b\bar{b}WW^*, WW^*\gamma\gamma, WW^*WW^*$ (AABOUD 18CW, AABOUD 18CQ, AABOUD 19A, AABOUD 190, AABOUD 18BU, and AABOUD 19T).
- ⁶ SIRUNYAN 19 search for HH production using $HH \rightarrow \gamma\gamma b\bar{b}$ with data of 35.9 fb^{-1} at $E_{\text{cm}} = 13 \text{ TeV}$. The quoted κ_λ is measured assuming all other Higgs boson couplings are at their SM value.
- ⁷ SIRUNYAN 19BE combine results of $13 \text{ TeV } 35.9 \text{ fb}^{-1}$ data: SIRUNYAN 19, SIRUNYAN 18A, SIRUNYAN 19AB, SIRUNYAN 19H, and SIRUNYAN 18F.
- ⁸ AABOUD 18CW search for HH production using $HH \rightarrow \gamma\gamma b\bar{b}$ with data of 36.1 fb^{-1} at $E_{\text{cm}} = 13 \text{ TeV}$. The quoted κ_λ is measured assuming all other Higgs boson couplings are at their SM value.
- ⁹ SIRUNYAN 18A search for HH production using $HH \rightarrow b\bar{b}\tau\tau$ with data of 35.9 fb^{-1} at $E_{\text{cm}} = 13 \text{ TeV}$. The upper limit on production cross section times branching fraction at 95% CL is shown as a function of κ_λ/κ_t in their Fig. 6 (top) where $\kappa_t = y_t / y_t^{SM}$ (top Yukawa coupling y_t).
- ¹⁰ KHACHATRYAN 16BQ search for HH production using $HH \rightarrow \gamma\gamma b\bar{b}$ with data of 19.7 fb^{-1} at $E_{\text{cm}} = 8 \text{ TeV}$.

Higgs-gauge boson quartic coupling modifier κ_{2V}

Signal strength relative to the SM prediction, $\kappa_{2V} = \lambda_{VVHH} / \lambda_{VVHH}^{SM}$, $V = W, Z$.

VALUE	CL%	DOCUMENT ID	TECN	COMMENT
$\bullet \bullet \bullet$ We do not use the following data for averages, fits, limits, etc. $\bullet \bullet \bullet$				
0.67 to 1.38	95	¹ CMS	22 CMS	$13 \text{ TeV}, b\bar{b}ZZ^*, b\bar{b}\gamma\gamma, b\bar{b}\tau\tau, b\bar{b}b\bar{b}$, multilepton
-0.1 to 2.2	95	² TUMASYAN	22AN CMS	$13 \text{ TeV}, b\bar{b}b\bar{b}$
-1.3 to 3.5	95	³ SIRUNYAN	21K CMS	$13 \text{ TeV}, \gamma\gamma b\bar{b}$
-0.43 to 2.56	95	⁴ AAD	20X ATLS	$13 \text{ TeV}, VBF, b\bar{b}b\bar{b}$

¹ CMS 22 report combined results (see their Extended Data Table 2) using 138 fb^{-1} of data at $E_{\text{cm}} = 13 \text{ TeV}$. See their Fig. 6 (right).

² TUMASYAN 22AN search for non-resonant HH production using $HH \rightarrow b\bar{b}b\bar{b}$ with data of 138 fb^{-1} at $E_{\text{cm}} = 13 \text{ TeV}$. The upper limit on the $pp \rightarrow HH$ production cross section at 95% CL is shown as a function of κ_{2V} in their Fig. 2 (bottom).

³ SIRUNYAN 21K search for non-resonant HH production using $HH \rightarrow \gamma\gamma b\bar{b}$ with data of 137 fb^{-1} at $E_{\text{cm}} = 13 \text{ TeV}$.

⁴ AAD 20X search for $HH \rightarrow b\bar{b}b\bar{b}$ process via VBF with data of 126 fb^{-1} at $E_{\text{cm}} = 13 \text{ TeV}$.

tH production

VALUE	DOCUMENT ID	TECN	COMMENT
$5.7 \pm 2.7 \pm 3.0$	¹ SIRUNYAN	21R CMS	$pp, 13 \text{ TeV}$
$\bullet \bullet \bullet$ We do not use the following data for averages, fits, limits, etc. $\bullet \bullet \bullet$			
	² AAD	20Z ATLS	$pp, 13 \text{ TeV}$
	³ SIRUNYAN	19BK CMS	$pp, 13 \text{ TeV}$
	⁴ KHACHATRY...16AU CMS		$pp, 8 \text{ TeV}$

¹ SIRUNYAN 21R search for tH in final states with electrons, muons and hadronically decaying τ leptons ($H \rightarrow WW^*, ZZ^*, \tau\tau$) with 137 fb^{-1} of pp collision data at $E_{\text{cm}} = 13 \text{ TeV}$. The quoted signal strength corresponds to a significance of 1.4 standard deviations and is given for $m_H = 125 \text{ GeV}$.

² AAD 20Z search for the tH associated production using $H \rightarrow \gamma\gamma$ in 139 fb^{-1} of data at $E_{\text{cm}} = 13 \text{ TeV}$. An upper limit on its rate is set to be 12 times the Standard Model at 95% CL ($m_H = 125.09 \text{ GeV}$).

³ SIRUNYAN 19BK search for the tH associated production using multilepton signatures ($H \rightarrow WW^*$, $H \rightarrow \tau\tau$, $H \rightarrow ZZ^*$) and signatures with a single lepton and a $b\bar{b}$ pair ($H \rightarrow b\bar{b}$) using 35.9 fb^{-1} at $E_{\text{cm}} = 13 \text{ TeV}$. Results are combined with $H \rightarrow \gamma\gamma$ (SIRUNYAN 18DS). The observed 95% CL upper limit on the tH production cross section times $H \rightarrow WW^* + \tau\tau + ZZ^* + b\bar{b} + \gamma\gamma$ branching fraction is 1.94 pb (assuming SM $t\bar{t}H$ production cross section). See their Table X and Fig. 14. The values outside the ranges of $[-0.9, -0.5]$ and $[1.0, 2.1]$ times the standard model top quark Yukawa coupling are excluded at 95% CL.

⁴ KHACHATRYAN 16AU search for the tH associated production in 19.7 fb^{-1} at $E_{\text{cm}} = 8 \text{ TeV}$. The 95% CL upper limits on the tH associated production cross section is measured to be 600–1000 fb depending on the assumed $\gamma\gamma$ branching ratios of the Higgs boson. The $\gamma\gamma$ branching ratio is varied to be by a factor of 0.5–3.0 of the Standard Model Higgs boson ($m_H = 125 \text{ GeV}$). The results of the signal strengths for a negative Higgs-boson trilinear coupling are given. The results are given for $m_H = 125 \text{ GeV}$.

H Production Cross Section in pp Collisions at $\sqrt{s} = 13 \text{ TeV}$

Assumes $m_H = 125 \text{ GeV}$

VALUE (pb)	DOCUMENT ID	TECN	COMMENT
56.9 ± 3.4 OUR AVERAGE			
58 ± 4 ± 4	¹ AAD	22N ATLS	$pp, 13 \text{ TeV}, \gamma\gamma$
53.5 ± 4.9 ± 2.1	² AAD	20BA ATLS	$pp, 13 \text{ TeV}, ZZ^* \rightarrow 4\ell (\ell = e, \mu)$
61.1 ± 6.0 ± 3.7	³ SIRUNYAN	19BA CMS	$pp, 13 \text{ TeV}, \gamma\gamma, ZZ^* \rightarrow 4\ell (\ell = e, \mu)$
• • • We do not use the following data for averages, fits, limits, etc. • • •			
57.0 ± 6.0 ± 4.0	⁴ AABOUD	18CG ATLS	$pp, 13 \text{ TeV}, \gamma\gamma, ZZ^* \rightarrow 4\ell (\ell = e, \mu)$
47.9 ± 9.1 ± 8.6	⁴ AABOUD	18CG ATLS	$pp, 13 \text{ TeV}, \gamma\gamma$
68 ± 11 ± 10	⁴ AABOUD	18CG ATLS	$pp, 13 \text{ TeV}, ZZ^* \rightarrow 4\ell (\ell = e, \mu)$
69 ± 10 ± 5	⁵ AABOUD	17CO ATLS	$pp, 13 \text{ TeV}, ZZ^* \rightarrow 4\ell$

¹ AAD 22N use 139 fb^{-1} of pp collisions at $E_{\text{cm}} = 13 \text{ TeV}$. The quoted value is given for $m_H = 125.09 \text{ GeV}$.

² AAD 20BA use 139 fb^{-1} of pp collisions at $E_{\text{cm}} = 13 \text{ TeV}$ with $H \rightarrow ZZ^* \rightarrow 4\ell$ where $\ell = e, \mu$. The quoted value is given for $m_H = 125 \text{ GeV}$ and assumes the Standard Model branching ratio.

³ SIRUNYAN 19BA use 35.9 fb^{-1} of pp collisions at $E_{\text{cm}} = 13 \text{ TeV}$.

⁴ AABOUD 18CG use 36.1 fb^{-1} of pp collisions at $E_{\text{cm}} = 13 \text{ TeV}$.

⁵ AABOUD 17CO use 36.1 fb^{-1} of pp collisions at $E_{\text{cm}} = 13 \text{ TeV}$ with $H \rightarrow ZZ^* \rightarrow 4\ell$ where $\ell = e, \mu$ for $m_H = 125 \text{ GeV}$. Differential cross sections for the Higgs boson transverse momentum, Higgs boson rapidity, and other related quantities are measured as shown in their Figs. 8 and 9.

H REFERENCES

AAD	22D	PL B829 137066	G. Aad <i>et al.</i>	(ATLAS Collab.)
AAD	22M	JHEP 2206 097	G. Aad <i>et al.</i>	(ATLAS Collab.)
AAD	22N	JHEP 2208 027	G. Aad <i>et al.</i>	(ATLAS Collab.)
AAD	22P	JHEP 2208 104	G. Aad <i>et al.</i>	(ATLAS Collab.)
AAD	22Q	JHEP 2208 175	G. Aad <i>et al.</i>	(ATLAS Collab.)

AAD	22S	EPJ C82 105	G. Aad <i>et al.</i>	(ATLAS Collab.)
AAD	22V	EPJ C82 622	G. Aad <i>et al.</i>	(ATLAS Collab.)
AAD	22W	EPJ C82 717	G. Aad <i>et al.</i>	(ATLAS Collab.)
AAD	22X	PR D105 092003	G. Aad <i>et al.</i>	(ATLAS Collab.)
AAD	22Y	PR D106 052001	G. Aad <i>et al.</i>	(ATLAS Collab.)
ATLAS	22	NAT 607 52	ATLAS Collaboration	(ATLAS Collab.)
Also		NAT 612 E24 (errat.)	ATLAS Collaboration	(ATLAS Collab.)
CMS	22	NAT 607 60	CMS Collaboration	(CMS Collab.)
TUMASYAN	22AM	NATP 18 1329	A. Tumasyan <i>et al.</i>	(CMS Collab.)
TUMASYAN	22AN	PRL 129 081802	A. Tumasyan <i>et al.</i>	(CMS Collab.)
TUMASYAN	22G	PR D105 092007	A. Tumasyan <i>et al.</i>	(CMS Collab.)
TUMASYAN	22Y	JHEP 2206 012	A. Tumasyan <i>et al.</i>	(CMS Collab.)
AAD	21	PL B812 135980	G. Aad <i>et al.</i>	(ATLAS Collab.)
AAD	21AB	EPJ C81 178	G. Aad <i>et al.</i>	(ATLAS Collab.)
AAD	21AJ	EPJ C81 537	G. Aad <i>et al.</i>	(ATLAS Collab.)
AAD	21F	PR D103 112006	G. Aad <i>et al.</i>	(ATLAS Collab.)
AAD	21H	PL B816 136204	G. Aad <i>et al.</i>	(ATLAS Collab.)
AAD	21I	PL B819 136412	G. Aad <i>et al.</i>	(ATLAS Collab.)
AAD	21M	JHEP 2103 268	G. Aad <i>et al.</i>	(ATLAS Collab.)
SIRUNYAN	21	PL B812 135992	A.M. Sirunyan <i>et al.</i>	(CMS Collab.)
SIRUNYAN	21A	EPJ C81 13	A.M. Sirunyan <i>et al.</i>	(CMS Collab.)
Also		EPJ C81 333 (errat.)	A.M. Sirunyan <i>et al.</i>	(CMS Collab.)
SIRUNYAN	21AE	PR D104 052004	A.M. Sirunyan <i>et al.</i>	(CMS Collab.)
SIRUNYAN	21C	JHEP 2101 148	A.M. Sirunyan <i>et al.</i>	(CMS Collab.)
SIRUNYAN	21K	JHEP 2103 257	A.M. Sirunyan <i>et al.</i>	(CMS Collab.)
SIRUNYAN	21L	JHEP 2103 011	A.M. Sirunyan <i>et al.</i>	(CMS Collab.)
SIRUNYAN	21O	JHEP 2107 027	A.M. Sirunyan <i>et al.</i>	(CMS Collab.)
SIRUNYAN	21R	EPJ C81 378	A.M. Sirunyan <i>et al.</i>	(CMS Collab.)
SIRUNYAN	21S	EPJ C81 488	A.M. Sirunyan <i>et al.</i>	(CMS Collab.)
SIRUNYAN	21Z	PR D104 032013	A.M. Sirunyan <i>et al.</i>	(CMS Collab.)
TUMASYAN	21D	JHEP 2111 153	A. Tumasyan <i>et al.</i>	(CMS Collab.)
AAD	20	PR D101 012002	G. Aad <i>et al.</i>	(ATLAS Collab.)
AAD	20A	PL B800 135069	G. Aad <i>et al.</i>	(ATLAS Collab.)
AAD	20AE	PRL 125 221802	G. Aad <i>et al.</i>	(ATLAS Collab.)
AAD	20AG	PL B809 135754	G. Aad <i>et al.</i>	(ATLAS Collab.)
AAD	20AQ	EPJ C80 957	G. Aad <i>et al.</i>	(ATLAS Collab.)
Also		EPJ C81 29 (errat.)	G. Aad <i>et al.</i>	(ATLAS Collab.)
Also		EPJ C81 398 (errat.)	G. Aad <i>et al.</i>	(ATLAS Collab.)
AAD	20BA	EPJ C80 942	G. Aad <i>et al.</i>	(ATLAS Collab.)
AAD	20C	PL B800 135103	G. Aad <i>et al.</i>	(ATLAS Collab.)
AAD	20E	PL B801 135145	G. Aad <i>et al.</i>	(ATLAS Collab.)
AAD	20F	PL B801 135148	G. Aad <i>et al.</i>	(ATLAS Collab.)
AAD	20N	PL B805 135426	G. Aad <i>et al.</i>	(ATLAS Collab.)
AAD	20X	JHEP 2007 108	G. Aad <i>et al.</i>	(ATLAS Collab.)
Also		JHEP 2101 145 (errat.)	G. Aad <i>et al.</i>	(ATLAS Collab.)
Also		JHEP 2105 207 (errat.)	G. Aad <i>et al.</i>	(ATLAS Collab.)
AAD	20Z	PRL 125 061802	G. Aad <i>et al.</i>	(ATLAS Collab.)
SIRUNYAN	20AE	JHEP 2003 131	A.M. Sirunyan <i>et al.</i>	(CMS Collab.)
SIRUNYAN	20AS	PRL 125 061801	A.M. Sirunyan <i>et al.</i>	(CMS Collab.)
SIRUNYAN	20BK	JHEP 2011 039	A.M. Sirunyan <i>et al.</i>	(CMS Collab.)
SIRUNYAN	20BL	JHEP 2012 085	A.M. Sirunyan <i>et al.</i>	(CMS Collab.)
SIRUNYAN	20C	EPJ C80 75	A.M. Sirunyan <i>et al.</i>	(CMS Collab.)
SIRUNYAN	20L	PL B805 135425	A.M. Sirunyan <i>et al.</i>	(CMS Collab.)
AABOUD	19A	JHEP 1901 030	M. Aaboud <i>et al.</i>	(ATLAS Collab.)
AABOUD	19AI	PL B793 499	M. Aaboud <i>et al.</i>	(ATLAS Collab.)
AABOUD	19AL	PRL 122 231801	M. Aaboud <i>et al.</i>	(ATLAS Collab.)
AABOUD	19AQ	PR D99 072001	M. Aaboud <i>et al.</i>	(ATLAS Collab.)
AABOUD	19F	PL B789 508	M. Aaboud <i>et al.</i>	(ATLAS Collab.)
AABOUD	19N	JHEP 1904 048	M. Aaboud <i>et al.</i>	(ATLAS Collab.)
AABOUD	19O	JHEP 1904 092	M. Aaboud <i>et al.</i>	(ATLAS Collab.)
AABOUD	19T	JHEP 1905 124	M. Aaboud <i>et al.</i>	(ATLAS Collab.)
AABOUD	19U	JHEP 1905 141	M. Aaboud <i>et al.</i>	(ATLAS Collab.)
AAD	19A	PL B798 134949	G. Aad <i>et al.</i>	(ATLAS Collab.)
SIRUNYAN	19	PL B788 7	A.M. Sirunyan <i>et al.</i>	(CMS Collab.)
SIRUNYAN	19AB	JHEP 1904 112	A.M. Sirunyan <i>et al.</i>	(CMS Collab.)
SIRUNYAN	19AF	JHEP 1906 093	A.M. Sirunyan <i>et al.</i>	(CMS Collab.)
SIRUNYAN	19AJ	EPJ C79 94	A.M. Sirunyan <i>et al.</i>	(CMS Collab.)
SIRUNYAN	19AT	EPJ C79 421	A.M. Sirunyan <i>et al.</i>	(CMS Collab.)
SIRUNYAN	19AX	PL B791 96	A.M. Sirunyan <i>et al.</i>	(CMS Collab.)
SIRUNYAN	19BA	PL B792 369	A.M. Sirunyan <i>et al.</i>	(CMS Collab.)
SIRUNYAN	19BE	PRL 122 121803	A.M. Sirunyan <i>et al.</i>	(CMS Collab.)

SIRUNYAN	19BK	PR D99	092005	A.M. Sirunyan <i>et al.</i>	(CMS Collab.)
SIRUNYAN	19BL	PR D99	112003	A.M. Sirunyan <i>et al.</i>	(CMS Collab.)
SIRUNYAN	19BO	PL B793	520	A.M. Sirunyan <i>et al.</i>	(CMS Collab.)
SIRUNYAN	19BR	PL B797	134811	A.M. Sirunyan <i>et al.</i>	(CMS Collab.)
SIRUNYAN	19BY	PR D100	072007	A.M. Sirunyan <i>et al.</i>	(CMS Collab.)
SIRUNYAN	19BZ	PR D100	112002	A.M. Sirunyan <i>et al.</i>	(CMS Collab.)
SIRUNYAN	19CG	JHEP	1910 139	A.M. Sirunyan <i>et al.</i>	(CMS Collab.)
SIRUNYAN	19E	PRL	122 021801	A.M. Sirunyan <i>et al.</i>	(CMS Collab.)
SIRUNYAN	19H	JHEP	1901 040	A.M. Sirunyan <i>et al.</i>	(CMS Collab.)
SIRUNYAN	19L	JHEP	1901 183	A.M. Sirunyan <i>et al.</i>	(CMS Collab.)
SIRUNYAN	19R	JHEP	1903 026	A.M. Sirunyan <i>et al.</i>	(CMS Collab.)
AABOUD	18	PL B776	318	M. Aaboud <i>et al.</i>	(ATLAS Collab.)
AABOUD	18AC	PR D97	072003	M. Aaboud <i>et al.</i>	(ATLAS Collab.)
AABOUD	18AJ	JHEP	1803 095	M. Aaboud <i>et al.</i>	(ATLAS Collab.)
AABOUD	18AU	JHEP	1807 127	M. Aaboud <i>et al.</i>	(ATLAS Collab.)
AABOUD	18BK	PL B784	173	M. Aaboud <i>et al.</i>	(ATLAS Collab.)
AABOUD	18BL	PL B786	134	M. Aaboud <i>et al.</i>	(ATLAS Collab.)
AABOUD	18BM	PL B784	345	M. Aaboud <i>et al.</i>	(ATLAS Collab.)
AABOUD	18BN	PL B786	59	M. Aaboud <i>et al.</i>	(ATLAS Collab.)
AABOUD	18BO	PR D98	052005	M. Aaboud <i>et al.</i>	(ATLAS Collab.)
AABOUD	18BP	PL B786	223	M. Aaboud <i>et al.</i>	(ATLAS Collab.)
AABOUD	18BQ	PR D98	052003	M. Aaboud <i>et al.</i>	(ATLAS Collab.)
AABOUD	18BU	EPJ C78	1007	M. Aaboud <i>et al.</i>	(ATLAS Collab.)
AABOUD	18CA	JHEP	1810 180	M. Aaboud <i>et al.</i>	(ATLAS Collab.)
AABOUD	18CG	PL B786	114	M. Aaboud <i>et al.</i>	(ATLAS Collab.)
AABOUD	18CQ	PRL	121 191801	M. Aaboud <i>et al.</i>	(ATLAS Collab.)
AABOUD	18CW	JHEP	1811 040	M. Aaboud <i>et al.</i>	(ATLAS Collab.)
AABOUD	18M	PRL	120 211802	M. Aaboud <i>et al.</i>	(ATLAS Collab.)
AABOUD	18T	PR D97	072016	M. Aaboud <i>et al.</i>	(ATLAS Collab.)
AAIJ	18AM	EPJ C78	1008	R. Aaij <i>et al.</i>	(LHCb Collab.)
AALTONEN	18C	PR D98	072002	T. Aaltonen <i>et al.</i>	(CDF Collab.)
SIRUNYAN	18A	PL B778	101	A.M. Sirunyan <i>et al.</i>	(CMS Collab.)
SIRUNYAN	18AE	PL B780	501	A.M. Sirunyan <i>et al.</i>	(CMS Collab.)
SIRUNYAN	18BD	JHEP	1806 101	A.M. Sirunyan <i>et al.</i>	(CMS Collab.)
SIRUNYAN	18BH	JHEP	1806 001	A.M. Sirunyan <i>et al.</i>	(CMS Collab.)
SIRUNYAN	18BQ	JHEP	1808 066	A.M. Sirunyan <i>et al.</i>	(CMS Collab.)
SIRUNYAN	18BU	EPJ C78	140	A.M. Sirunyan <i>et al.</i>	(CMS Collab.)
SIRUNYAN	18BV	EPJ C78	291	A.M. Sirunyan <i>et al.</i>	(CMS Collab.)
SIRUNYAN	18DB	PRL	121 121801	A.M. Sirunyan <i>et al.</i>	(CMS Collab.)
SIRUNYAN	18DQ	JHEP	1811 152	A.M. Sirunyan <i>et al.</i>	(CMS Collab.)
SIRUNYAN	18DS	JHEP	1811 185	A.M. Sirunyan <i>et al.</i>	(CMS Collab.)
SIRUNYAN	18E	PRL	120 071802	A.M. Sirunyan <i>et al.</i>	(CMS Collab.)
SIRUNYAN	18F	JHEP	1801 054	A.M. Sirunyan <i>et al.</i>	(CMS Collab.)
SIRUNYAN	18L	PRL	120 231801	A.M. Sirunyan <i>et al.</i>	(CMS Collab.)
SIRUNYAN	18S	PR D97	092005	A.M. Sirunyan <i>et al.</i>	(CMS Collab.)
SIRUNYAN	18Y	PL B779	283	A.M. Sirunyan <i>et al.</i>	(CMS Collab.)
AABOUD	17AW	JHEP	1710 112	M. Aaboud <i>et al.</i>	(ATLAS Collab.)
AABOUD	17BA	JHEP	1712 024	M. Aaboud <i>et al.</i>	(ATLAS Collab.)
AABOUD	17BD	EPJ C77	765	M. Aaboud <i>et al.</i>	(ATLAS Collab.)
AABOUD	17CO	JHEP	1710 132	M. Aaboud <i>et al.</i>	(ATLAS Collab.)
AABOUD	17Y	PRL	119 051802	M. Aaboud <i>et al.</i>	(ATLAS Collab.)
AAD	17	EPJ C77	70	G. Aad <i>et al.</i>	(ATLAS Collab.)
KHACHATRY...	17F	JHEP	1702 135	V. Khachatryan <i>et al.</i>	(CMS Collab.)
SIRUNYAN	17AM	PL B775	1	A.M. Sirunyan <i>et al.</i>	(CMS Collab.)
SIRUNYAN	17AV	JHEP	1711 047	A.M. Sirunyan <i>et al.</i>	(CMS Collab.)
SIRUNYAN	17CN	PR D96	072004	A.M. Sirunyan <i>et al.</i>	(CMS Collab.)
AABOUD	16I	PR D94	052002	M. Aaboud <i>et al.</i>	(ATLAS Collab.)
AABOUD	16K	PRL	117 111802	M. Aaboud <i>et al.</i>	(ATLAS Collab.)
AABOUD	16X	JHEP	1611 112	M. Aaboud <i>et al.</i>	(ATLAS Collab.)
AAD	16	PL B753	69	G. Aad <i>et al.</i>	(ATLAS Collab.)
AAD	16AC	PR D93	092005	G. Aad <i>et al.</i>	(ATLAS Collab.)
AAD	16AF	JHEP	1601 172	G. Aad <i>et al.</i>	(ATLAS Collab.)
AAD	16AL	JHEP	1605 160	G. Aad <i>et al.</i>	(ATLAS Collab.)
AAD	16AN	JHEP	1608 045	G. Aad <i>et al.</i>	(ATLAS Collab.)
AAD	16AO	JHEP	1608 104	G. Aad <i>et al.</i>	(ATLAS Collab.)
AAD	16BL	EPJ C76	658	G. Aad <i>et al.</i>	(ATLAS Collab.)
AAD	16K	EPJ C76	6	G. Aad <i>et al.</i>	(ATLAS Collab.)
KHACHATRY...	16AB	PL B759	672	V. Khachatryan <i>et al.</i>	(CMS Collab.)
KHACHATRY...	16AR	JHEP	1604 005	V. Khachatryan <i>et al.</i>	(CMS Collab.)
KHACHATRY...	16AU	JHEP	1606 177	V. Khachatryan <i>et al.</i>	(CMS Collab.)
KHACHATRY...	16B	PL B753	341	V. Khachatryan <i>et al.</i>	(CMS Collab.)

KHACHATRY...	16BA	JHEP 1609 051	V. Khachatryan <i>et al.</i>	(CMS Collab.)
KHACHATRY...	16BQ	PR D94 052012	V. Khachatryan <i>et al.</i>	(CMS Collab.)
KHACHATRY...	16CD	PL B763 472	V. Khachatryan <i>et al.</i>	(CMS Collab.)
KHACHATRY...	16G	EPJ C76 13	V. Khachatryan <i>et al.</i>	(CMS Collab.)
AAD	15	PL B740 222	G. Aad <i>et al.</i>	(ATLAS Collab.)
AAD	15AA	PR D92 012006	G. Aad <i>et al.</i>	(ATLAS Collab.)
AAD	15AH	JHEP 1504 117	G. Aad <i>et al.</i>	(ATLAS Collab.)
AAD	15AQ	JHEP 1508 137	G. Aad <i>et al.</i>	(ATLAS Collab.)
AAD	15AX	EPJ C75 231	G. Aad <i>et al.</i>	(ATLAS Collab.)
AAD	15B	PRL 114 191803	G. Aad <i>et al.</i>	(ATLAS and CMS Collabs.)
AAD	15BC	EPJ C75 349	G. Aad <i>et al.</i>	(ATLAS Collab.)
AAD	15BD	EPJ C75 337	G. Aad <i>et al.</i>	(ATLAS Collab.)
AAD	15BE	EPJ C75 335	G. Aad <i>et al.</i>	(ATLAS Collab.)
AAD	15CE	PR D92 092004	G. Aad <i>et al.</i>	(ATLAS Collab.)
AAD	15CI	EPJ C75 476	G. Aad <i>et al.</i>	(ATLAS Collab.)
Also		EPJ C76 152 (errat.)	G. Aad <i>et al.</i>	(ATLAS Collab.)
AAD	15CX	JHEP 1511 206	G. Aad <i>et al.</i>	(ATLAS Collab.)
AAD	15F	PR D91 012006	G. Aad <i>et al.</i>	(ATLAS Collab.)
AAD	15G	JHEP 1501 069	G. Aad <i>et al.</i>	(ATLAS Collab.)
AAD	15I	PRL 114 121801	G. Aad <i>et al.</i>	(ATLAS Collab.)
AAD	15P	PRL 115 091801	G. Aad <i>et al.</i>	(ATLAS Collab.)
AAD	15T	PL B749 519	G. Aad <i>et al.</i>	(ATLAS Collab.)
AALTONEN	15	PRL 114 151802	T. Aaltonen <i>et al.</i>	(CDF and D0 Collabs.)
AALTONEN	15B	PRL 114 141802	T. Aaltonen <i>et al.</i>	(CDF Collab.)
KHACHATRY...	15AM	EPJ C75 212	V. Khachatryan <i>et al.</i>	(CMS Collab.)
KHACHATRY...	15AN	EPJ C75 251	V. Khachatryan <i>et al.</i>	(CMS Collab.)
KHACHATRY...	15BA	PR D92 072010	V. Khachatryan <i>et al.</i>	(CMS Collab.)
KHACHATRY...	15H	PL B744 184	V. Khachatryan <i>et al.</i>	(CMS Collab.)
KHACHATRY...	15Q	PL B749 337	V. Khachatryan <i>et al.</i>	(CMS Collab.)
KHACHATRY...	15Y	PR D92 012004	V. Khachatryan <i>et al.</i>	(CMS Collab.)
KHACHATRY...	15Z	PR D92 032008	V. Khachatryan <i>et al.</i>	(CMS Collab.)
AAD	14AR	PL B738 234	G. Aad <i>et al.</i>	(ATLAS Collab.)
AAD	14AS	PL B738 68	G. Aad <i>et al.</i>	(ATLAS Collab.)
AAD	14BC	PR D90 112015	G. Aad <i>et al.</i>	(ATLAS Collab.)
AAD	14BJ	JHEP 1409 112	G. Aad <i>et al.</i>	(ATLAS Collab.)
AAD	14J	PL B732 8	G. Aad <i>et al.</i>	(ATLAS Collab.)
AAD	14O	PRL 112 201802	G. Aad <i>et al.</i>	(ATLAS Collab.)
AAD	14W	PR D90 052004	G. Aad <i>et al.</i>	(ATLAS Collab.)
ABAZOV	14F	PRL 113 161802	V.M. Abazov <i>et al.</i>	(D0 Collab.)
CHATRCHYAN	14AA	PR D89 092007	S. Chatrchyan <i>et al.</i>	(CMS Collab.)
CHATRCHYAN	14AI	PR D89 012003	S. Chatrchyan <i>et al.</i>	(CMS Collab.)
CHATRCHYAN	14AJ	NATP 10 557	S. Chatrchyan <i>et al.</i>	(CMS Collab.)
CHATRCHYAN	14B	EPJ C74 2980	S. Chatrchyan <i>et al.</i>	(CMS Collab.)
CHATRCHYAN	14G	JHEP 1401 096	S. Chatrchyan <i>et al.</i>	(CMS Collab.)
CHATRCHYAN	14K	JHEP 1405 104	S. Chatrchyan <i>et al.</i>	(CMS Collab.)
KHACHATRY...	14D	PL B736 64	V. Khachatryan <i>et al.</i>	(CMS Collab.)
KHACHATRY...	14H	JHEP 1409 087	V. Khachatryan <i>et al.</i>	(CMS Collab.)
KHACHATRY...	14P	EPJ C74 3076	V. Khachatryan <i>et al.</i>	(CMS Collab.)
AAD	13AJ	PL B726 120	G. Aad <i>et al.</i>	(ATLAS Collab.)
AAD	13AK	PL B726 88	G. Aad <i>et al.</i>	(ATLAS Collab.)
Also		PL B734 406 (errat.)	G. Aad <i>et al.</i>	(ATLAS Collab.)
AALTONEN	13L	PR D88 052013	T. Aaltonen <i>et al.</i>	(CDF Collab.)
AALTONEN	13M	PR D88 052014	T. Aaltonen <i>et al.</i>	(CDF and D0 Collabs.)
ABAZOV	13L	PR D88 052011	V.M. Abazov <i>et al.</i>	(D0 Collab.)
CHATRCHYAN	13BK	PL B726 587	S. Chatrchyan <i>et al.</i>	(CMS Collab.)
CHATRCHYAN	13J	PRL 110 081803	S. Chatrchyan <i>et al.</i>	(CMS Collab.)
CHATRCHYAN	13X	JHEP 1305 145	S. Chatrchyan <i>et al.</i>	(CMS Collab.)
CHATRCHYAN	13Y	JHEP 1306 081	S. Chatrchyan <i>et al.</i>	(CMS Collab.)
HEINEMEYER	13A	arXiv:1307.1347	S. Heinemeyer <i>et al.</i>	(LHC Higgs CS Working Group)
AAD	12AI	PL B716 1	G. Aad <i>et al.</i>	(ATLAS Collab.)
AAD	12DA	SCI 338 1576	G. Aad <i>et al.</i>	(ATLAS Collab.)
AALTONEN	12Q	PRL 109 111803	T. Aaltonen <i>et al.</i>	(CDF Collab.)
AALTONEN	12R	PRL 109 111804	T. Aaltonen <i>et al.</i>	(CDF Collab.)
AALTONEN	12S	PRL 109 111805	T. Aaltonen <i>et al.</i>	(CDF Collab.)
AALTONEN	12T	PRL 109 071804	T. Aaltonen <i>et al.</i>	(CDF and D0 Collabs.)
ABAZOV	12K	PL B716 285	V.M. Abazov <i>et al.</i>	(D0 Collab.)
ABAZOV	12O	PRL 109 121803	V.M. Abazov <i>et al.</i>	(D0 Collab.)
ABAZOV	12P	PRL 109 121804	V.M. Abazov <i>et al.</i>	(D0 Collab.)
CHATRCHYAN	12BY	SCI 338 1569	S. Chatrchyan <i>et al.</i>	(CMS Collab.)
CHATRCHYAN	12N	PL B716 30	S. Chatrchyan <i>et al.</i>	(CMS Collab.)

DITTMAIER 12 arXiv:1201.3084
DITTMAIER 11 arXiv:1101.0593

S. Dittmaier *et al.* (LHC Higgs CS Working Group)
S. Dittmaier *et al.* (LHC Higgs CS Working Group)
